SAFETY IN MINES RESEARCH ADVISORY COMMITTEE

SIMRAC

Final Project Report

Title: THE SAFE USE OF MINE WINDING ROPES

Volume 6 : Studies towards a Code of Practice
for the Performance, Operation, Testing and
Maintenance of Drub Winders

Author/s: G F K Hecker and J Kroonstuiver

Research
Agency: Mine Hoisting Technology
CSIR

Project No: GAP 054

Date: April 1996

INVESTIGATION INTO ROPE FORCES
GENERATED DURING EMERGENCY
BRAKING EVENTS
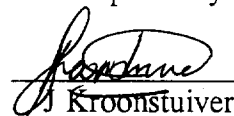
by

J. Kroonstuiver

CSIR Contract Report No 940189
Job No.: MST(94)MC2208
September 1994

Submitted to:
  The SIMRAC Engineering Advisory Committee

Issued By:
  Mine Hoisting, Metallurgical and Corrosion Services
  Division of Materials Science and Technology
  CSIR
  Private Bag x28, Auckland Park, 2006

  Telephone   (011) 726 7100
  Telefax   (011) 726 6418

Prepared by:

J Kroonstuiver

Reviewed by:

G/F K Hecker

SYNOPSIS

This study was commissioned to determine the maximum rope force in the rope of a mine winding system subsequent to a brake control system failure. Four different winders were evaluated: a 4000m Blair multi rope system; a 2300m Blair multi rope system; a 2500m double drum system; and a 1800m double drum system.

The deeper shaft systems exhibited higher rope forces than the shallower systems. The 4000m system had the highest rope force as a fraction of the rope breaking strength. A rope force of 60% of the rope breaking strength was calculated for this system. The lower static factors of the deeper winds resulted in the higher rope forces calculated for these winding systems.

Slack rope occurred in the 4000m mine winding system after the occurrence of a brake control system failure. Slack rope could be prevented and the maximum rope force in the system could be reduced by increasing the number of independent brake systems on a winder.

LIST OF SYMBOLS

a	Design brake deceleration
ρ	Rope Mass per metre
$[C]$	Discrete element damping matrix
D_w	Winder diameter (Includes motors and wound up rope)
D_s	Head sheave diameter
F	Maximum equivalent braking force
I_w	Winder inertia
I_s	Head sheave inertia
z	Shaft depth
M_c	Mass of conveyance and attachments
M_l	Mass of payload
$[M]$	Discrete element mass matrix
$[K]$	Discrete element stiffness matrix
$[\zeta_r]$	Modal damping matrix
$[\omega_r]$	Diagonal natural frequency matrix
$[\phi]$	Mode shape
$[\phi]^T$	Mode shape transposed

Young's Modulus

σ	Rope stress based on cross sectional area.
k_1	173 GPa
k_2	22,7 (GPa)^2
k_3	0,197 GPa

Force Ratio

(Rope force)/(Rope breaking force)

LIST OF FIGURES

CONTENTS

1. INTRODUCTION

The safe design of mine winding systems can be achieved with a better understanding of rope forces occurring in winding installations. Dynamic events at the winder can be included in a numerical analysis to determine the effect that these events have on the ropes of the winding system. Dynamic events at the winder include normal braking, normal acceleration, impulse type events (e.g. as at a motor short circuit) and emergency braking events (trip-out, uncontrolled braking and controlled emergency braking).

This study was undertaken to determine the forces in a winding system subsequent to and during an uncontrolled emergency braking event. To obtain a better understanding of the effect of this braking event different winding systems were analyzed: a 4000m Blair multi rope system; a 2300m Blair multi rope system; a 2500m double drum system and a 1800m double drum system. These four winding system were hypothetical and the ropes were selected to obtain a static factor of 2500/(4000 + L). Some of the physical parameters of the winding systems (e.g. the drum inertia, rope diameters etc.) were obtained by considering existing winding systems. The 4000m winding system was included in the analysis to illustrate the behaviour of a deep level winding system. The brake policy adopted in existing winder systems was adopted in the numerical system, so that simulation results remained valid.

2. MODEL DEFINITION

A discrete numerical model representing the winder system was defined using the MATLAB package (version 4.2b) in conjunction with the SIMULINK dynamic systems simulation software (version 1.3a). Figure 1 illustrates the model used. Masses numbered M1 to M4 represent: the ascending conveyance mass; the sheave wheel inertia; the winder inertia and the descending conveyance mass respectively. The number of elements defined in the ropes (L1 to L4) could be varied. Velocities, accelerations and displacements were considered positive towards the right of the diagram.

Torque vs time profiles could be entered directly into the model. The braking events considered in this investigation represented a failure of the brake control mechanism. The accuracy of the simulation results was controlled by a relative error input defined in SIMULINK.
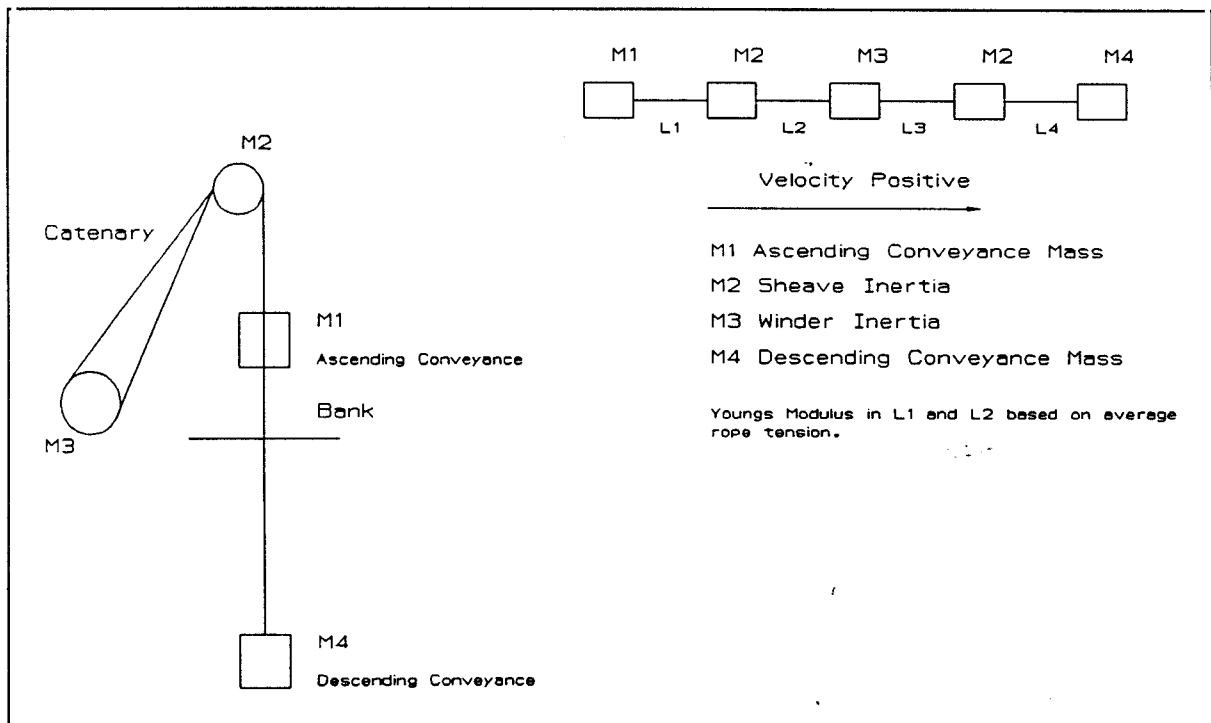
**Figure 1**   Numerical lumped parameter model used in simulations

3. BRAKE TORQUE

The maximum brake torque applied to the winder during emergency braking was the torque capacity of a single brake. The four winders investigated each had two brakes. The maximum torque applied by a single brake was sufficient to decelerate the winder at a minimum deceleration of 2,5m/s². This deceleration could increase, depending on the imbalance load applied to the winder drum by the rope and payload mass.

The brake force applied to the lumped mass of the winder (M3) by a single brake was determined by using the equation given below:

$$F = (\rho z + M_l)g + \left[\rho z + 2M_c + M_l + \frac{I_w + 2I_s}{\left[\frac{D_w}{2} \right]^2} \right] a$$

Two dynamic braking events were considered in this investigation. A stepped torque/time profile and an exponential torque/time profile. The stepped profile represented to the situation where, after an emergency trip-out, the hydraulic mechanism failed. Brake hydraulic pressure would be lost immediately causing the immediate uncontrolled application of the brakes. The exponential profile represented the case where, at motor trip-out, brake hydraulic pressure was gradually released. For this situation the brakes would be applied uncontrolled but at a predetermined rate. The torque curves in figure 2 were normalised with respect to the maximum brake torque applied by a single brake.
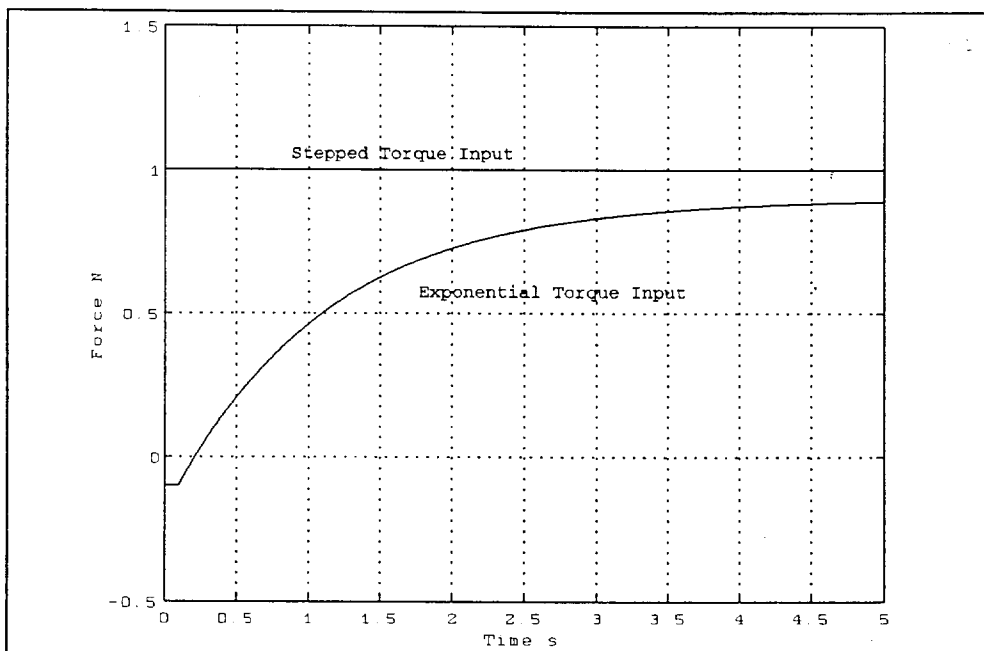
Figure 2   Torque vs time profiles applied to winder drum during braking

5. YOUNG'S MODULUS

Work carried out by Van Zyl [1992] illustrated that the rope stiffness was a function of mean rope tension. Constancon [1993] also found that the damping coefficient was dependent on the mean rope tension. A constant rope stiffness and a constant damping factor ζ was used in these simulations, the value chosen for the Young's Modulus was based on the mean rope tension.

The equation below illustrates the Young's modulus model derived by van Zyl [1992].

$$E = k_1 - \left(\frac{k_2}{\sigma + k_3} \right)$$

The mean stress in the rope was determined to calculate the 'average' value of Young's modulus. The mean stress was determined by considering the stress levels in a rope with a loaded conveyance only. The mean stress was taken as the average of the stress in the rope at the winder at maximum and at minimum depth (with a loaded conveyance).

6. SIMULATION PARAMETERS

HYPOTHETICAL SHAFT SYSTEMS				
SYSTEM PARAMETERS	SYSTEM 1 BMR	SYSTEM 2 BMR	SYSTEM 3 D-DRUM	SYSTEM 4 D-DRUM
Shaft Depth (m)	4000	2300	2500	1800
Static factor	3,13	3,97	3,85	4,31
Rope Diameter (mm)	64	38	54	44
Rope Area (mm^2)	3 743	1 319	1 333	885
Rope Mass per Metre (kg/m)	34	12	12,39	8,24
Rope Breaking Strength (kN)	5882	2070	2 117	1 408
Winder Inertia (kg•m^2)	10 056 430	1 430 000	2 200 000	1 006 500
Winder Diameter (m)	7,20	4,27	6,00	4,88
Sheave Inertia (kg•m^2)	75 000	15 570	21 600	11 600
Sheave Diameter (m)	7,20	4,27	6,00	4,88
Conveyance Mass (kg)	15 952	7 551	7 540	5 550
Payload Mass (kg)	37 222	17 755	17 593	12 952
Young's Modulus (MPa)	123 000	124 000	124 000	127 000
Maximum Brake Torque (MNm)	13,86	2,97	3,80	1,90
Winding Velocity (m/s)	18	18	18	18

7. RESULTS

7.1 System 1:

In this simulation a number of results are presented to allow the reader to obtain an overview of the forces in a rope/winder system subsequent to a brake control failure. In figure 3 a loaded descending conveyance at maximum shaft depth (4000m) with an empty ascending at minimum shaft depth (at 30m) was decelerated using the instantaneous (stepped) brake input. The rope forces in the system were normalised (with respect to the rope breaking strength of 5882 kN) to facilitate a comparison between different rope/winder systems. The force ratio plotted on the ordinate axis represents this normalised force.
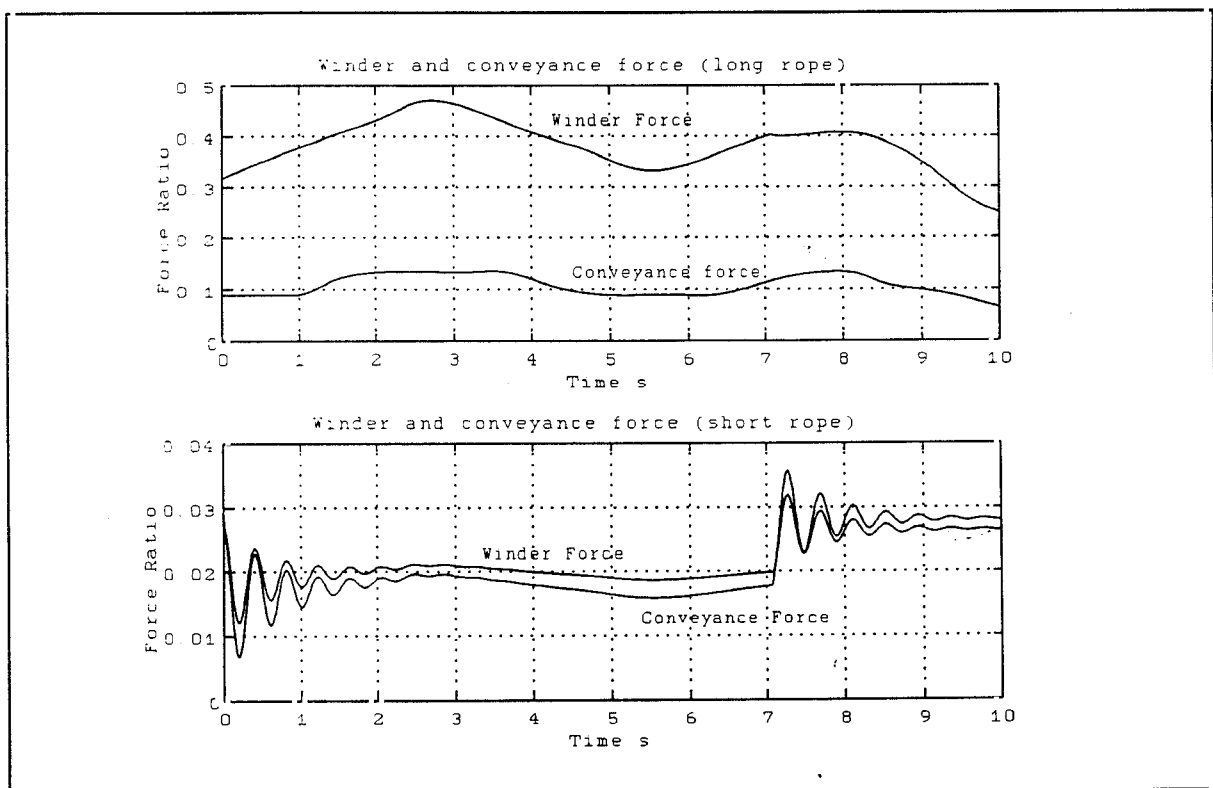
Figure 3   Rope forces resulting from an instantaneously applied brake, a loaded descending conveyance at 4000m and an empty ascending conveyance at 30m.

The same system (as presented in figure 3) was decelerated with the exponential brake profile. The results are presented in figure 4. Rope forces obtained with the exponential profile are lower than those obtained with the stepped brake profile. The force in the long rope first decreases before it increases. This results from the 100ms delay that occurs before the winder brakes are applied (i.e. after the motor has tripped). The average rope force in the short rope is the same for both the exponential and the stepped brake profile.
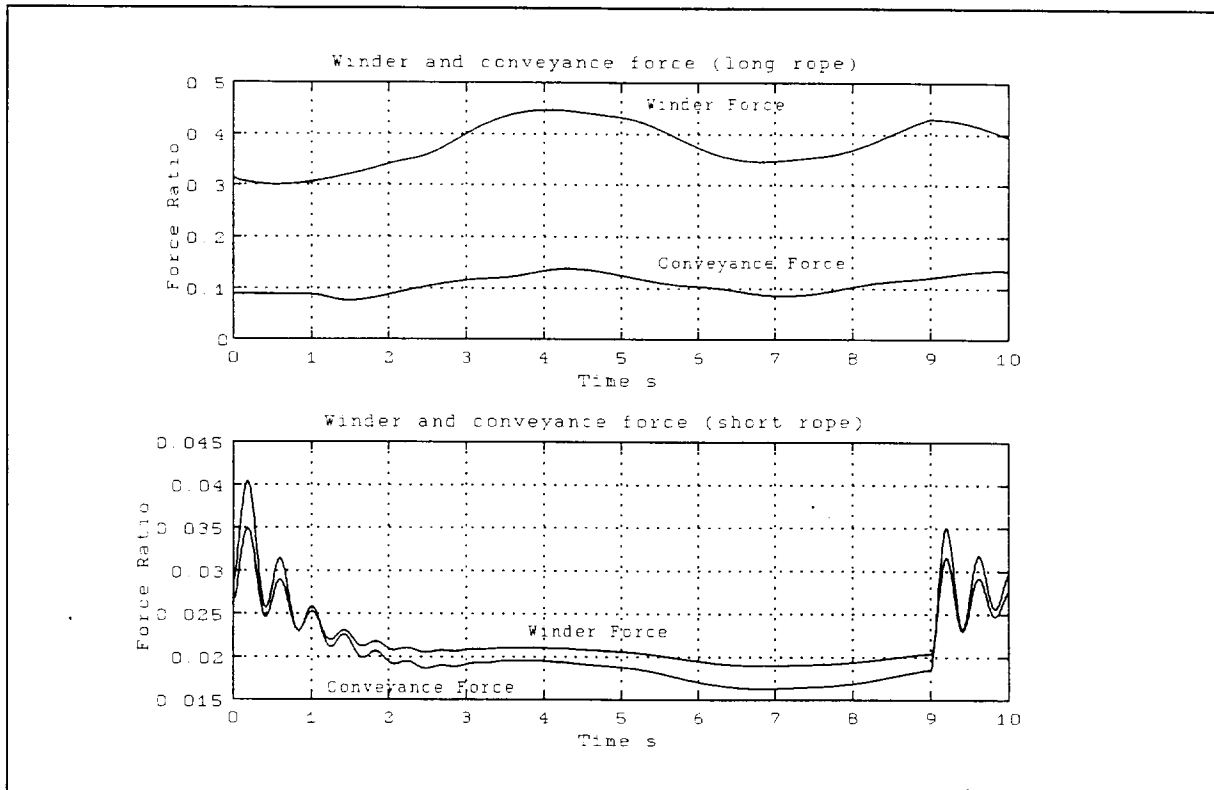
Figure 4   Rope forces with an exponentially applied brake, a loaded descending
                conveyance at 4000m and an empty ascending conveyance at 30m

The maximum rope force occurred in this system when the imbalance force (due to the rope mass and the payload mass) assisted the brakes in decelerating the winder. In figure 5 the following two cases are presented: a loaded descending conveyance at maximum shaft depth (4000m) with an empty ascending at minimum shaft depth (see figure 3); and a loaded ascending conveyance at maximum shaft depth with an empty descending conveyance at minimum shaft depth (30m). The maximum force obtained in the latter case was 60% of the rope breaking strength.
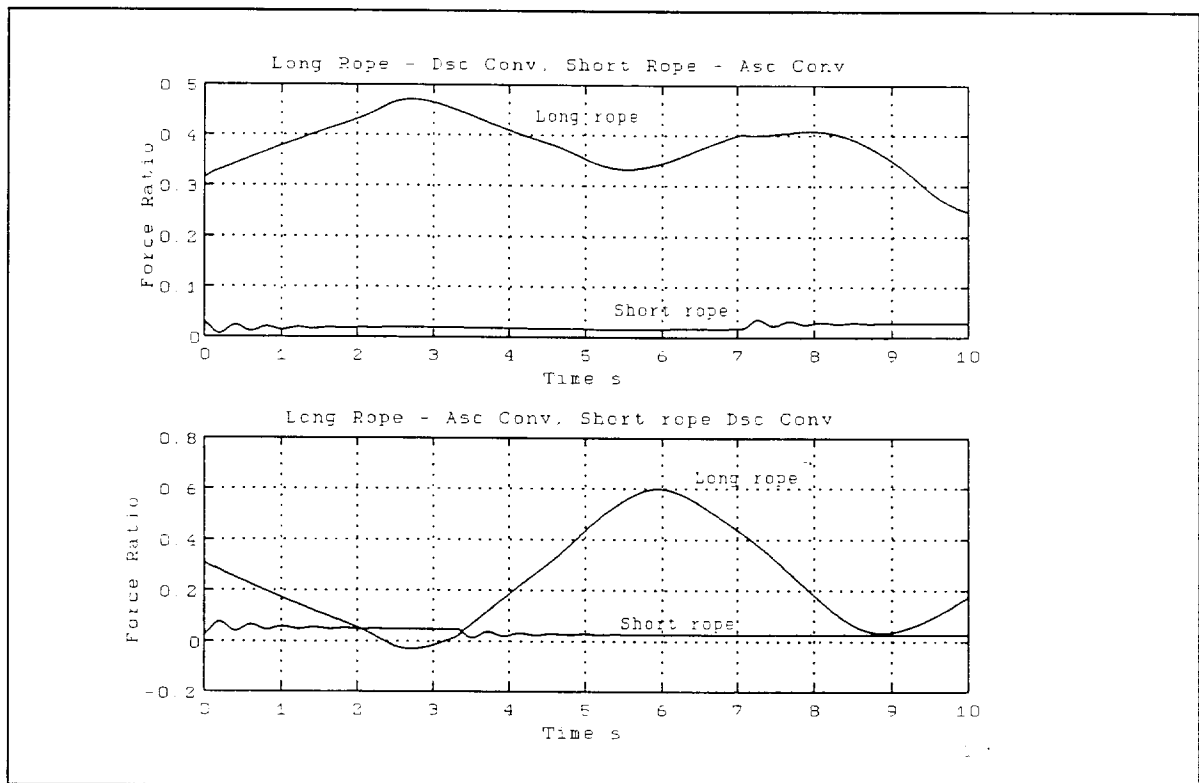

Figure 5   Rope forces with and instantaneously applied brake, a loaded conveyance at 4000m and an empty conveyance at 30m

In figure 6 the maximum force in the long rope for the ascending case is presented. The rope is seen to go into a slack condition (compression). The duration of slack rope at the conveyance is approximately two seconds.
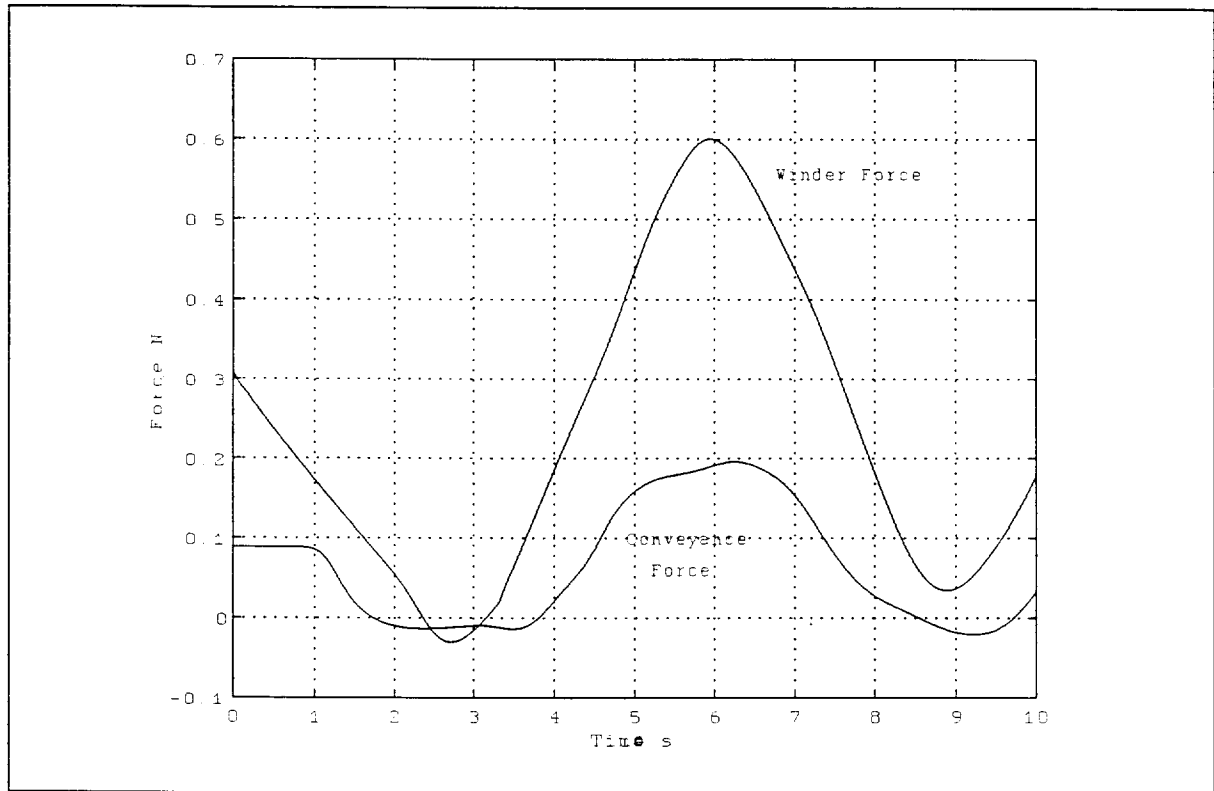
Figure 6   Forces in long rope at winder and conveyance, a loaded ascending conveyance at 4000m and an empty descending conveyance at 30m

The model used in these simulations was not adjusted during slack rope. The negative rope forces present in the model may have distorted the results slightly. The forces acting on the section of the rope that was slack should only have been gravitational pull, as opposed to gravity and compressive rope forces. The magnitude of the negative rope forces was small, the effect of including these forces in the simulation was negligible and did not detract the validity of the solution.

7.2 System 2

The in shaft conveyance positions resulting in maximum rope forces for the other winder systems were determined. These positions were: an ascending loaded conveyance at maximum shaft depth with an empty conveyance at bank level; a descending loaded conveyance at maximum shaft depth with an empty conveyance at bank level. These positions were considered in the calculations that were carried out for the other shaft systems.

Figure 7 presents the two cases considered in this winder system. A loaded ascending conveyance at maximum shaft depth (empty conveyance at bank level) and a loaded descending conveyance at maximum shaft depth are considered (empty conveyance at bank level).
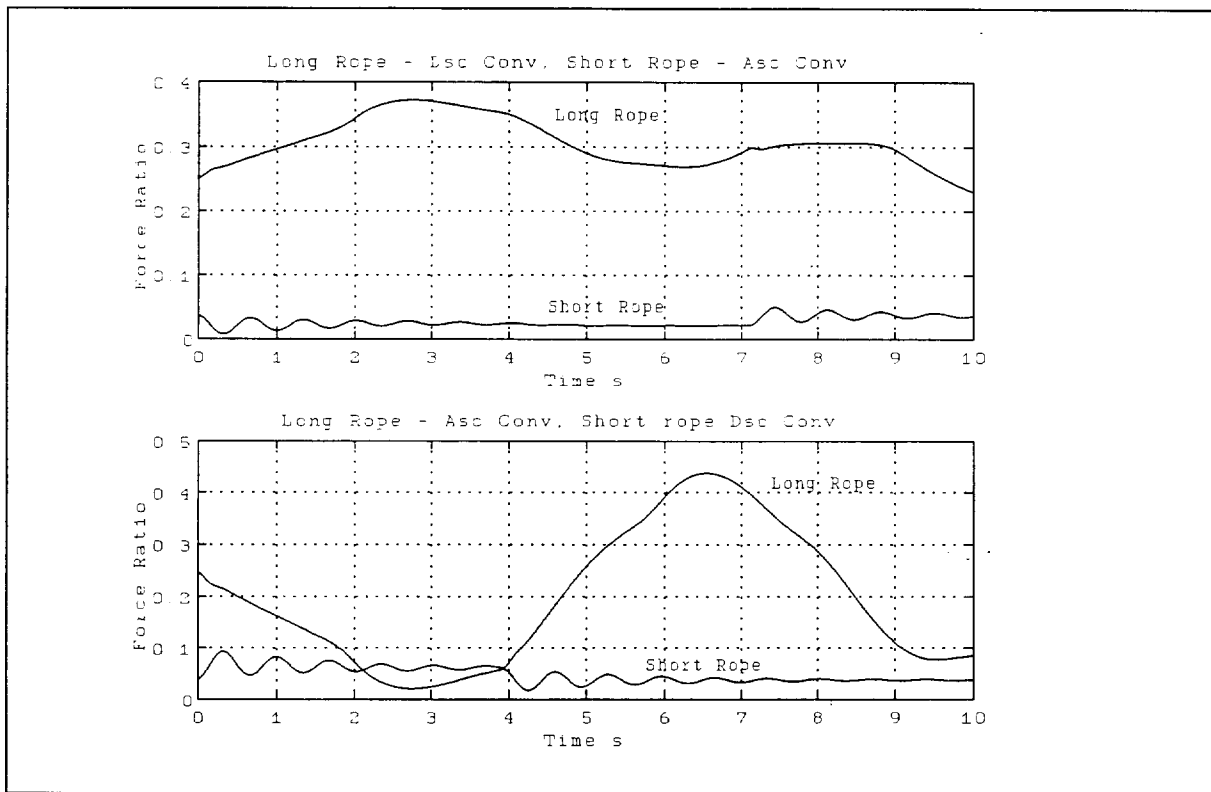
Figure 7   Winder forces in long and short rope, a loaded long rope conveyance and an empty short rope conveyance

When an ascending conveyance is decelerated in the long rope the rope force levels obtained are higher than for the case where a descending conveyance is decelerated in the long rope. The maximum force level of 45 % of rope breaking strength was obtained for the ascending loaded conveyance. Slack rope did not occur in this system.

7.3 System 3

The results obtained for two cases for this winder system are presented in figure 8. Each case considered a loaded conveyance at maximum shaft depth and an empty conveyance at bank level. The first simulation considers a loaded descending conveyance, while the second simulation considers a loaded ascending conveyance.

Figure 8   Winder forces in long and short rope, a loaded long rope conveyance and an empty short rope conveyance

When the loaded ascending conveyance is decelerated, the imbalance force in the system assists the brakes in stopping the winder. This results in a larger winder deceleration. The direction of the deceleration results in an initial decrease in the rope force. When the brakes are released (i.e. after the winder has stopped) the overshoot subsequent to the release of the brakes results in the higher force levels observed. Slack rope did not occur in this simulation.

7.4 System 4

In Figure 9 the forces at the winder for the long and short rope are presented. A fully loaded conveyance was placed at maximum depth and an empty conveyance at minimum depth. In the first case the loaded conveyance was ascending, while in the second case the loaded conveyance was descending. The brakes were applied to retard the motion of the system.
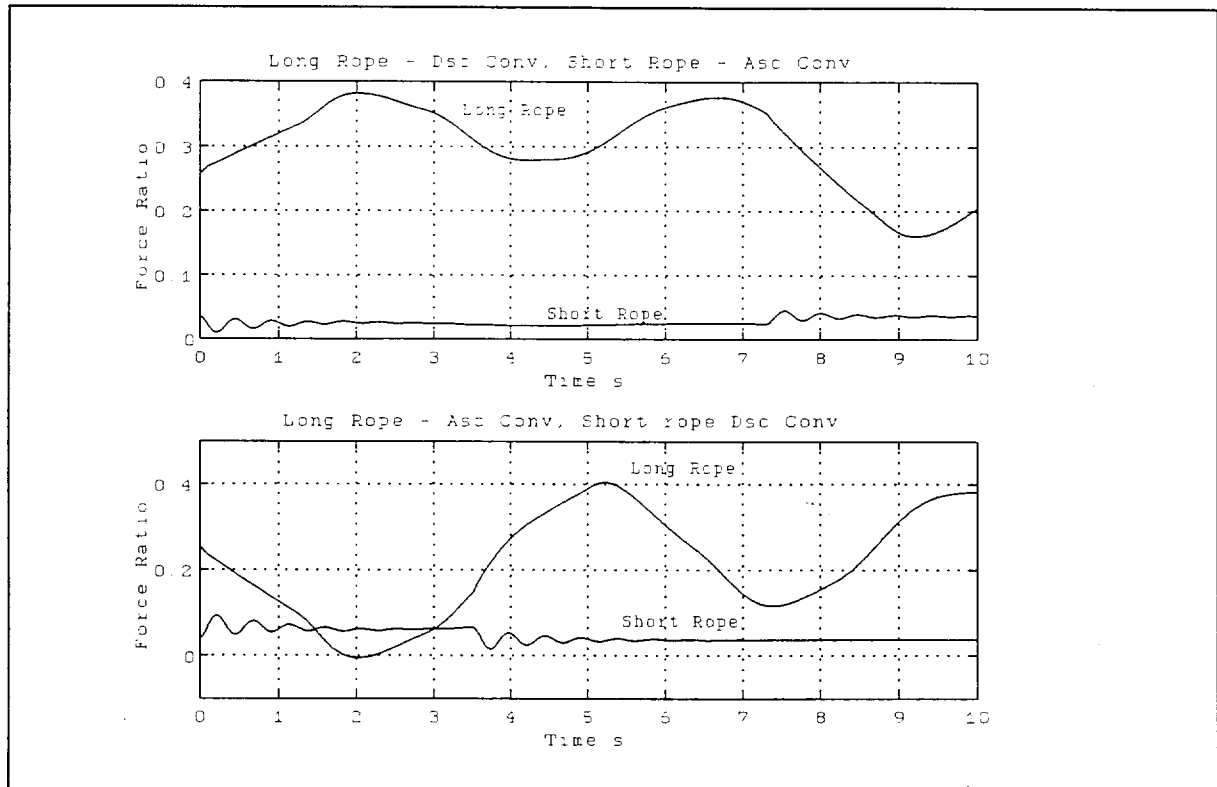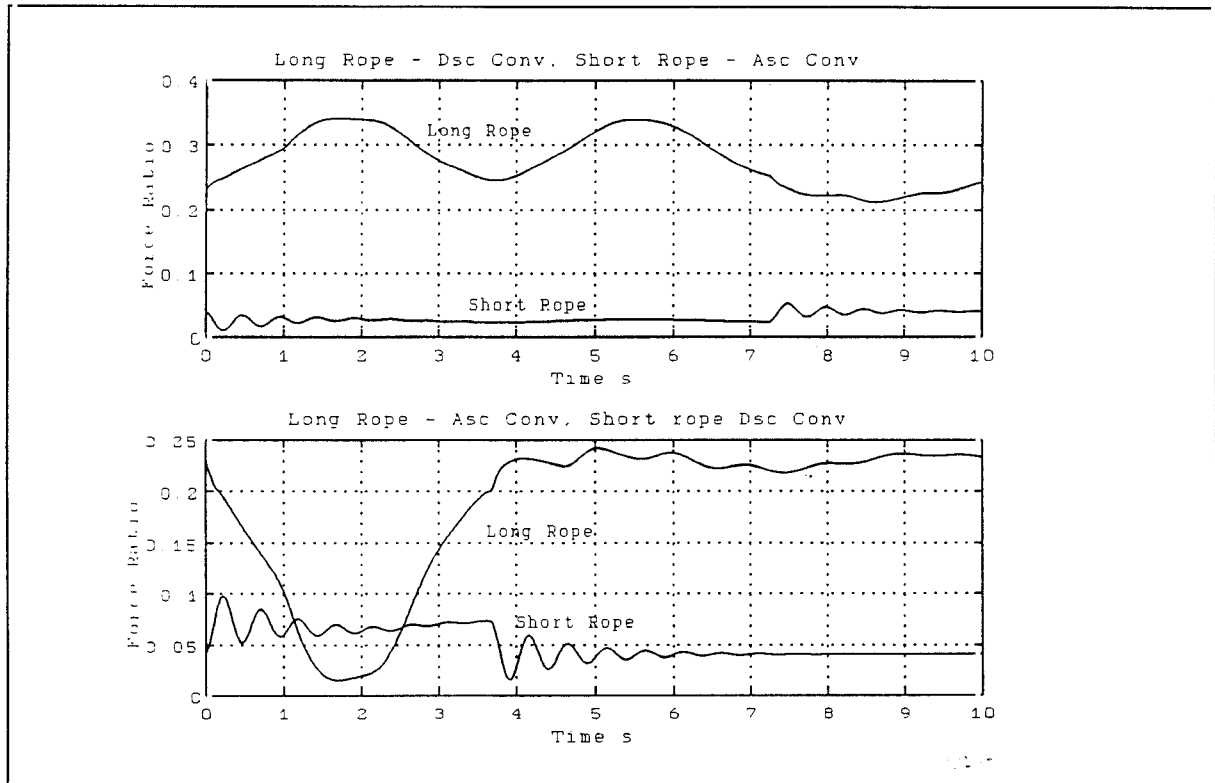

Figure 9   Winder forces in long and short rope, a loaded long rope conveyance and an empty short rope conveyance

It is interesting to note that in this system the maximum force occurs with the loaded conveyance descending at maximum shaft depth. The reason for this is point at which the brakes are released (i.e. when the winder stops). When the winder is stopped (winder acceleration is zero) no appreciable overshoot occurred. A maximum force of 35% rope braking strength occurred in this winder configuration (for a loaded, descending conveyance). Slack rope did not occur in this simulation.

8. SLACK ROPE

Slack rope only occurred in the 4000m system when the imbalance force was assisting the brakes in decelerating the winder. The 4000m design considered in this numerical simulation consisted of a two brake winder. Slack rope would be prevented if the deceleration of the winder was reduced. This could be achieved by reducing the braking effort during emergency braking. If three brakes were used per winder then slack rope would be prevented.

9. CONCLUSIONS

9.1   If the maximum brake torque can be considered a function of the maximum imbalance force in the system then the maximum force obtained in the mine winding rope as a result of a brake control system failure will increase with increasing shaft depth. The maximum force obtained in the deep level system was 60% of the rope breaking strength.

9.2   Slack rope occurred in the 4000m wind after the brake control failure occurred. A slack rope duration of 2 seconds was observed. Slack rope can be prevented by increasing the number of brakes on a winder. The maximum torque applied to the system during brake failure or uncontrolled braking trip-out will then also be reduced.

9.3   A stepped brake profile results in higher rope force levels than the exponential brake profile. Slack rope will also be less severe for the exponential profile.

10. REFERENCES

1. van Zyl, M., *Load Ranges Experienced By Drum Winder Ropes*, CSIR Contract Report (MST(92)MC996), November 1992.

2. van Zyl, M., *Drum Winder Rope Forces Generated By the Occurrence of Slack Rope - A Mathematical Model*, CSIR Contract Report (MST(91)MC867), September 1991.

3. Greenway, M.E., *An Engineering Evaluation of the Limits to Hoisting From Great Depth*, Anglo American Corporation of S.A. Ltd, June 1991.

4. Massey, D.S., *An Initial Investigation into Rope Forces Generated by Flashover Torques*, CSIR Interim Report, May 1994.

5. Constancon, C.P., **THE DYNAMICS OF MINE HOIST CATENARIES**, PhD Thesis, University of the Witwatersrand, 1993.

6. Kroonstuiver, J., *Investigation of forces in a 4000m Mine Winding Rope Resulting From a Flashover/Short Circuit torque*, CSIR Contract report 940192, October 1994.

ROPE FORCE MEASUREMENTS DURING EMERGENCY BRAKING

by

G F K Hecker

CSIR Contract Report No 940190
Job No.: MST(94)MC2208
September 1994

Submitted to:
    The SIMRAC Engineering Advisory Committee

Issued By:
    Mine Hoisting, Metallurgical and Corrosion Services
    Division of Materials Science and Technology
    CSIR
    Private Bag x28, Auckland Park, 2006

    Telephone   (011) 726 7100
    Telefax   (011) 726 6418

Prepared by:

_____
G F K Hecker

Reviewed by:

_____
R A Backeberg

SYNOPSIS

The Working Group drafting the Safety Standard for the Performance, Operation, Maintenance and Testing of Mine Winders (SABS TC 801.19 - WG2) has requested an analysis of rope forces that occur during a trip out with the view to determine whether it is necessary to measure rope forces at the headgear sheave or at the conveyance when the dynamic factor of safety of the rope is being established.

The drum speed traces obtained during brake tests of several winders were used to calculate the dynamic rope forces. Based on these measurements, a simple method was devised with which the dynamic factor could be established.

LIST OF SYMBOLS

a_c conveyance acceleration

F_b back end rope force

F_f front end rope force

F_{stat} static back end rope force

g gravitational acceleration

M_c conveyance mass

M_p payload mass

M_r rope mass

1. INTRODUCTION

The task group members compiling the section on brake specifications in the safety standard for the performance, operation, maintenance and testing of mine winding plant[1] have drafted a section that prescribes the measurement of rope forces to ascertain the dynamic factor of safety of the rope. The question arose whether the forces should be measured at the back end of the rope or whether front end force measurements or conveyance acceleration measurements could be used as well. It was therefore requested to analyse the dynamic rope forces that occur during a trip out with the view to establish which measurements should be prescribed in the safety standard. The analyses that were done are an extension of previous work on dynamic rope forces that occured during brake tests[2].

2. ANALYSIS OF DYNAMIC ROPE FORCES

Most rope force analyses were based on drum speed traces recorded during trip out tests such as the one shown in Figure 1.

Chart Speed: .....25.mm/sec. MIDSHAFT TRIP-OUT   Tripped At: 14.17 m/s
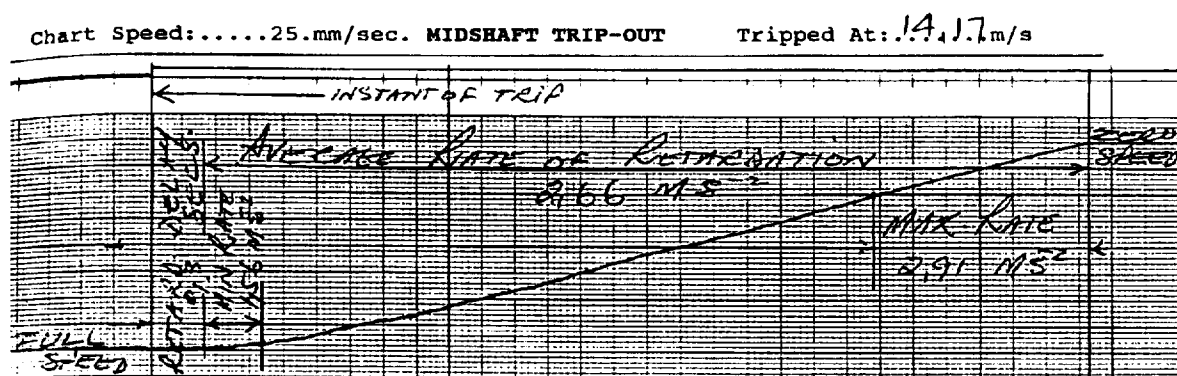
Figure 1:   Example of a speed trace recorded during a trip out test

Traces such as this one were obtained from representatives of mining groups. They were digitized and speed-time histories were generated. In some cases the drum speed was recorded directly onto a computer, providing more detailed and accurate measurements. The speed values, together with the rope properties and conveyance masses, were used to obtain rope force histories. The analyses were done with the aid of a finite difference rope model which ignored the presence of sheaves and catenaries but included a viscous damping model and an incompressible rope which changed in length while winding. This model was used to calculate the forces at the back and front ends of the rope.
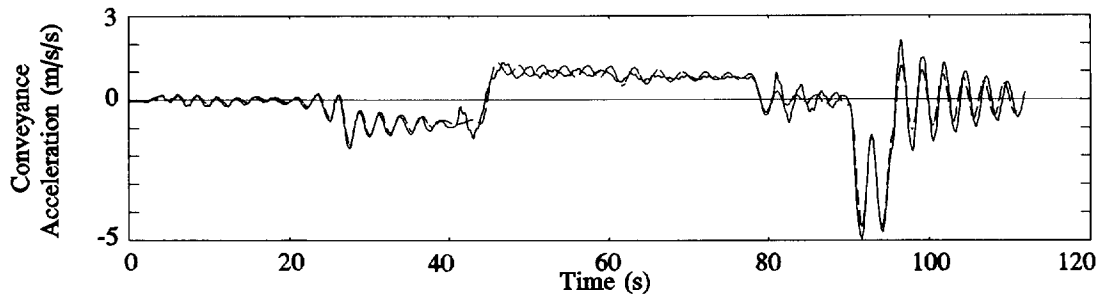
Figure 2: Measured Conveyance Accelerations compared to those obtained by Finite Difference Analysis

The model was validated by comparing the calculated conveyance accelerations with measured accelerations. The drum motion was measured during winding and a trip out and using these measurements as input data to the model. The conveyance accelerations were measured using an accelerometer on the conveyance. Figure 2 shows the conveyance accelerations obtained with the finite difference model as a solid line and those measured on the conveyance as a dashed line.
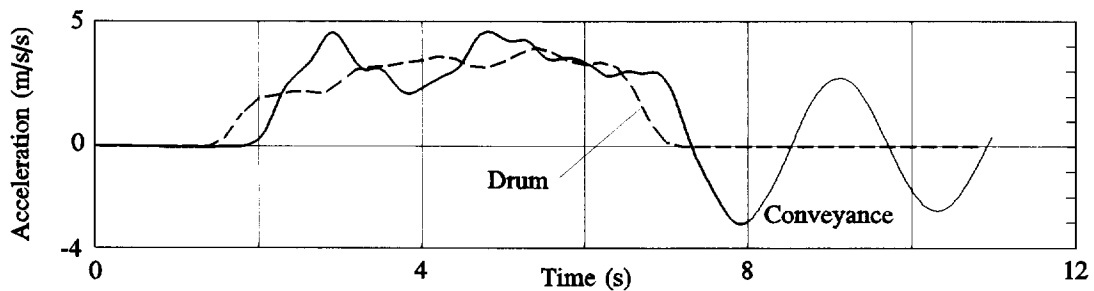
Figure 3: Drum and Conveyance Accelerations

Figure 3 shows the drum accelerations obtained from differentiating the speed profile shown in Figure 1 and the conveyance accelerations calculated with the aid of the finite difference model. The rope forces obtained with the model for this case are shown in Figure 4.
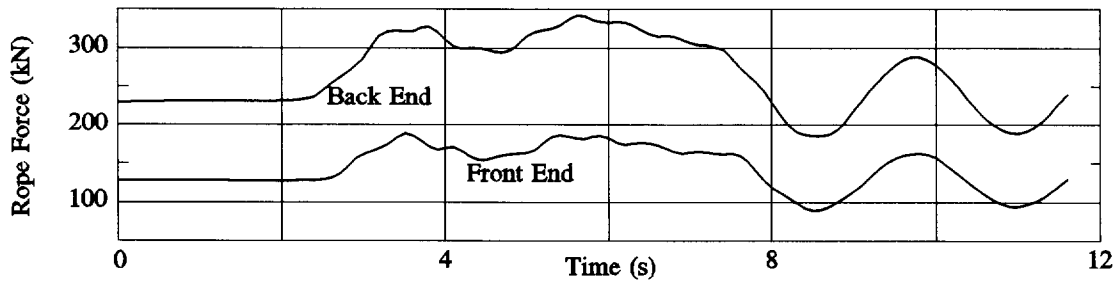
Figure 4: Calculated Rope Forces

3. ESTIMATING BACK END FORCES FROM MEASURED FRONT END FORCES

If one assumes that the rope behaves like a rigid body with the same dynamics as the conveyance, the back end forces can be approximated as

$$F_b \approx F_{stat} \left[1 + \frac{a_c}{g} \right]$$

If the front end rope force is measured instead of the conveyance acceleration, the conveyance acceleration can be calculated as

$$a_c = \frac{F_f}{M_c + M_p} - g$$

It is then possible to estimate the back end rope force as

$$F_b \approx \left(M_r + M_c + M_p \right) \cdot \left(a_c + g \right)$$

$$= \left(M_r + M_c + M_p \right) \cdot \left[\frac{F_f}{M_c + M_p} - g + g \right] \quad \text{from the previous equation}$$

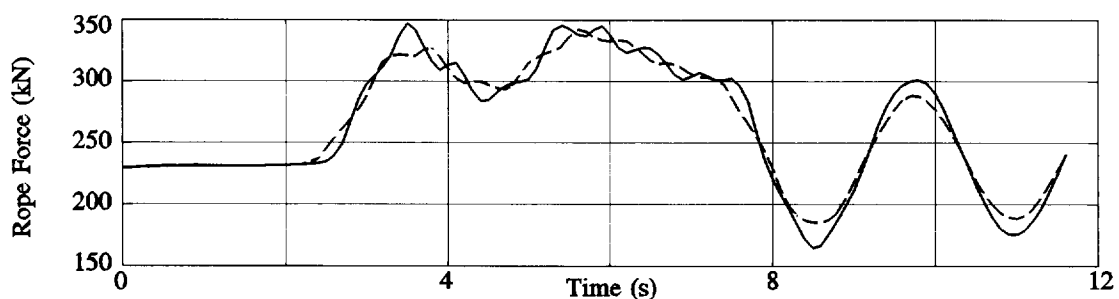$$= F_f \cdot \frac{M_r + M_c + M_p}{M_c + M_p}$$

Figure 5:   Back end Rope Force Approximation

The front end rope force shown in Figure 4 was multiplied by $(M_r + M_c + M_p)/(M_c + M_p)$ to approximate the back end force. The solid line in Figure 5 shows the back end force

obtained by this approximation, compared to the actual* back end force shown by the dashed line. This figure shows that the solid line approximates the dashed line with reasonable accuracy. The static force and the rigid body acceleration forces are, by definition of the preceding equations, reproduced accurately. The forces for higher modes of vibration, even the first fundamental, are higher than the true back end forces because there are longitudinal dynamic strain variations in the rope and these are not taken into account.

The peak conveyance acceleration of 4,71 (see Figure 3) and the static rope force can be used to estimate the dynamic rope force as follows:

$$F_b \approx F_{stat} \left[1 + \frac{a_c}{g} \right]$$

$$= 234 \left[1 + \frac{4,71}{9,8} \right]$$

$$= 346 \text{ kN}$$

The actual back end force for this case was calculated to be 342 kN.

4. TEST CASES

The rope force approximation described in the previous section was done for all the winders where speed-time traces could be located. The purpose of the investigation was to verify that the peak back end rope force could be approximated from the peak front end rope force or from the peak conveyance acceleration. Therefore only the peak rope forces are tabled and not the entire set of results.

The term $(1 + a_c/g)$ is an approximation of the dynamic amplification factor, i.e. the factor by which the dynamic rope force is larger than the static rope force. The actual dynamic amplification factor, on the other hand, is the ratio between the peak dynamic and the static back end rope forces as determined by measurement or detailed modelling. The accuracy of the approximation was verified by comparing the approximated dynamic amplification factor with the actual one.

---

* In this report the term *actual back end forces* is used for the back end forces obtained with the finite difference model.

Figure 6 shows a comparison between the estimated and the actual dynamic amplification factors for the cases analysed. In all cases the estimated rope forces were higher than the actual forces.

This leads to a conservative approximation of the dynamic factor. If the dynamic factor is calculated using the approximation, it will be slightly lower than the actual dynamic factor. In other words: If the approximated dynamic factor complies with that specified in the code of practice, then the actual dynamic factor is higher.
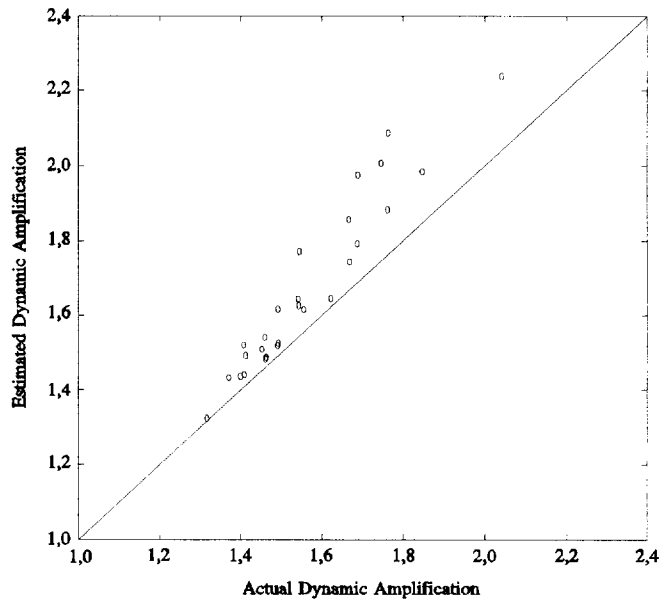
Figure 6: Comparison between estimated and actual dynamic amplification

Figure 7 shows how the accuracy of the approximated dynamic factor varies with peak conveyance acceleration. Where small conveyance accelerations occur, as will be the requirement for many winders to conform with the code of practice, high accuracies are being obtained. Where higher accelerations occur, the level of higher modes of vibrations in the rope will be larger, leading to larger approximation errors.
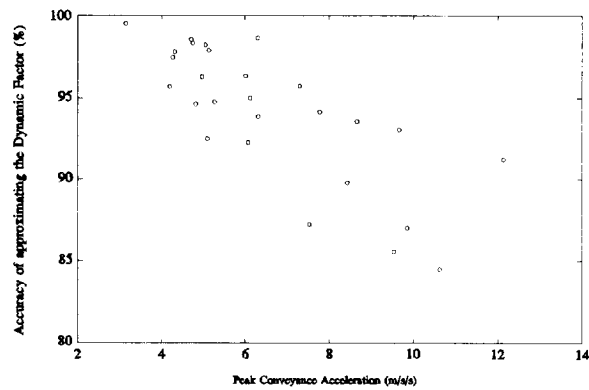
Figure 7: Accuracy of approximating the dynamic factor as a function of peak conveyance acceleration

5. CONCLUSIONS

- From this brief study it can be concluded that the peak back end rope forces that occur during emergency braking can be estimated from front end rope force measurements or from conveyance acceleration measurements.

- The accuracy of the estimated back end forces is within a few percent when the peak accelerations are low.

- With higher accelerations the estimate becomes less accurate. The final result, however, is conservative because the actual dynamic forces are lower than the estimated ones.

REFERENCES

1. *CODE OF PRACTICE: PERFORMANCE, OPERATION, MAINTENANCE AND TESTING OF MINE WINDING PLANT* Draft document prepared for the SABS Working Group TC 801.19 - WG2

2. Hecker, G.F.K. *Rope Forces during Dynamic Brake Tests* CSIR Conttract Reoirt MST(92)MC1220, July 1992

INVESTIGATION OF FORCES IN A 4000m
MINE WINDING ROPE RESULTING
FROM A FLASHOVER/SHORT CIRCUIT.

by

J. Kroonstuiver
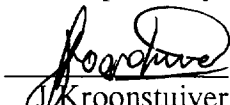
Submitted to:
    The SIMRAC Engineering Advisory Committee

Issued By:
    Mine Hoisting, Metallurgical and Corrosion Services
    Division of Materials Science and Technology
    CSIR
    Private Bag x28, Auckland Park, 2006

    Telephone   (011) 726 7100
    Telefax   (011) 726 6418

Prepared by:

J. Kroonstuiver

Reviewed by:

R. A. Backeberg

SUMMARY

This report presents the findings of a numerical study into the investigation of flashover torque in a hypothetical deep winding application. The objectives of this study were to determine the maximum forces in the ropes and the dynamic response of a deep level mine winding system. A numerical model defined in the MATLAB/SIMULINK environment was used to simulate the mine winding system.

Slack rope could occur in the short rope (conveyance close to bank) for the impulse durations considered. It was found that slack rope of duration 0,44s could occur. During this time the amount of rope that went slack was 0,252m. The maximum force in the rope after slack rope was 30% of the rope breaking strength.

At 200ms 40% of the rope breaking strength was achieved in the ropes of the hypothetical 4000m winding system. Further simulations would have to be carried out to determine the allowable short circuit torque duration for other winder configurations.

CONTENTS

LIST OF FIGURES

1. INTRODUCTION

The SABS working group on the Code of Practice for the Performance, Operation, Maintenance and Testing of Winding Plant (SABS TC 801.19 - WG2) has requested an analysis of the dynamic rope forces resulting from a winder motor short circuit torque.

The purpose of this analysis is to determine whether it is necessary to prescribe a maximum allowable short circuit torque in the code of practice. This report describes a numerical analysis of the dynamic response of a hypothetical winder system to the occurrence of a short circuit torque. The force levels in the ropes, and the dynamic response of the system to a short circuit event were investigated. The following features of the system response were considered important and were determined for the 4000m winder:

a).   The maximum force occurring in the rope.

b).   The severity of slack rope.

c).   The short circuit torque duration required to achieve 40% (to ensure a dynamic factor of 2,5) of the rope breaking strength.

2. MODEL DEFINITION

A discrete numerical model was defined using the MATLAB package (version 4.2b) in conjunction with the SIMULINK dynamic systems simulation software (version 1.3a). Figure 1 shows a schematic illustration of the discrete model. The lumped masses numbered M1 to M4 represent: The ascending conveyance mass; Sheave inertia on ascending side; Winder inertia; Sheave inertia on descending side and descending conveyance mass respectively. The ascending rope could be the overlay or the underlay rope. The winder and sheave inertias were transformed to the linear plane. The torque applied at the winder was converted to a force. Velocities, accelerations and displacements were considered positive towards the right of the diagram. The rope segments numbered L1 to L4 represent the different segments in the winding system: From ascending conveyance to sheave; From sheave to drum (ascending side catenary); From drum to sheave (descending side catenary) and from sheave to descending conveyance respectively.

Each of the rope segments was subdivided into a discrete number of elements. The segments were only allowed a single degree of freedom, lateral motion was not allowed. The equations of motion were defined for each element and combined into a matrix. The impulse torque function was applied to the lumped mass representing the winder. The torque was converted to a linear force which was applied at the winder.
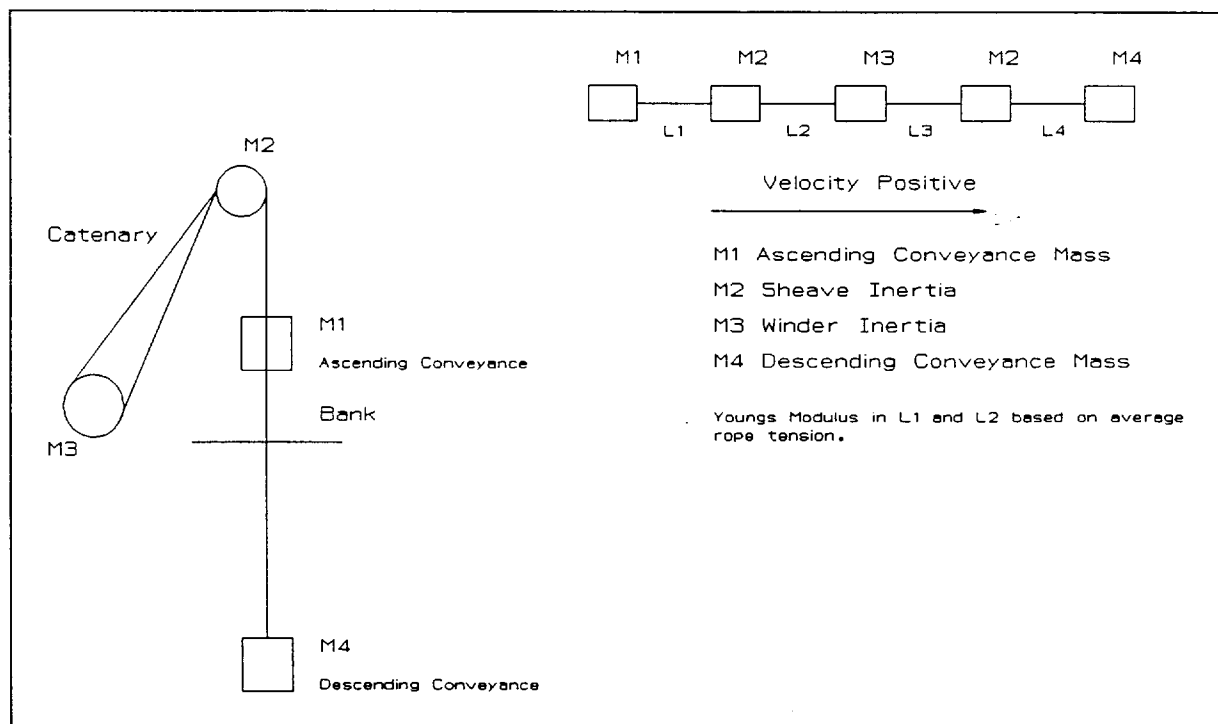
Figure 1   Lumped parameter model of mine winding system.

Rope stiffness was defined as a continuous function. The rope was allowed to withstand compression. It was assumed that compressive forces would be of short duration (high frequency), and have a small effect on the winder motion.

3. PARAMETERS

Maximum rope forces were determined by varying the position and the mass of the conveyances. The parameters listed in the table were used in the simulations. These parameters present a hypothetical deep level (4000m) BMR winder system.

HYPOTHETICAL SHAFT SYSTEM	
SYSTEM PARAMETERS	2 Ropes per conveyance
Shaft Depth (m)	4 000
Safety Factor	3,13
Rope Diameter (mm)	64
Rope Area (mm^2)	3 743
Rope Mass per metre (kg/m)	34
Rope Breaking Strength (kN)	6 000
Winder Inertia (kg•m^2)	18 670 000
Winder Diameter (m)	8,50
Sheave Inertia (kg•m^2)	200 000
Sheave Diameter (m)	8,50
Conveyance Mass (kg)	20 000
Payload Mass (kg)	40 000
Youngs Modulus (GPa)	110 000
Flashover Torque (MNm)	22
Damping Factor (s)	0,0135
Flashover Duration (ms)	200
Bank to Head sheave (m)	30
Catenary Length (m)	70

The winder parameters in the table were calculated using the proposed regulations as outlined by Hecker [5]. The damping factor used was derived using the formulation by van Zyl [11].

4. RESULTS

Loading conditions and in shaft conveyance positions resulting in maximum rope forces were determined. Case 1 presents the highest loading condition (40% rope breaking strength) while case 2 presents the worst slack rope condition for this system (highest compressive forces).

4.1 Case 1:

Fully loaded descending conveyance at 4000m.
Empty ascending conveyance at 30m (distance between skip and head sheave).

This position, conveyance loading configuration and direction of travel yielded the largest tensile forces in the long rope. The maximum force in the long rope was 2,4 MN. This was 40% of the rope breaking strength (at an impulse duration of 200ms). Slack rope can be identified as a negative resultant force (compressive force) in the rope. Figure 2 illustrates the loading condition in the rope on the ascending and descending side of the winder. Slack rope is evident in the short rope, while a force of 40% the rope breaking strength occurs in the long rope.
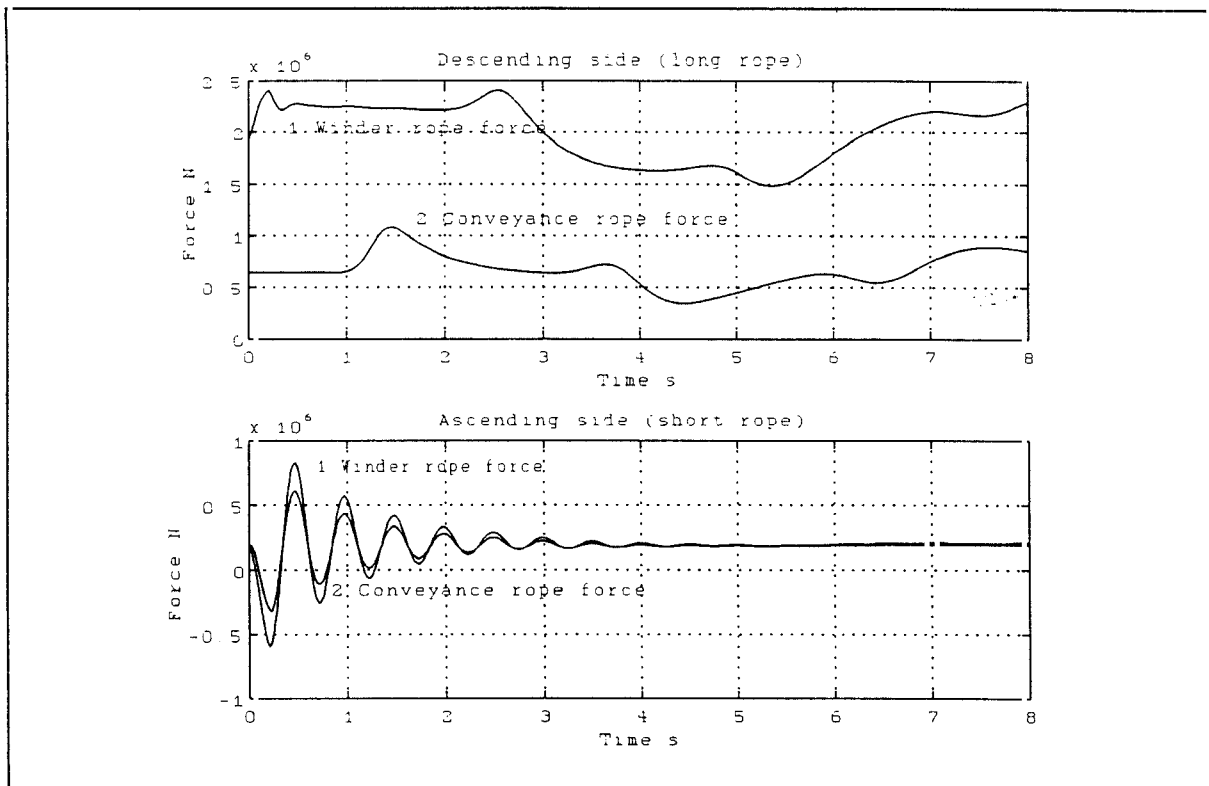
Figure 2   Forces obtained in the long and short rope at the winder and conveyance.

The rope forces on either side of the head sheave are shown in figure 3. The rope forces on the catenary side are greater in magnitude than the forces on the conveyance side.
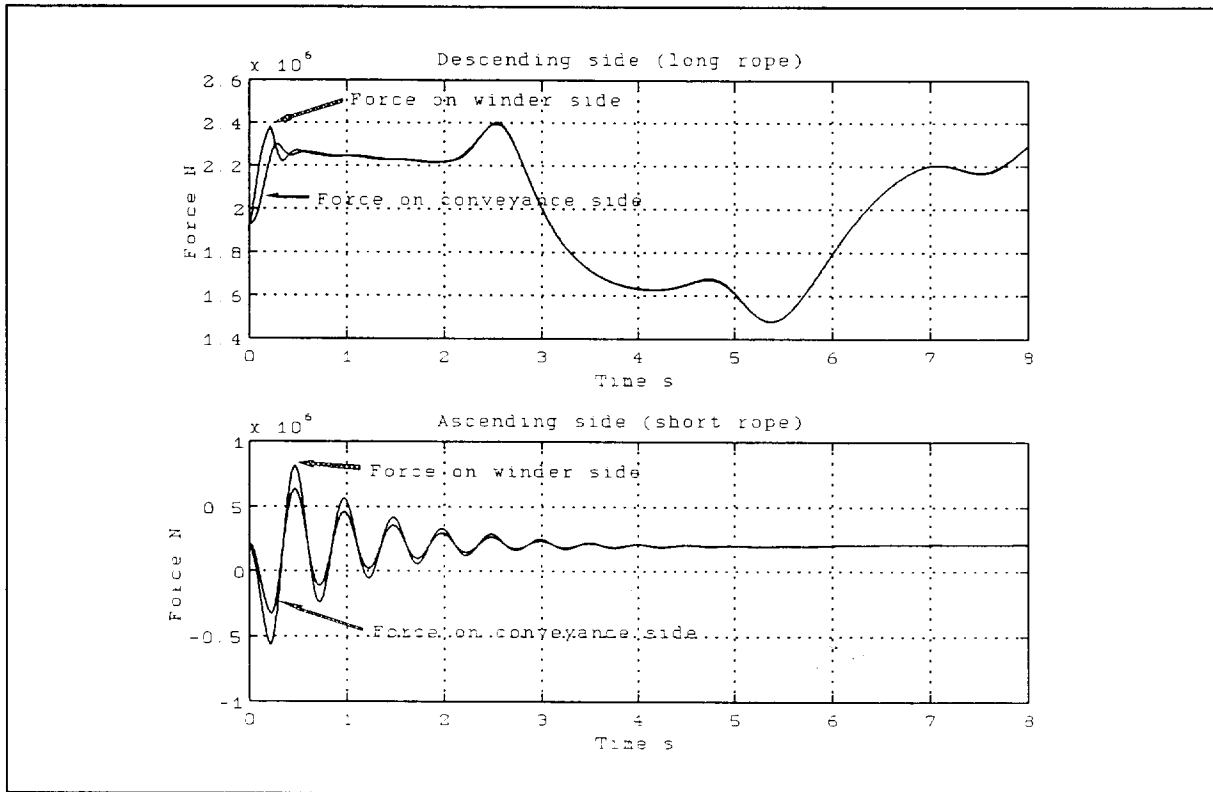
Figure 3   Forces before and after the sheave wheel at the long and short rope.

Figure 4 shows the acceleration of the drum and conveyance on the short rope and the velocity of the drum and both conveyances. Winder acceleration subsequent to the impulse duration is small. The dynamic forces in the short rope do not have an appreciable effect on the motion of the winder drum. The velocity of the drum, ascending (short rope) and descending conveyances (long rope) are compared in figure 4. The drum motion is out of phase with the motion of the long rope conveyance.
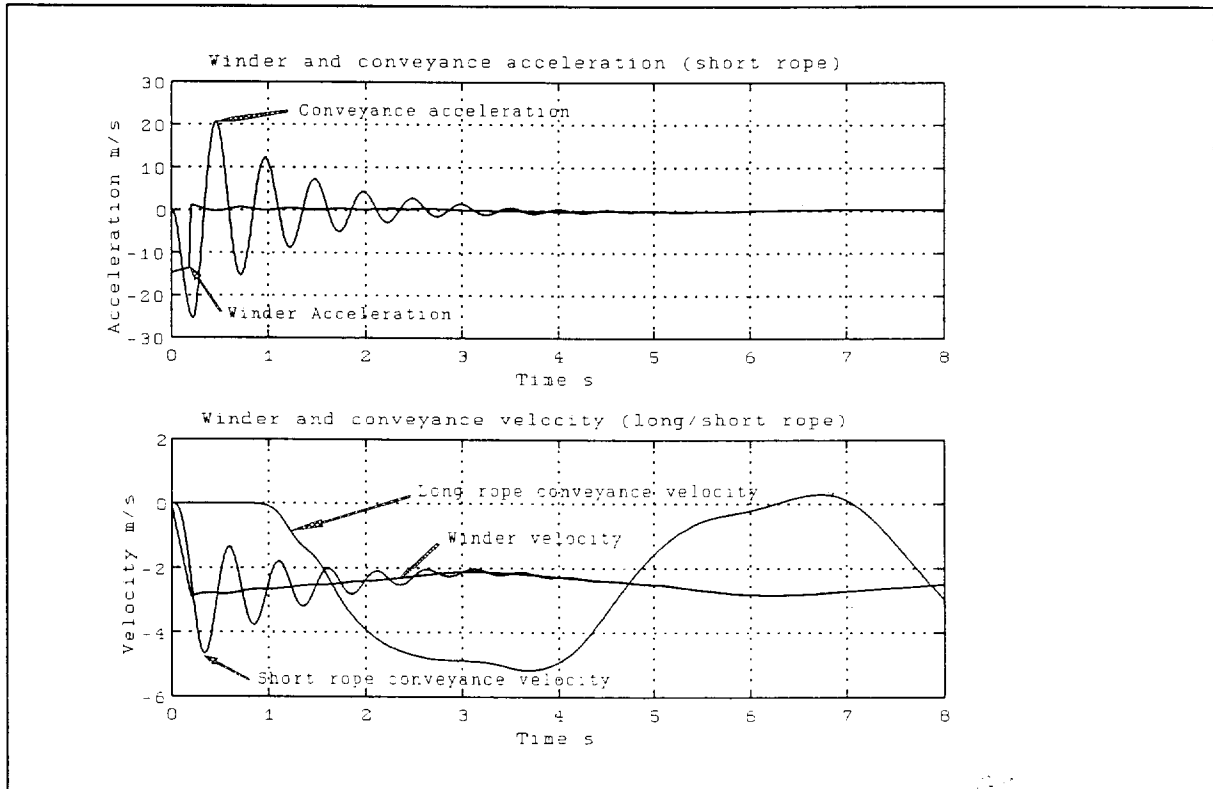
Figure 4   Velocity and acceleration vs time for the winder and conveyances.

4.2 Case 2

The parameters of the numerical model were changed until the worst case slack rope condition was identified. This position was found to be the following:

Fully loaded ascending conveyance at bank level (100m rope length between conveyance and winder). Empty descending conveyance at 4000m (4100m rope length between winder and conveyance).

Figure 5 illustrates the forces obtained for the slack rope case. The catenary side, of the short rope, exhibits higher compressive forces than the conveyance side, indicating that slack rope will first be evident in the catenary.
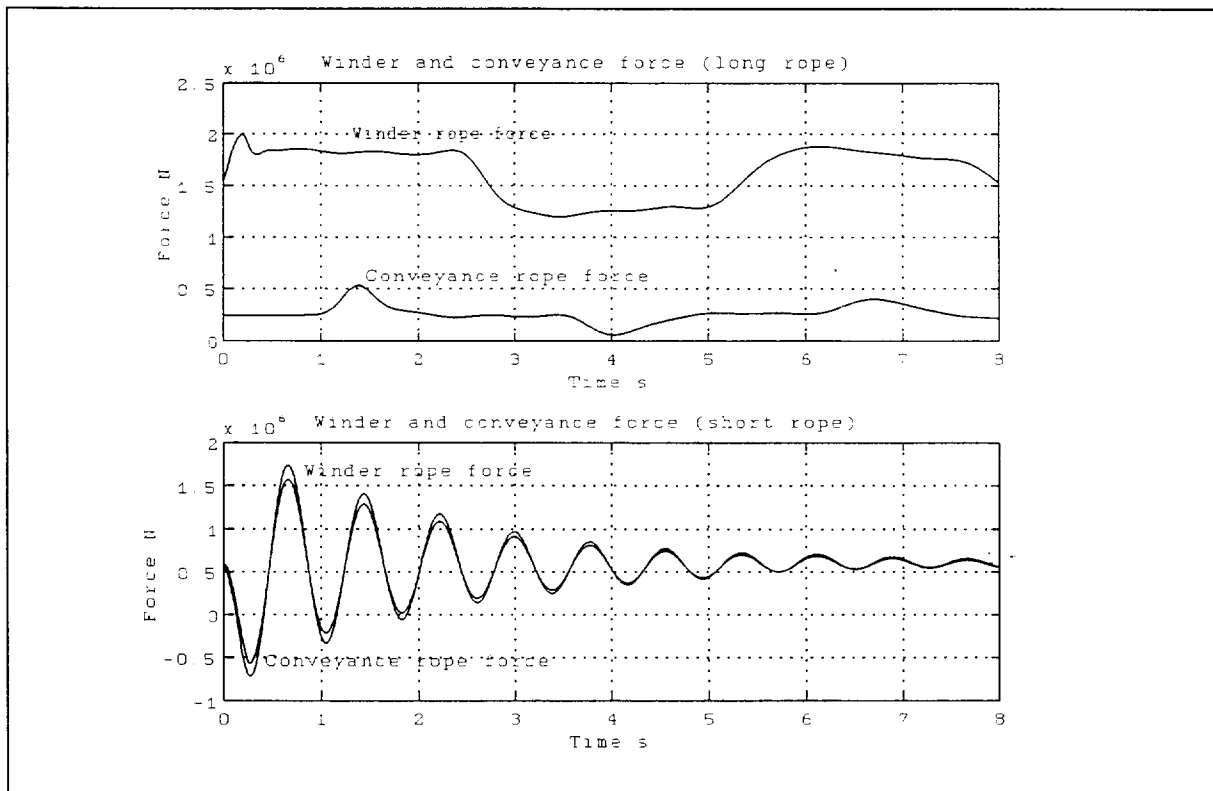
Figure 5   Forces obtained in the long and short rope at the winder and the conveyance.

5. FACTORS AFFECTING ROPE FORCES

5.1 Effect of Damping model.

The maximum force, and severity of slack rope was dependent on the damping model. The viscous/proportional damping model was seen to reduce the effect of the higher frequencies more quickly than the non-proportional modal damping model (based on 3% of critical damping). Constancon [1] found that the damping factor (ζ) did not increase in proportion to the modal frequency but maintained a constant value of about 3%. His findings were based on drop tests carried out at Elandsrand Gold Mine.

In the viscous proportional damping model the damping was defined as $[C] = 0.0135[K]$. Where [C] is the viscous damping matrix and 0.0135 the proportional damping coefficient (van Zyl [11]). The stiffness matrix [K] was based on discrete element rope stiffnesses.

For the modal damping model the damping was defined using the following transformation:

$$2 * [\zeta_r][\omega_r] = \frac{[\phi]^T[C][\phi]}{[\phi]^T[M][\phi]}$$

Where [ζ_r] is the diagonal damping factor matrix, [ω_r] is the diagonal natural frequency matrix, [C] is the damping matrix, [M] is the mass matrix, and [ϕ] and [ϕ]^T are the undamped mode shape matrix and mode shape matrix transposed respectively. A damping factor (ζ) of 3% was used throughout all comparative simulations.

Figure 6 compares forces obtained in the long rope at the winder using the different damping models. Forces shown were obtained with an empty, descending conveyance at a depth of 4000m. Choice of damping model becomes apparent after 200ms (i.e. after the torque pulse). The higher frequencies in the proportional model decay more rapidly than the same frequencies in the non proportional model. The maximum force obtained in the system (in this case) remains largely unaffected by the choice of damping model.
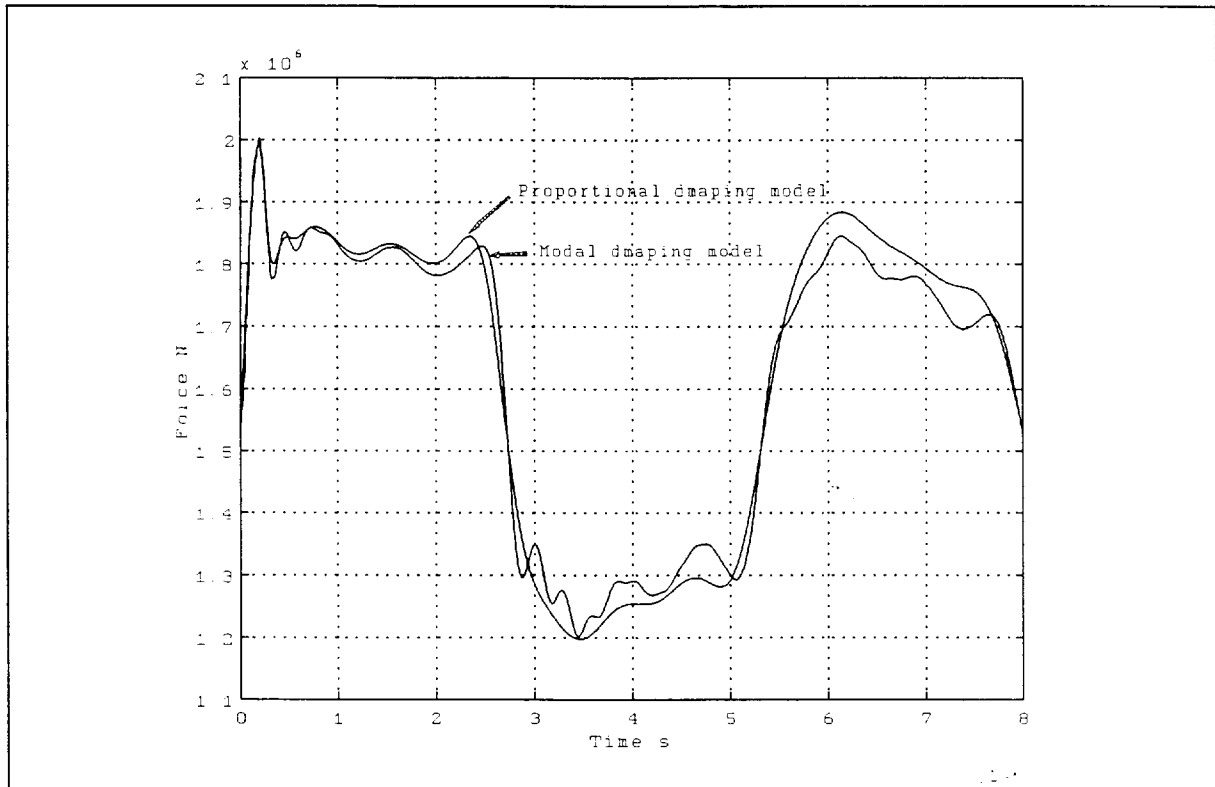
Figure 6   Comparison between Proportional and Modal damping models.

5.2 Effect of damping coefficient.

In figure 7 a comparison is made between simulations using different damping coefficients. The viscous proportional damping model was used in this comparison. Forces at the winder for a rope length of 4000m and an empty, descending conveyance are shown. The peak rope force remains unaffected when increasing the damping coefficient. Plots 1 to 4 were obtained by using damping coefficients 0.0135, 0.027, 0.0405 and 0.054 respectively.
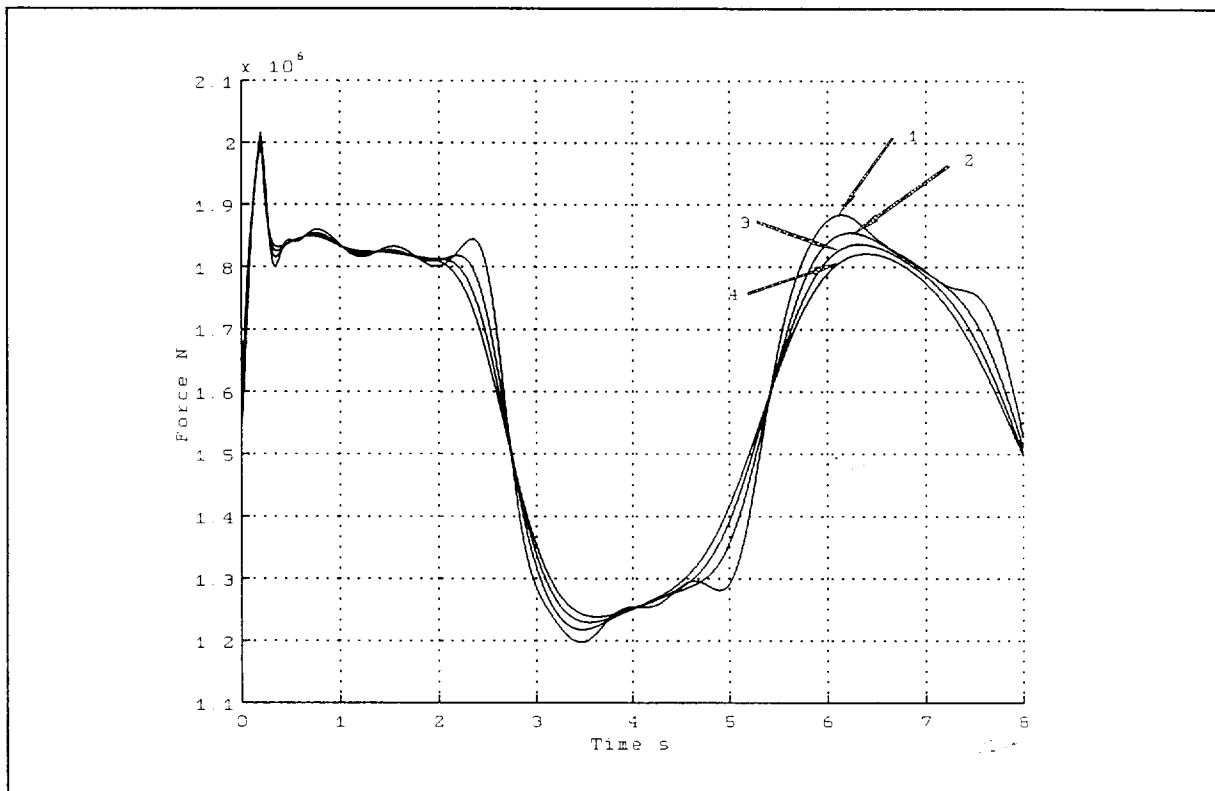
Figure 7   Effect of damping coefficient on rope forces.

5.3 Effect of Impulse Duration.

In figure 8 the duration of the torque pulse for the general viscous proportional damping model was increased. Plots 1 to 4 show the rope forces resulting from impulse durations 400ms, 200ms, 100ms and 50ms respectively. As the impulse duration is increased the dynamic forces in the rope are increased. The increase in dynamic rope force will be evident until the duration of the impulse exceeds 1/4 of the first natural period of the system. In this simulation an empty, descending conveyance was placed at a depth of 4000m. The forces illustrated are those calculated at the winder in the long rope.
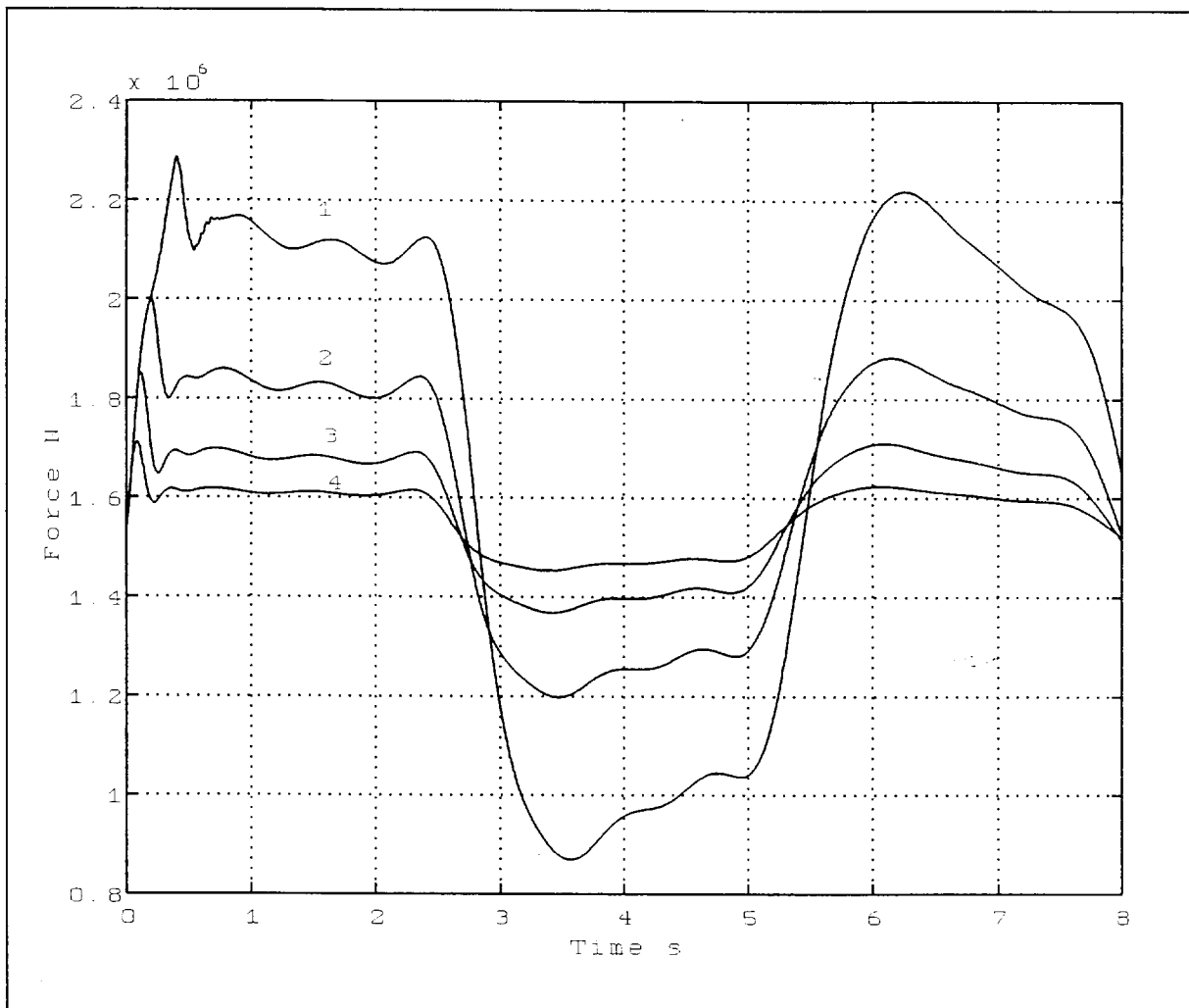
Figure 8   Effect of impulse duration on rope forces.

5.4 Effect of conveyance position in shaft on rope force levels.

The static force in the rope is a function of the position of the conveyance in the shaft. The static force in the rope at the winder will increase as the conveyance is placed at greater shaft depths. The dynamic characteristics of the rope/winder system changes as the conveyance position in the shaft is varied. The first natural frequency of the system decreases as conveyance moves deeper down the shaft. The dynamic response of the winder/conveyance system to impulse torques applied at the winder changes with the conveyance at different positions in the shaft.

A loaded descending conveyance was placed at different positions in the shaft. An impulse of duration 200ms was applied to the system and the resultant forces calculated. Numbered 1 to 6 the positions were 4000m, 3200m, 2400m, 1600m, 1200m and 800m respectively. The plots illustrated on figure 9 show the dynamic forces at the winder after a short circuit torque.
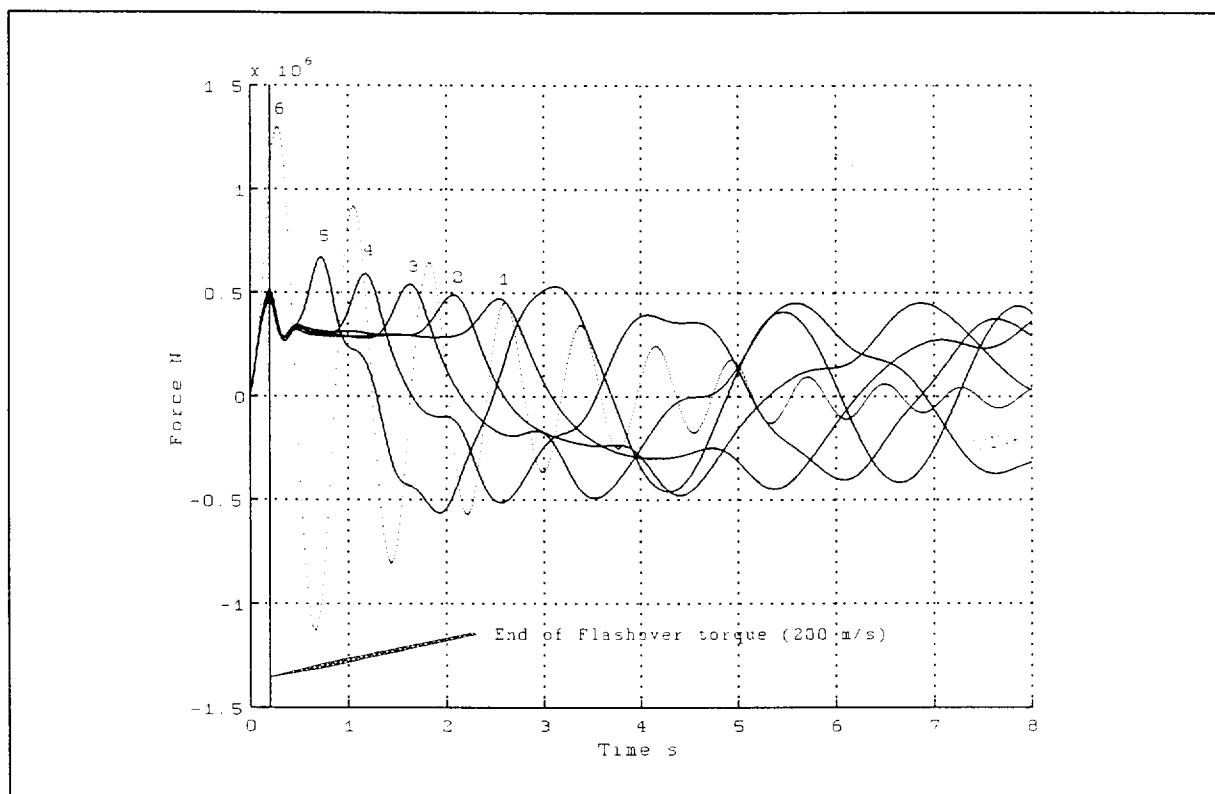
Figure 9　　　Dynamic forces in the long rope as a function of shaft depth.

The magnitude of the reflected wave (indicated by 1 to 5) on figure 9 can be seen to increase with decreasing shaft depth. The increase in dynamic response is a result of the change in the dynamic characteristics of the system. When 1/4 of the first natural frequency of the system is less than 200m/s (the applied impulse duration) the resulting waveform in the rope will have the shape of plot 6 on figure 9.

Although the dynamic forces in the system increased with decreasing shaft depth the total force in the rope (i.e. the sum of static and dynamic forces) decreased with decreasing shaft depth. In figure 10 below the rope static forces are added to the dynamic forces of figure 9. Plots 1 to 5 were obtained for a loaded, descending conveyance at positions 4000m, 3200m, 2400m, 1600m, 1200m, and 800m respectively. Forces at the winder are presented. A flashover torque of 200m/s was applied to the winder. In figure 9 the maximum force obtained at the winder was 1,4MN (dynamic) when the conveyance was at bank level. In figure 10 the maximum force obtained was 2,4MN when the conveyance was at maximum shaft depth.
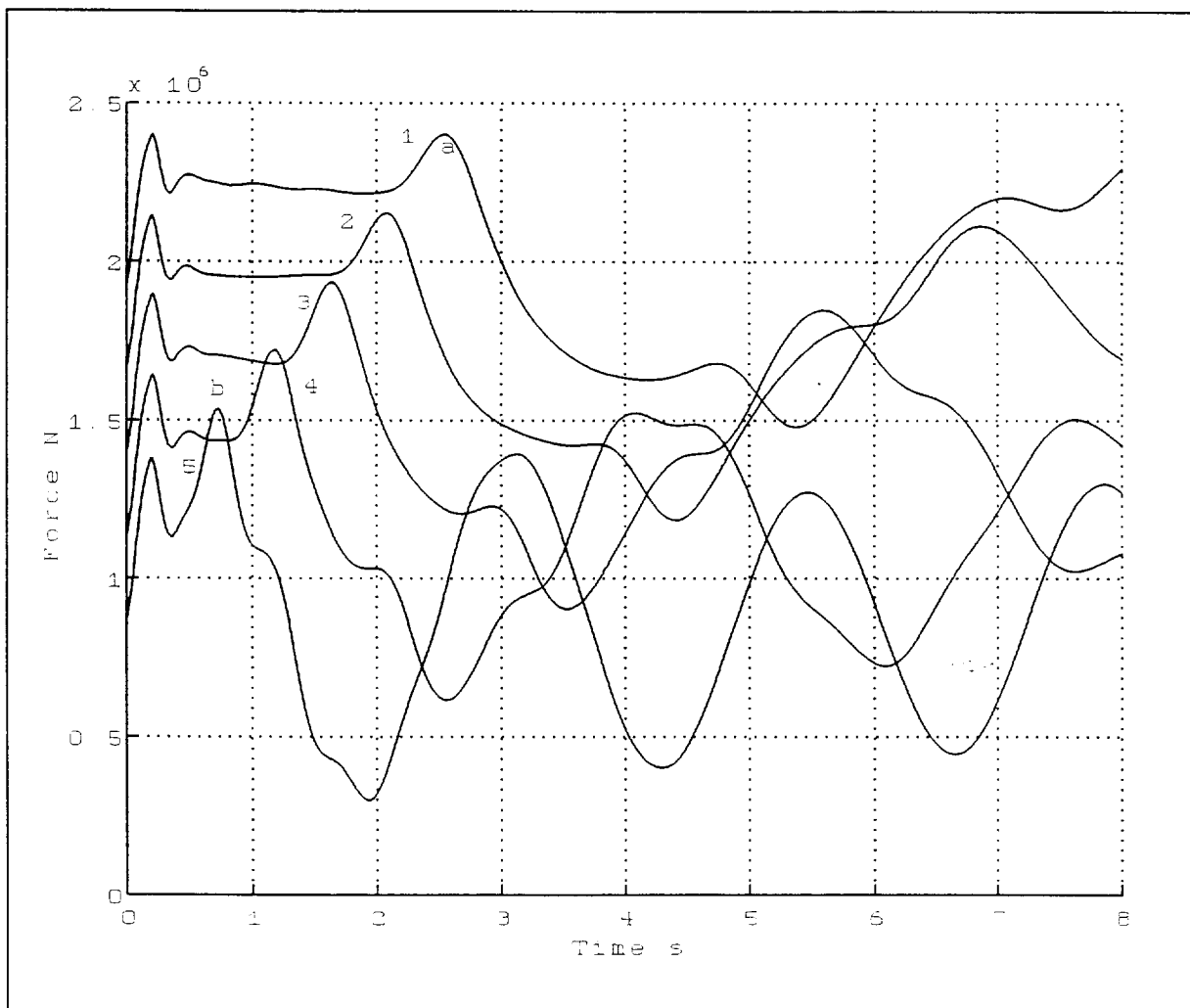
Figure 10   Rope force as a function of conveyance position in shaft.

5.5 Effect of including a Sheave in the model.

Figure 10 illustrates the effect of including the sheave in the simulation. The forces at the winder on the long rope side are plotted. A system including a sheave wheel inertia is compared to a system excluding a sheave wheel inertia. An empty conveyance was placed at 4000m. Plot 1 shows the force level in a rope system including a sheave wheel while plot 2 excludes the sheave wheel. The vertical line indicates the end of the impulse (200m/s).

When comparing plots 1 and 2 the effect of the sheave can clearly be seen. During the impulse the forces in the catenary were higher when including the sheave in the simulation. Subsequent to the impulse (i.e. after 200ms) the forces obtained were very similar for both the sheave or no sheave case. The sheave increases the stiffness of the rope seen by the winder, resulting in the higher initial force.
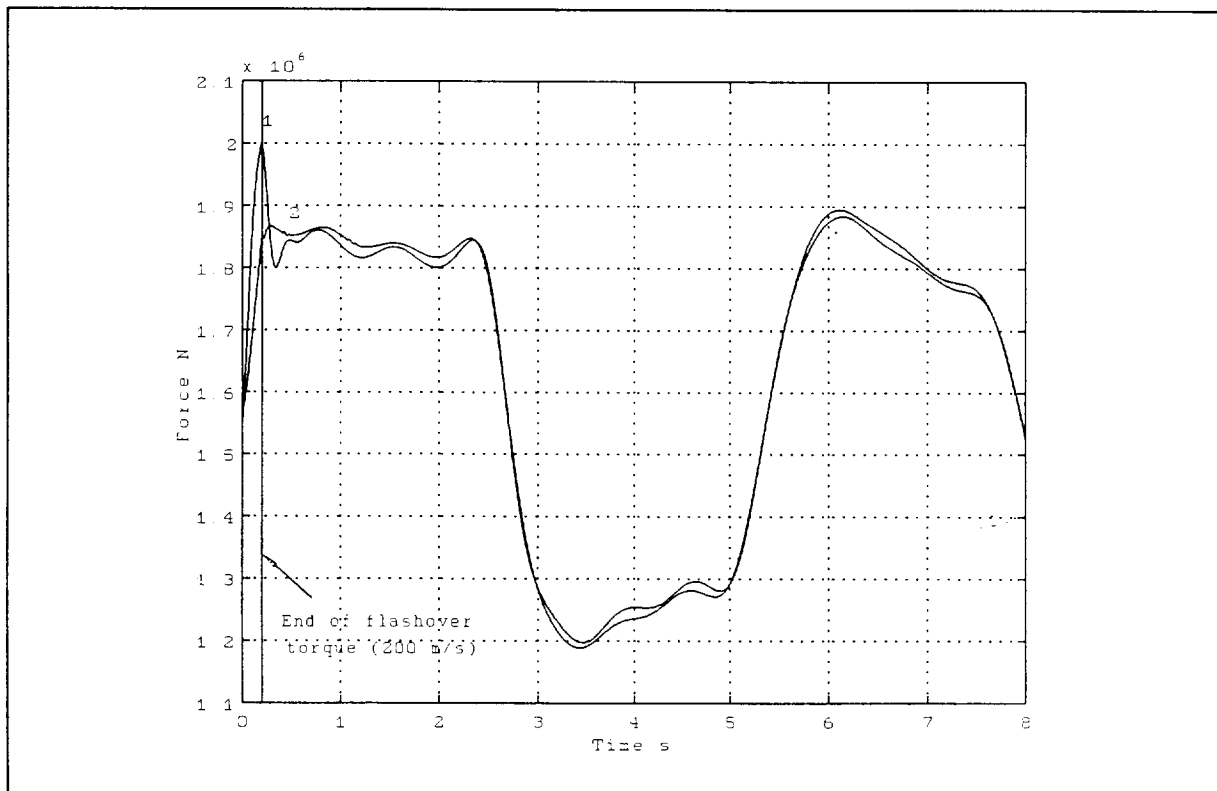
Figure 11   Comparison between simulation including and excluding sheave inertia.

5.6 Effect of shape of impulse torque function.

The shape of the impulse wave form was altered to investigate its effect on force levels in the system. In figure 12 an empty, descending conveyance, at 4000m was considered. The impulse values were kept constant while varying the shape of the function. Plot 1 shows the response with a descending ramp, plot 2 with an ascending ramp and plot 3 with a square wave. The impulse duration was kept at 200ms while the shape of the function was altered.
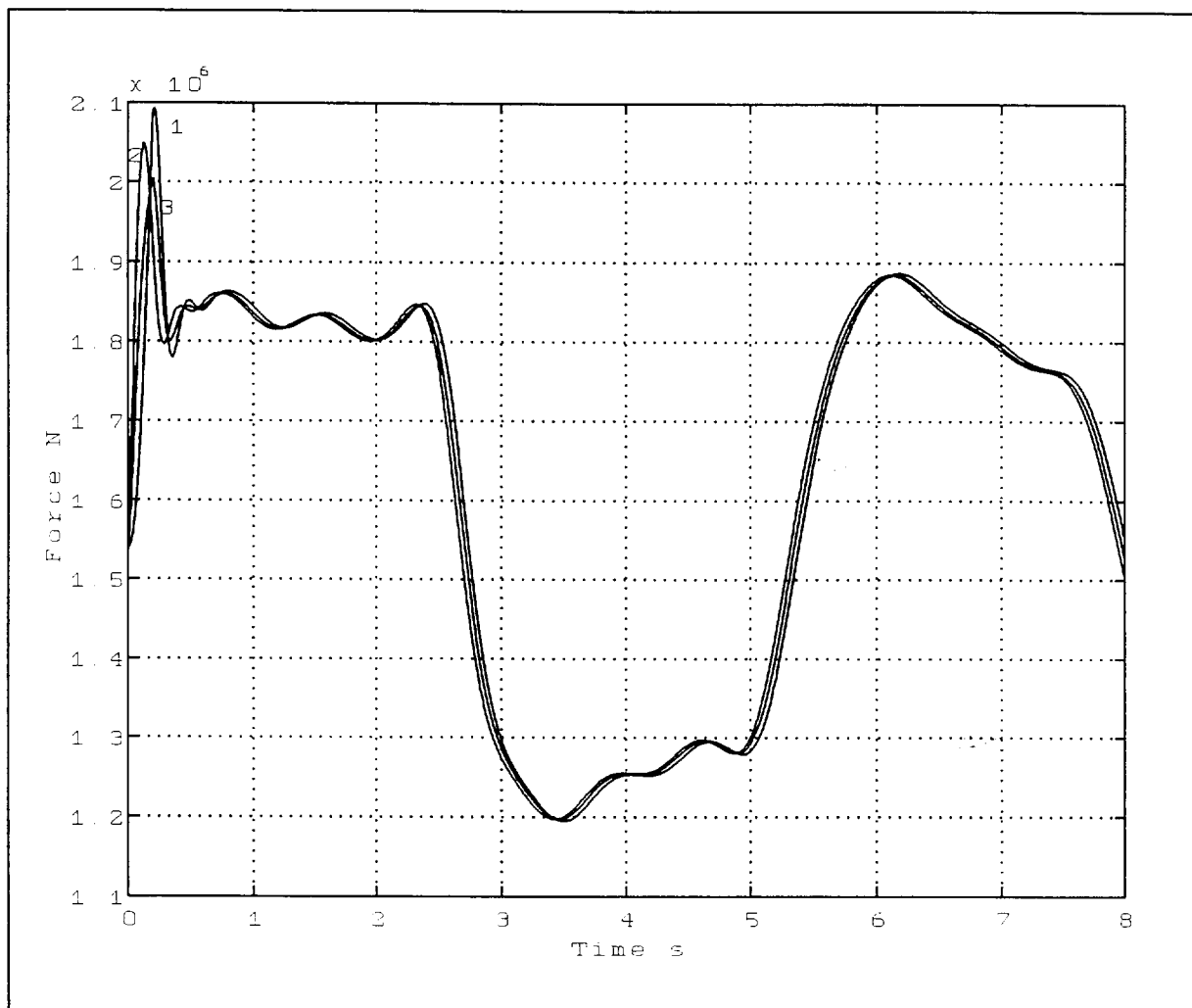
Figure 12   Comparison between different impulse functions.

It is clear that the maximum force in the rope at the winder remains largely unaffected by varying the impulse shape. The force decreases slightly from descending ramp to ascending ramp to square wave. The forces are nearly identical for the three impulse shapes considered.

In figure 13 the impulse time was varied and the torque magnitude was changed to maintain a constant impulse magnitude. The impulse was maintained as a square wave. Plot 1 for a 100ms impulse, plot 2 for a 200ms impulse and plot 3 for a 400ms impulse.
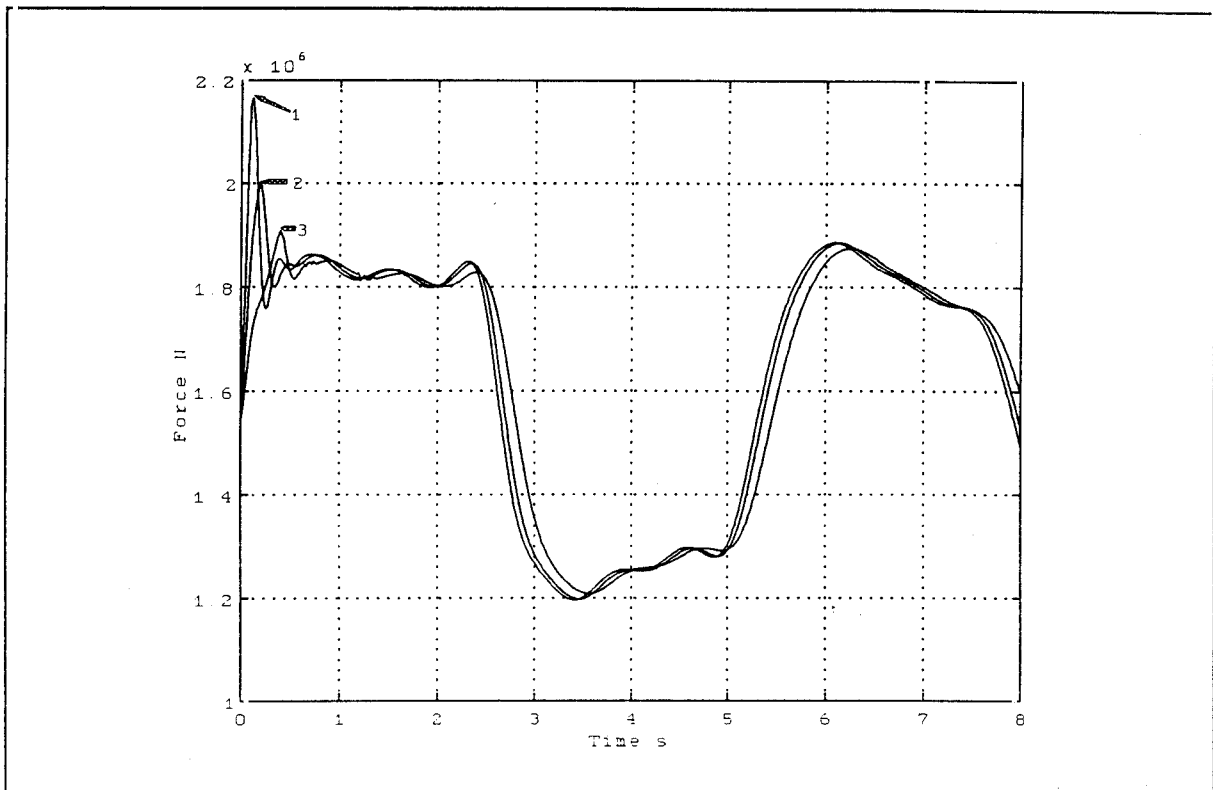
Figure 13   Force in the long rope for a changing impulse duration.

Even though the energy input to the system was kept constant the effect of changing the impulse duration on the rope forces was very significant. The duration of the impulse as a fraction of the first natural frequency of the system appears to be important, rather than the energy input to the system.

6. SLACK ROPE

In figure 4 the drum motion was presented for an applied impulse. From this diagram it was evident that the initial impulse motion of the drum can be approximated. The drum acceleration can be calculated by dividing the applied torque function by the winder drum inertia. This results in a stepped acceleration or ramp velocity change for the winder. The stepped acceleration change was applied to a single degree of freedom model to calculate rope forces after slack rope.

A single degree of freedom model including a tensile rope was used for the slack rope analysis in the short rope. Dynamic short rope forces did not have a substantial effect on the motion of the winder (figure 4), it was therefore not necessary to the effect of the short rope forces (slack rope) on the remaining winding system. Of interest here was the rope force in the short rope after going slack. Damping was also excluded from the simulation as only the first force peak was of interest, forces thereafter were of little concern. The stepped acceleration was derived using the following formula:

$$a = \frac{10 * \dfrac{T}{r}}{\dfrac{I_w}{r^2}}$$

Where **T** is the maximum imbalance torque of the system and I_w the winder inertia. The winder radius **r** is used to convert the inertia and torque to translating quantities. The acceleration a is the maximum linear acceleration at the winder (see figure 9). This acceleration would apply for the duration of the impulse. Once the impulse ceased no force other than the rope forces would be applied to the drum. An ascending, fully loaded conveyance was placed at 100m.

The non-linear single degree of freedom model was used to derive the result illustrated in figure 14.
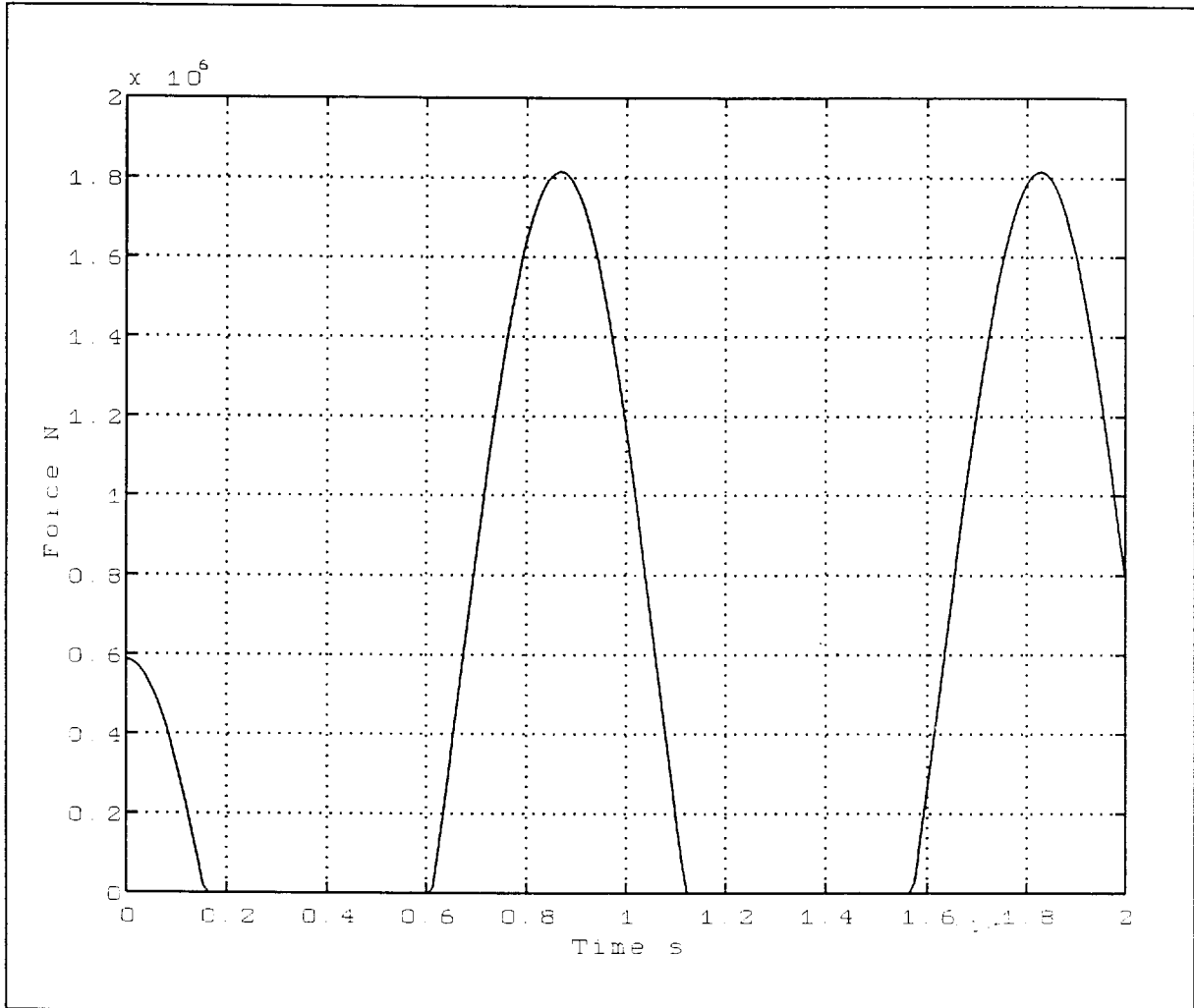
Figure 14   Rope forces at the winder in the short rope for the slack rope condition.

The slack rope duration was calculated to be 0,44 seconds. The maximum force occurring in the rope was 30% of the rope breaking strength.

The motion of the winder (plot 1) and the conveyance (plot 2) are shown in figure 15. The difference in motion between winder and conveyance is also shown (plot 3).
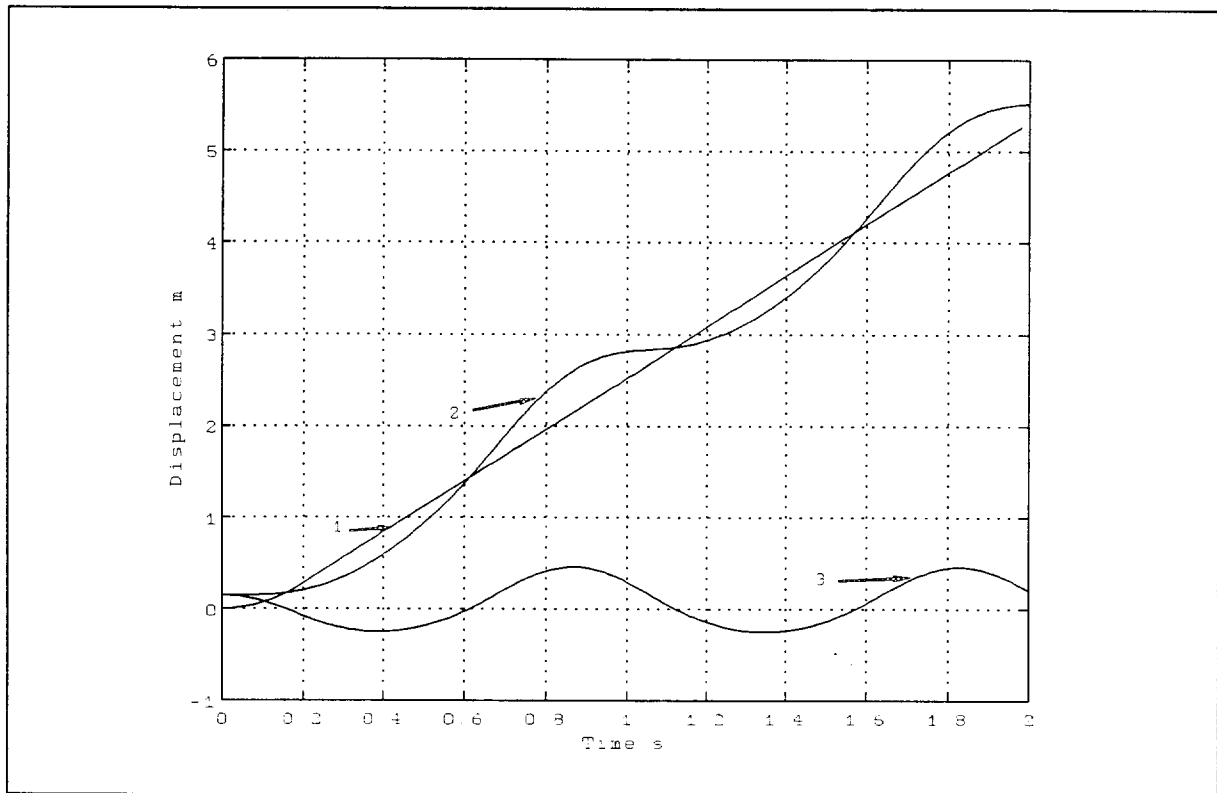
Figure 15   Motion of winder and conveyance during slack rope

The maximum slack rope difference between the displacement of the winder and the conveyance in this figure was 0,252m. The forces calculated and presented in figure 14 indicate that the slack rope condition will not result in a failure of the rope.

7. CONCLUSIONS

1. The maximum force obtained in the ropes as a result of the short circuit was dependent on the impulse duration. At a duration of 200ms 40% of the rope breaking strength was achieved. This relatively short impulse duration indicates that careful consideration has to the allowable flashover impulse duration in winder systems. For hypothetical 4000m winding system a limit of 200m/s would have to be placed on the winder (for an overload torque of 10 times the imbalance torque).

2. For stated short circuit torques slack rope will occur in the short rope of the 4000m winding system. In the 4000m winding system the worst slack rope condition occurred in the ascending wind with a full conveyance at or near bank level. For a 200ms impulse duration slack rope was not sufficient to break the rope, nor exceed 40% of the rope breaking strength.

3. Altering the shape of the impulse torque while maintaining a constant impulse magnitude did not have a large influence on the maximum force in the rope. Altering the impulse duration while maintaining a constant impulse magnitude changed the maximum rope forces significantly. The impulse duration has a large influence on the maximum force obtained in the rope.

4. The influence the sheave wheel on rope forces is considerable. Rope forces in the catenary were increased by the introduction of the sheave wheel. An increase of 10% for the maximum force was obtained when the sheave wheels were included in the simulation.

8. RECOMMENDATIONS

1. The slack rope condition should be discussed and investigated in greater detail.

2. The exact duration and magnitude of the impulse likely to occur with different winder motors should be documented. This will enable the calculation of forces in the ropes of different winder configurations. The required limit for the impulse duration to prevent rope forces in excess of 40% of the rope breaking force for other winding systems will have to be determined.

9. REFERENCES

1.   Constancon, C.,P., *The Dynamics of Mine Hoist Catenaries*, PhD Thesis, University of the Witwatersrand, 1994.

2.   Greenway, M.E., *Dynamic Loads in Winding Ropes - An Analytical Approach*, Internal Report, Anglo American Corporation, February 1989.

3.   Greenway, M.E. *Dynamic Rope Loads in Response to Instantaneous Winder Braking*, Internal Report, Anglo American Corporation, June 1991.

4.   Hecker, G.,F.,K., *Rope Forces During Dynamic Brake Tests*, CSIR Contract Report, July 1992.

5.   Hecker., G.F.K., *Proposed Changes to Rope Safety Regulations*, CSIR Contract Report, September 1992.

6.   Information received from Mr W. Hilmer, Siemens, November 1993.

7.   Kuun, T.C., *Dynamic Loads in Winding Ropes*,Internal Report, Anglo American Corporation, December 1988.

8.   Massey, D.,S., *Initial Investigation Into Rope Forces Generated By Flashover Torques*, CSIR Interim Report, May 1994.

9.   Perry, J.,F., *Mechanical braking and its influence on winding equipment*, Proc.Inst.Mech.Eng.,1937,vol 32.,P 537.

10.   Thomas, G.,R., *An Investigation into the Dynamic Rope Loads in Drum Winder Systems*, SDRC Contract Report,July 1988.

11.   van Zyl, M., *Drum Winder Rope Forces Generated During Emergency Braking, Normal Acceleration, Skip Loading*, CSIR Contract Report, April 1991.

12.   van Zyl, M., *Load Ranges Experienced by Drum Winder Ropes*, CSIR Contract Report, November 1992.

13.   van Zyl., M., *Drum Winder Rope Forces Generated By the Occurrence of Slack Rope - An Analytical Model*, September 1991.

LOAD RANGES DURING A
NORMAL WINDING CYCLE.

by

J Kroonstuiver

Submitted to: SIMRAC Engineering Advisory Committee

J Kroonstuiver

Reviewed by:

G/F.K Hecker

SYNOPSIS

This report describes an investigation carried out by the CSIR to derive methods that may be used to determine the load range in a winding rope of a vertical winding system. Four methods for obtaining the load range are presented: A calculation used to estimate the load range, a direct measurement of the load range with sheave load cells and two methods using conveyance mounted load cells. The methods presented calculate the load range after the completion of the winding cycle.

LIST OF SYMBOLS

$$\eta = \frac{\text{Suspended rope Mass}}{\text{Attached Mass}}$$

$$1 + \eta = \frac{\text{Rigid body rope force at winder}}{\text{Rigid body rope force at conveyance}}$$

a_m = Maximum winder acceleration

a = Winder acceleration

u = Displacement of rope

x = Position in rope, measured from sheave to skip

t = Time during winding cycle

ϕ_i = Normal coordinate for the i'th mode of vibration

X_i = Normal function or mode shape

ζ_i = Dimensionless rope/conveyance system natural frequency

$$= \frac{\omega_i l}{c}$$

ω_i = System i'th natural frequency

l = Suspended rope length

$$c = \text{Wave velocity in rope} = \sqrt{\frac{E}{\rho}}$$

E = Effective Young's modulus

A = Rope steel cross sectional area

ρ = Density of steel in rope

ρ_r = Rope mass per metre

C_i, D_i = Arbitrary Constants

M = Attached mass

M_c = Empty conveyance mass

M_p = Mass of payload

M_r = Suspended rope mass

ω_1 = 1'st natural frequency (Hz)

F_1 = 1st natural frequency (rad.s^{-1})

D_r = Dynamic force ratio

S_r = Rigid bodyf force ratio

Measured sheave force = Rope force measured at the head sheave

Skip force = Rope force measured at conveyance load cell

CONTENTS

LIST OF FIGURES

LIST OF TABLES

1   INTRODUCTION

The load range acting in a drum winder rope is defined as the difference between the maximum and minimum tension that any part of the rope experiences during a winding cycle. In the *"Code of Practice Performance, Operation, Testing and Maintenance of Drum Winders"* limitations have been placed on the load range allowed in the winding rope. The load range at any point in the rope is not to exceed the 15% of the rope breaking strength more than once every ten trips.

This document describes an investigation carried out by the CSIR to derive methods that may be used to determine the load range during winding. Chapters 1 and 2 of the report introduce the subject matter and describe the relationship between rope forces measured at the conveyance and head sheave. Chapter 3 covers the in rope position of the maximum load range and the different methods of calculating the load range are discussed. The methods of calculating the load range in a winding rope are verified by comparing the calculated load range to data from rock and man winder cycles. Recorded data from a South African rock winder is used while hypothetical data created with a numerical simulation is used for the man winder. The results of this investigation are relevant to man and rock winders since both winders are considered in this investigation.

Chapter 4 briefly outlines the conclusions and recommendations found in this report.

2   ROPE FORCES

2.1   Winder Parameters

The calculations derived in this report were designed using measured data from a South African rock winder cycle and calculated data for a man winder cycle. The rock winder cycle data was available from a previous CSIR investigation (report No. MST(92)MC996), while the man winder cycle data was created using a finite difference model. An example of the measured quantities of the rock winder cycle are listed in Appendix A. The calculated quantities of a man winder cycle are listed in Appendix B. The rock winder cycle starts with an empty skip at the bank, followed by a wind to the loading bay, loading, a wind back to the bank and unloading. The man winding cycle starts with a loaded conveyance at the bank, winding to shaft bottom, unloading, winding back to mid shaft, loading with 50% payload, winding to shaft bottom, unloading and winding an empty conveyance back to the bank.

2.2   Rigid body and dynamic rope forces

The rigid body rope force is the non-oscillatory force in the rope. It is the force resulting from gravitational acceleration (g) and constant acceleration (a). A rigid body force will be the only rope force in a stationery winder. The total rope force is the sum of the rigid body rope force and the dynamic rope force. The rigid body rope force is calculated by filtering the measured rope force with a low bandpass filter. The dynamic rope force is calculated by subtracting the rigid body rope force from the measured rope force. Typical filter characteristics required for this purpose are illustrated in Appendix F.

2.3   The Rigid body force ratio

The free body diagram in Figure 1 illustrates the relationship between the rigid body sheave and the rigid body skip force. When the system is moving at constant velocity and when the system is accelerating (a in Figure 1) the rigid body sheave force divided by the rigid body skip force is the ratio $(1+\eta)$. The rigid body rope force is a maximum at the sheave and a minimum at the skip. The ratio $(1+\eta)$ is independent of the winder acceleration, it is only dependent on the ratio of suspended rope mass to attached mass (η). In Figure 2 the rigid body force at the sheave and at the conveyance and the rigid body force ratio are plotted as a function of time during the rock winder cycle.

Figure 1   Free body diagram of rope and attached mass showing the ratio of rigid body
sheave force to rigid body skip force

Figure 2   Rigid body sheave and skip force and rigid body ratio vs time

2.4   The dynamic force ratio

The dynamic rope forces are obtained by subtracting the rigid body forces in Figure 2 from the measured rope forces. The dynamic rope force at the head sheave and at the skip for a segment of the rock winder cycle in Appendix A are plotted as a function of time in Figure 3. The dynamic ratio is the ratio of the dynamic sheave force to the dynamic skip force. This ratio is also dependent on η (Rope mass/attached mass).
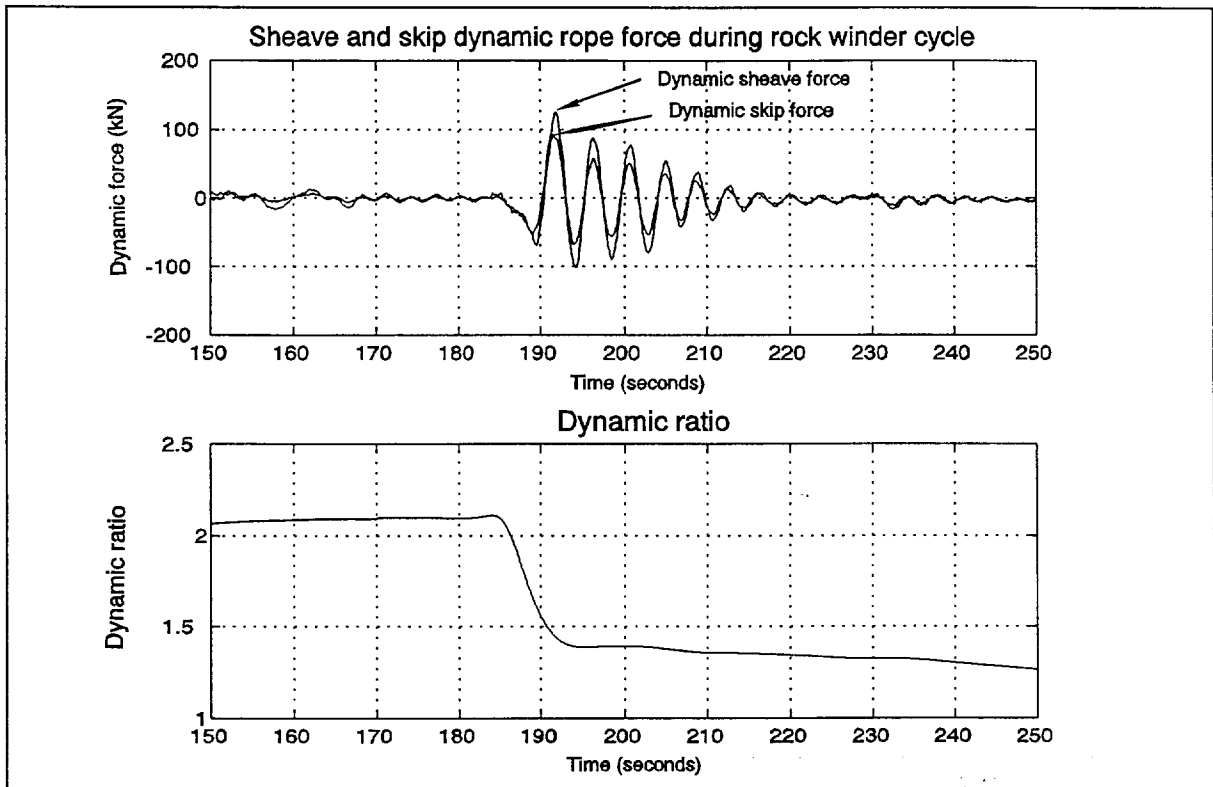
Figure 3   Dynamic sheave and skip force and dynamic ratio vs time

To derive the relationship between the η and the dynamic ratio a solution for harmonic oscillation of the rope with attached mass is considered. In a previous report by Greenway (ref 2) a normal mode solution was used to predict the displacement and the forces in the rope of the winder system. Greenway noted (2) ..."in the normal mode method the displacement function u(x,t) is expressed as a summation of products of time functions $\Phi_i(t)$ and normal mode-shape displacement functions $X_i(x)$ as follows:..."

$$u(x,t) = \sum_{1}^{\infty} \phi_i(t)X_i(x) \quad \cdots\cdots\cdots\cdots\cdots\cdots \quad (1)$$

Equation 1 represents a displacement solution of a rope with an attached mass as a function of time and position along the rope while the system is undergoing harmonic oscillation.

The solution to Equation 1 is of the form:

$$X_i = C_i \cos\frac{\omega_i X}{c} + D_i \sin\frac{\omega_i X}{c} \quad \cdots\cdots\cdots\cdots\cdots\cdots \quad (2)$$

Assuming that the system is initially at rest and that the static tension is taken as the initial zero condition the following boundary conditions result:

$$\begin{aligned} \text{at } t=0 \quad u(x,t)=0 \quad &\therefore \; C_i=0 \quad &\text{...BC(1)} \\ \text{at } x=1 \quad EA\frac{\partial(1,t)}{\partial x} &= -M\frac{\partial^2 u(1,t)}{\partial t^2} \quad &\text{...BC(2)} \end{aligned} \quad \cdots\cdots\cdots\cdots \quad (3)$$

Boundary condition BC(1) reduces the normal mode solution to:

$$u(x,t) = \sum_{1}^{\infty} \phi_i(t)X_i(x)$$

Where: $\cdots\cdots$ (4)

$$X_i(x) = D_i \sin\left[\frac{\omega_i X}{c}\right]$$

ϕ_i = Function of time dependant on initial conditions

Boundary condition BC(2) results in the system natural frequencies which are obtained by solving the equation:

$$\zeta_i \tan(\zeta_i) = \eta$$

Where: $\cdots\cdots\cdots\cdots\cdots\cdots\cdots$ (5)

$$\zeta_i = \frac{\omega_i 1}{c}$$

The first derivative of the rope displacement with respect to x yields the rope force:

$$\text{Rope force} = EA\frac{\partial u(x,t)}{\partial x}$$

$$EA\frac{\partial u(x,t)}{\partial x} = EA\sum_{1}^{\infty}\phi_i(t)\frac{\partial X_i(x)}{\partial x} \quad\ldots\ldots\ldots\ldots\ldots (6)$$

$$\frac{\partial X_i(x)}{\partial x} = D_i\frac{\omega_i}{c}\cos\left[\frac{\omega_i x}{c}\right]$$

The dynamic ratio is then obtained:

$$\frac{F_{\text{head sheave}}}{F_{\text{conveyance}}} = \frac{EA\dfrac{\partial u(0,t)}{\partial x}}{EA\dfrac{\partial u(l,t)}{\partial x}}$$

$$= \frac{\displaystyle\sum_{1}^{\infty}\phi_i(t)\dfrac{\partial X_i(0)}{\partial x}}{\displaystyle\sum_{1}^{\infty}\phi_i(t)\dfrac{\partial X_i(l)}{\partial x}} \quad\ldots\ldots\ldots\ldots (7)$$

$$= \frac{\displaystyle\sum_{1}^{\infty}\phi_i(t)\,D_i\dfrac{\omega_i}{c}\cos\left[\dfrac{\omega_i 0}{c}\right]}{\displaystyle\sum_{1}^{\infty}\phi_i(t)\,D_i\dfrac{\omega_i}{c}\cos\left[\dfrac{\omega_i l}{c}\right]}$$

As most of the energy in the system response is in the first mode of vibration the higher frequency terms may be neglected. This reduces the dynamic ratio to:

$$\frac{F_{head\ sheave}}{F_{conveyance}} = \frac{E A \dfrac{\partial u(0,t)}{\partial x}}{E A \dfrac{\partial u(l,t)}{\partial x}}$$

$$= \frac{\phi_1(t)\ D_1\dfrac{\omega_1}{c}\cos\left[\dfrac{\omega_1 0}{c}\right]}{\phi_1(t)\ D_1\dfrac{\omega_1}{c}\cos\left[\dfrac{\omega_1 l}{c}\right]} \quad \cdots\cdots\cdots\cdots\cdots \quad (8)$$

$$= \frac{1}{\cos\left[\dfrac{\omega_1 l}{c}\right]}$$

$$= \frac{1}{\cos(\zeta_1)}$$

The dynamic ratio is therefore approximated by a function of ζ_1 which in turn is a function of ω_1. From Equation 5 the system first natural frequency is a function of η (the rope mass to attached mass ratio). By solving the first natural frequency equation and plotting the dynamic force ratio as a function of η it is possible to obtain a polynomial equation relating the dynamic force ratio to η. A least squares fit was applied to calculated values of the dynamic ratio, the curve obtained is illustrated in Figure in 4. The polynomial relating the dynamic ratio to η is obtained as:

$$\text{Dynamic ratio} = 0,00948\eta^2 + 0,54426\eta + 0,9825$$

$$\eta = \frac{\text{Rope mass}}{\text{Attached mass}} \quad \cdots\cdots\cdots\cdots (9)$$

2.5   Comparison between static and dynamic ratio

In Figure 4 the rigid body force ratio and dynamic force ratio are plotted as a function of η and as a function of time during the rock winder cycle. The rigid body force ratio is larger than the dynamic ratio for all values of η.
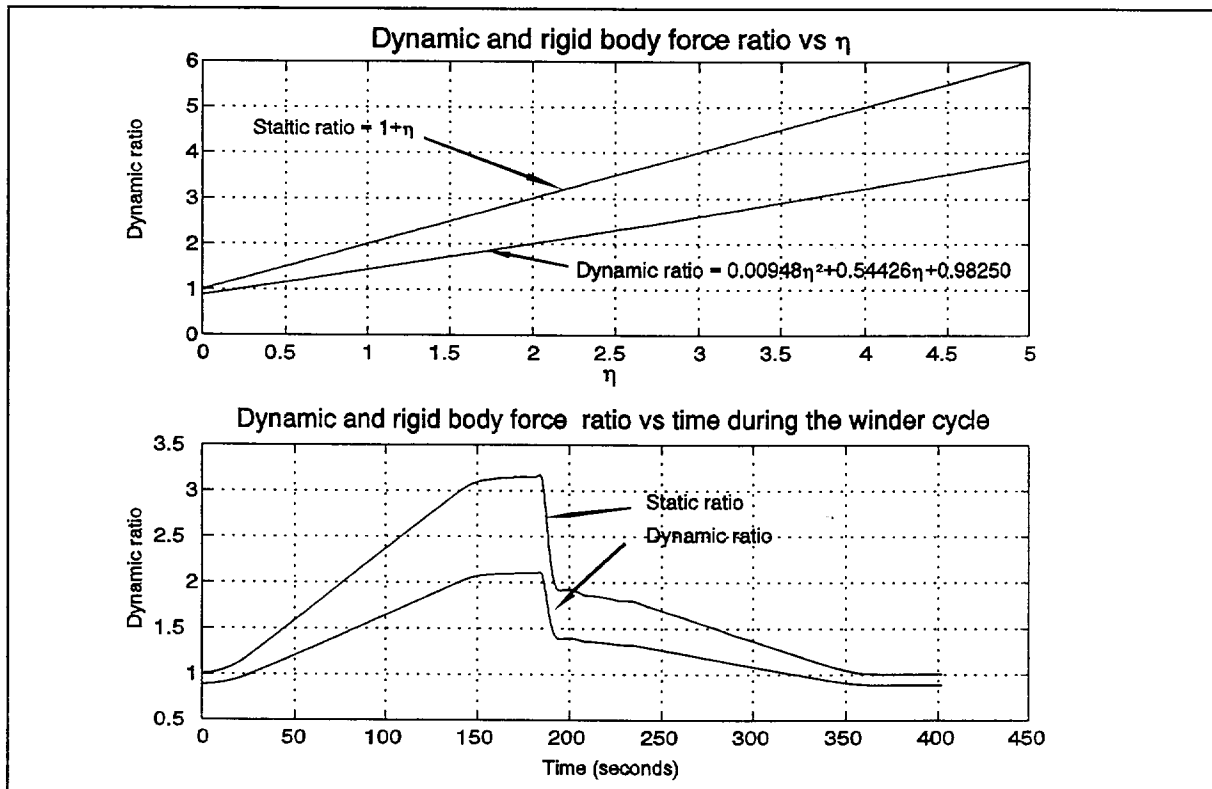
Figure 4   Comparison of static and dynamic ratio

2.6   Calculation of rope forces

If the rope force is measured at either the conveyance or at the headsheave then the dynamic ratio and rigid body ratio may be used to calculate the rope force at the rope end opposite to the side of the rope where the force measurement was made. Both ratios are a function of η, so the attached mass and the rope mass must be known throughout the wind.

$$F_{skip} = \frac{F_{sheave\ dynamic}}{D_r} + \frac{F_{sheave\ rigid\ body}}{S_r}$$

$$F_{sheave} = (F_{skip\ dynamic})D_r + F_{skip\ rigid\ body}S_r$$

$$
\begin{aligned}
F_{skip} &= \text{Calculated skip force} \\
F_{skip\ dynamic} &= \text{Dynamic skip force} \\
F_{skip\ rigid\ body} &= \text{Rigid body skip force} \\
F_{sheave} &= \text{Calculated sheave force} \\
F_{sheave\ dynamic} &= \text{Dynamic sheave force} \\
F_{sheave\ rigid\ body} &= \text{Rigid body sheave force} \\
D_r &= \text{Dynamic ratio} \\
S_r &= \text{Rigid body ratio}
\end{aligned}
\qquad \cdots \cdots \cdots \text{(10)}
$$

The accuracy of this calculation is dependent on filter characteristics used to calculate the static and dynamic rope forces.

2.7   Conclusion

Section 2 has been a brief overview of the rope forces of a mine winding system. The basic relationship between the measured sheave and the measured skip force is illustrated. Equation 10 in section 2.6 is used as a basis for calculating forces in the rope when measurements at either end of the rope are made.

3   LOAD RANGE

3.1   Position in the rope of the maximum load range

To determine the position in the rope where the maximum load range occurs the load range was calculated at points in the rope that were 100m apart. These calculations were carried out for the rock winder cycle (Appendix A) and the man winder cycle (Appendix B).

(i)   Rock winder cycle

The maximum load range in the rope of a rock winder occurs at the highest point in the rope when the rope is fully paid out. The maximum rope force occurs while a loaded skip is accelerating from the loading bay, sometimes the maximum force occurs during skip loading. The minimum rope force occurs with the empty skip approaching the shaft bottom while the winder is decelerating.

(ii)   Man winder cycle

The same calculation was carried out on a number of hypothetical man winder cycles, a specific point in the rope where the maximum load range occurred can not be identified. It is therefore concluded that the position in the rope of maximum load range is a function of the winding cycle.

3.2   Load range of equivalent sheave force

The equivalent sheave force is obtained by subtracting the rope weight from the measured sheave force. The sheave force is measured with a load cell at the head sheave sole plates. The load range of the equivalent sheave force is the difference between the maximum equivalent sheave force less the minimum equivalent sheave force. The load range represents the load range across the entire length of the rope during the wind. The load range of specific points in the rope will be less or equal to the load range of the equivalent sheave force. This holds true for man and rock winders. The maximum load range at any point in a winding rope can therefore be approximated from the load range of the equivalent sheave force for the winder cycle.

3.3   Load range - Method 1

(i) Load range equation

Method 1 uses a calculation that estimates the load range of the equivalent sheave force of a typical rock winder cycle. Figure 5 shows the characteristic equivalent sheave force of a typical rock winder cycle. The winder is initially at rest with the skip at the shaft bottom. After loading, an overshoot occurs in the equivalent sheave force, during acceleration a 100% force overshoot is assumed to occur. The winder winds to the bank, the skip is unloaded and the skip returns to the shaft bottom. When the skip approaches the shaft bottom, and during deceleration another 100% force overshoot (this time reducing the force magnitude) occurs.
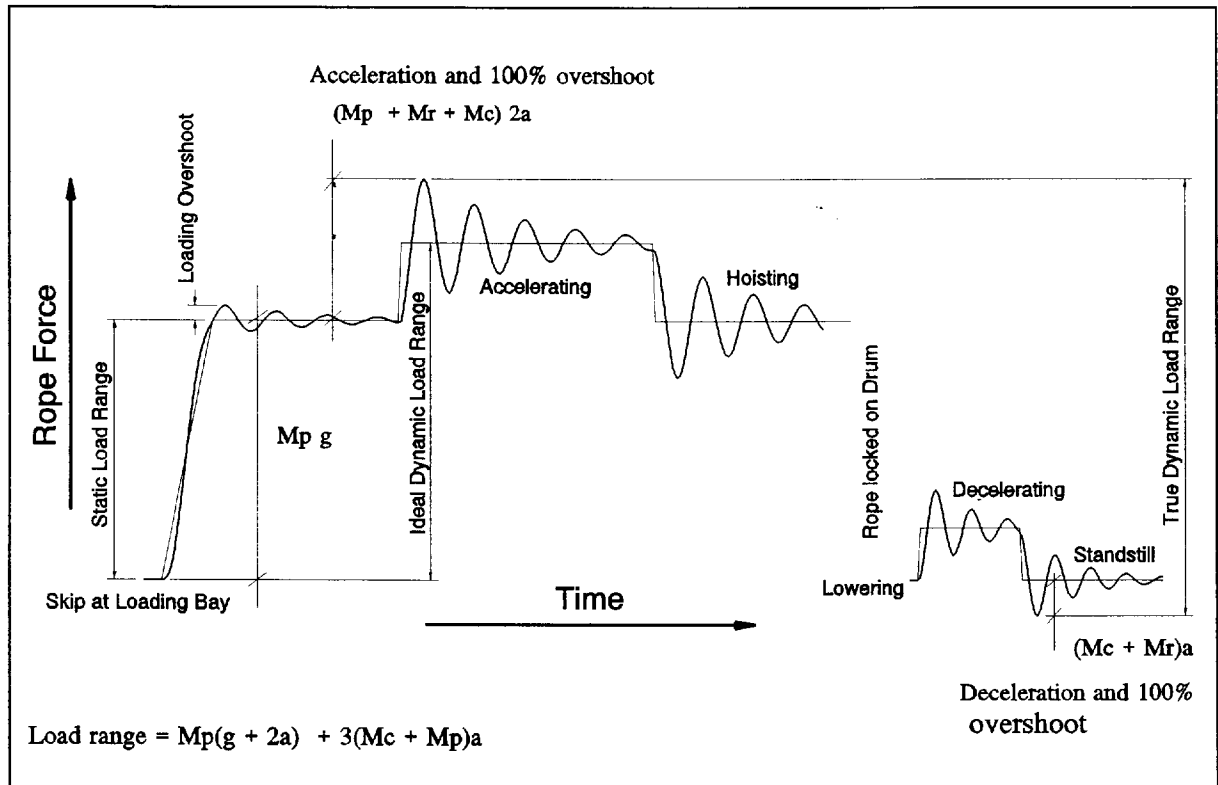
Figure 5   Rock winder cycle with derivation of loadrange method 1

The load range is calculated as:

$$\text{Load range} = F_p + F_a + F_{a\ 100} + F_{d\ 100}$$

$$\text{Load range} = M_p(g + 2a_m) + 3a_m(M_c + M_r)\ldots\ldots(\text{Rock winder})$$

$$\text{Load range} = M_p(g + 3a_m) + 3a_m(M_c + M_r)\ldots\ldots(\text{Man winder})$$

Where: F_p = Payload force = $M_p g$

F_a = Acceleration force = $(M_p + M_c + M_r)a_m$

$F_{a\ 100}$ = 100% overshoot after acceleration = $(M_p + M_c + M_r)a_m$ (11)

$F_{d\ 100}$ = 100% after deceleration = $(M_c + M_r)a_m$...(Rock winder)

$F_{d\ 100}$ = 100% after deceleration = $(M_p + M_c + M_r)a_m$...(Man winder)

M_p = Mass of payload
M_c = Mass of conveyance
M_r = Mass of rope
a_m = Maximum winder acceleration
g = Gravitational acceleration

In the typical rock winder cycle the maximum rope force usually occurs during winder acceleration as the skip leaves the loading bay. Sometimes the loading overshoot is larger than the acceleration overshoot. For the winder cycles considered in this investigation the loading overshoot was larger than the acceleration overshoot, however the 100% acceleration overshoot used in Equation 11 exceeded the loading overshoot. This should be checked for the individual winder systems where the method is used. The magnitude of the forces during loading may be measured to check that the calculated maximum rope force (using equation 11) is larger than the largest rope force during loading. If forces resulting from loading dynamics exceed the calculated maximum force then Equation 11 should be adjusted for that specific winding system or the skip loading method altered.

In the case of a man winder loading is carried out gradually and the maximum force will occur during winder acceleration or deceleration. The minimum rope force occurs with the winder decelerating with an empty conveyance while approaching the shaft bottom.

(ii) Application of method

Inputs to Equation 11 are the maximum winder acceleration (or deceleration) and the maximum payload during any one winding cycle. The payload is measured with either the conveyance or sheave load cell using the method shown in Appendix D.

3.4   Load range - Method 2

The load range of the equivalent sheave force is a good estimate of the maximum load range that may occur in the rope (Section 3.2). This characteristic of the winding system is used in method 2. The equivalent sheave force is calculated by subtracting the rope weight from the measured sheave force signal (Appendix C) during the wind. The load range of winding rope is the difference between the maximum peak and the minimum trough of the equivalent sheave force for each trip.
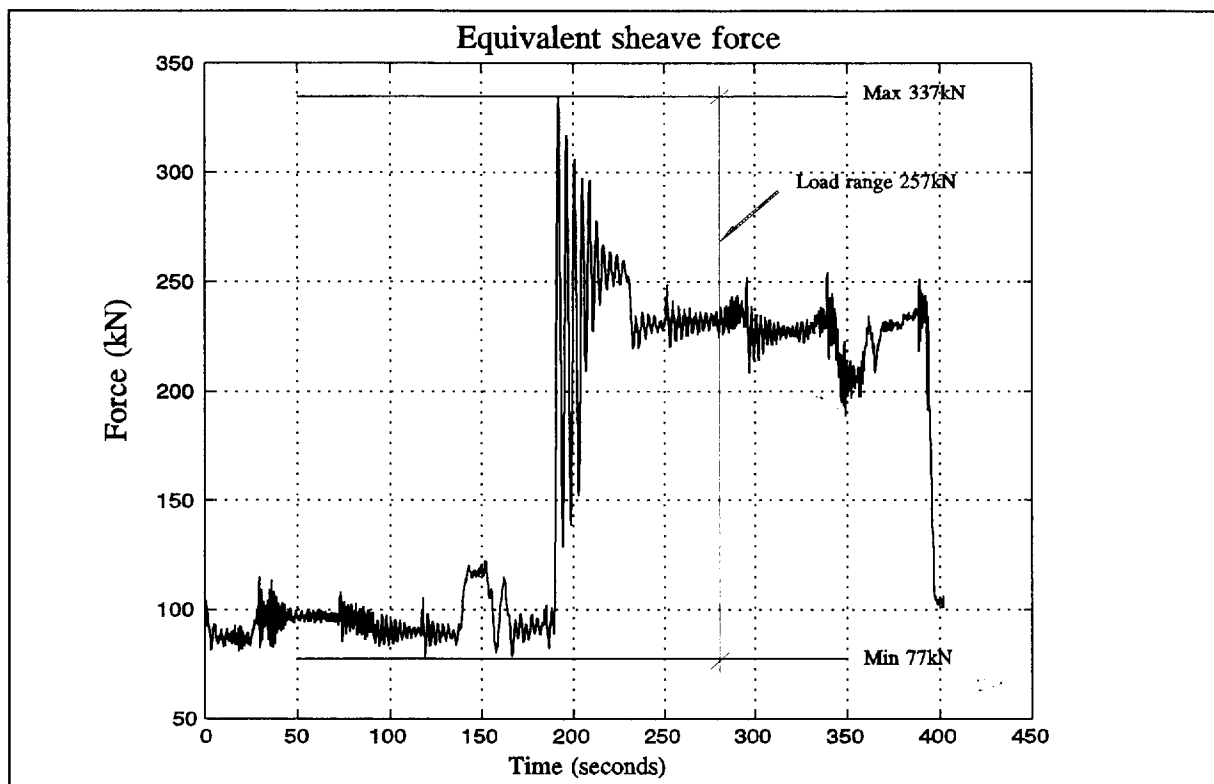
Figure 6   Load range of the equivalent sheave force

The load range of the equivalent sheave force is normally larger than the maximum load range of the winding rope. Method 2 remains conservative if a sufficiently accurate load cell is used. In Appendix G the measurement accuracies of the various instruments are discussed and the required accuracies for each instrument recommended.

3.5   Load range - Method 3

This method is based on a force measurement at the conveyance load cell and measurement of the conveyance position. The load range in the rope is calculated from the force measured at the conveyance. The rigid body ratio is used to calculate the sheave force. The rigid body and dynamic component of the measured conveyance force are both multiplied by the rigid body ratio to obtain the sheave force estimate. The modified Equation 10 used in this method is repeated as equation 12:

$$F_{sheave} = (F_{Measured\ skip\ force})\ S_r$$

$$
\begin{aligned}
F_{Measured\ skip\ force} &= \text{Measured skip force} \\
S_r &= \text{Rigid body ratio} \\
S_r &= 1 + \eta \\
\eta &= \frac{M_r}{M_c + Mp} \\
M_r &= \text{Suspended rope mass} \\
M_c &= \text{Conveyance mass} \\
M_p &= \text{Payload}
\end{aligned}
\qquad \ldots\ldots\ldots\ldots (12)
$$

The rigid body ratio is larger than the dynamic ratio (see Figure 4) for all values of η in the range of interest. By using the rigid body ratio in the place of the dynamic ratio the dynamic forces in the calculated sheave force are overestimated, making this method conservative.

For a rock winder during loading the value of η becomes difficult to determine. The CSIR used a filter to determine η while loading, however the filter characteristics used depended on the skip loading rate; it is therefore not practical to define a filter applicable to all winder applications. To counter this problem Equation 12 is used while the winder has an absolute velocity of at least $0,5m.s^{-1}$. The method is applied differently to man and rock winders:

(i) Man winder

The maximum rope force occurs when a loaded conveyance is acclerated from the deepest level in the shaft. It is assumed for a man winder that the loading dynamics are not severe and do not result in higher forces than the winding dynamics. To calculate η at any point in the trip it is necessary that the attached mass during every portion of the winding trip is known. The attached mass is calculated by the method presented in Appendix D. The suspended rope mass is calculated from the conveyance position, the rigid body ratio is calculated using Equation 12.

Method 3 is applied to the man winder as follows:

●   Record the conveyance position and conveyance force as a function of time and store

the recorded data.

This method is applied after every wind, therefore the data has to be stored so that subsequent calculations can be carried out.

- Locate data where winder velocity is $> 0,5 \text{m.s}^{-1}$.

  The conveyance must be freely suspended and not being loaded when the calculation is carried out, by checking that the velocity is larger than $0,5 \text{m.s}^{-1}$ this is achieved. Once this data set has been identified subsequent calculations are carried out on it.

- Find the maximum rope force, the suspended rope mass at that point and the attached mass at that point and calculate η.

  The maximum force is found and η is calculated at that point. This is carried out so that Equation 12 can be used to calculate the estimate maximum sheave force.

- Find the minimum rope force, the suspended rope mass and the attached mass at that point and calculate η.

  The minimum force is found and η is calculated at that point. This is carried out so that Equation 12 can be used to calculate the minimum estimate sheave force.

- Calculate the maximum and minimum estimate sheave force using (Equation 12)
- Subtract the relevant rope weight from the maximum and minimum sheave force to obtain the maximum and minimum equivalent sheave force.

  The rope weights when the maximum and minimum rope forces occur are determined so that the maximum and minimum equivalent sheave force can be calculated. The maximum and minimum equivalent sheave forces are obtained by subtracting the suspended rope weight form the maximum and minimum sheave force.

- The load range is calculated as the difference between the maximum and minimum equivalent sheave force.

(ii)   Rock winder

In a rock winder the rope forces during loading of the skip can exceed those forces in the rope during winding. To allow for larger forces during loading it is necessary to adjust the calculated value of the maximum equivalent sheave force when applying method 3 to a rock winder system. The adjustment is made by monitoring the maximum rope force during loading, and comparing this value to the maximum rope force during winding. If the loading force is found to exceed the winding force then the calculated maxim effective sheave force is multiplied by the maximum loading force to maximum winding force ratio.

Equation 12 is applied to the measured data while absolute winder velocity is larger than

$0,5\text{m.s}^{-1}$ (i.e. the winding force). The steps for applying this method to a rock winder are as follows:

- Record the conveyance position and conveyance force as a function of time
- Locate data where winder velocity is $> 0,5\text{m.s}^{-1}$ and hence identify the loading force (velocity larger than $0,5\text{m.s}^{-1}$) and winding rope force (velocity less than $0,5\text{m.s}^{-1}$)

  The loading and winding part of the cycle are identified so that the ratio of maximum loading force to maximum winding force can be calculated.

- Identify the maximum rope force during loading .
- Find the maximum rope force during winding and calculate η at that point.
- Find the minimum rope force during winding and calculate η at that point.
- Calculate the ratio of maximum loading force to maximum winding force.
- Calculate the estimate maximum and minimum sheave force using Equation 12.
- Subtract the rope weight from the maximum and minimum estimate sheave force to obtain the maximum and minimum equivalent sheave force.
- If the loading force to winding force ratio is >1 then multiply the maximum equivalent sheave force with this ratio.

  In the rock winder it may occur that the maximum loading force may exceed the maximum winding force. When this occurs it is necessary to adjust the maximum equivalent sheave force. This is carried out by finding the ratio of loading to winding force and multiplying this ratio with the maximum equivalent sheave force (if this ratio is larger than 1.

- The load range is calculated as the difference between the maximum and minimum equivalent sheave force.

In Figure 7 a winding cycle is shown. Equation 13 shows how information from the winding cycle is used to calculate the load range of a typical rock winder cycle. The maximum force during the winding cycle is adjusted as the loading forces are higher than the forces during winding. The steps carried out for rock winder are described in the equation:

Maximum forces:

$$F_{max\ skip} = 268kN\ (During\ winding)$$

$$F_{max\ skip} = 298kN\ (During\ loading)$$

Force ratio:

$$Ratio = \frac{Max\ loading\ force}{Max\ winding\ force} = \frac{298}{268} = 1,11$$

Equivalent force:

$$F_{Max\ sheave} = (1+\eta)F_{Max\ skip} = 514kN$$

$$F_{Min\ sheave} = (1+\eta)(F_{Min\ skip}) = 84kN \quad\quad\quad\quad \ldots\ldots (13)$$

$$F_{Equivalent\ max} = F_{Max\ sheave} - Rope_{weight} = 304kN$$

$$F_{Equivalent\ min} = F_{Min\ sheave} - Rope_{weight} = 84kN$$

Adjust force:

$$F_{Equivalent\ max} = 304\,kN(1,11) = 337\,kN$$

Load range:

$$Load\ range = 337kN - 84kN = 253kN$$
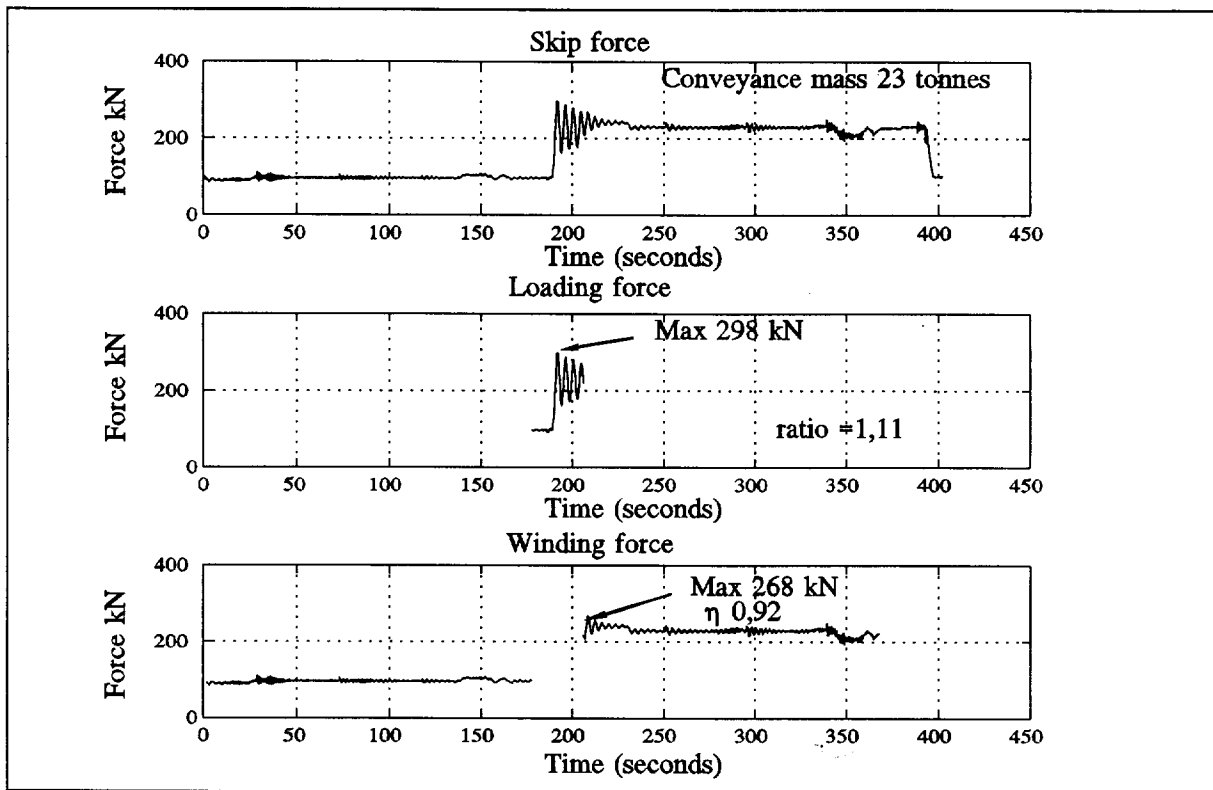
Figure 7   Skip force during loading and during winding

The load range calculated with method 3 is listed in table 1.

Force	Measured forces	Calculated forces
Maximum skip force	298	-----
Minimum skip force	84	-----
Maximum sheave force	545	-----
Minimum sheave force	84	-----
Maximum equivalent sheave force	335	337*
Minimum equivalent sheave force	84	84**
Load range	251	253

   *   Rigid body ratio 1,92
  **   Rigid body ratio 1,00

Table 1   Load range calculated by method 3

In figure 8 the calculated values in table 1 are plotted on the same axis as the measured equivalent sheave force.
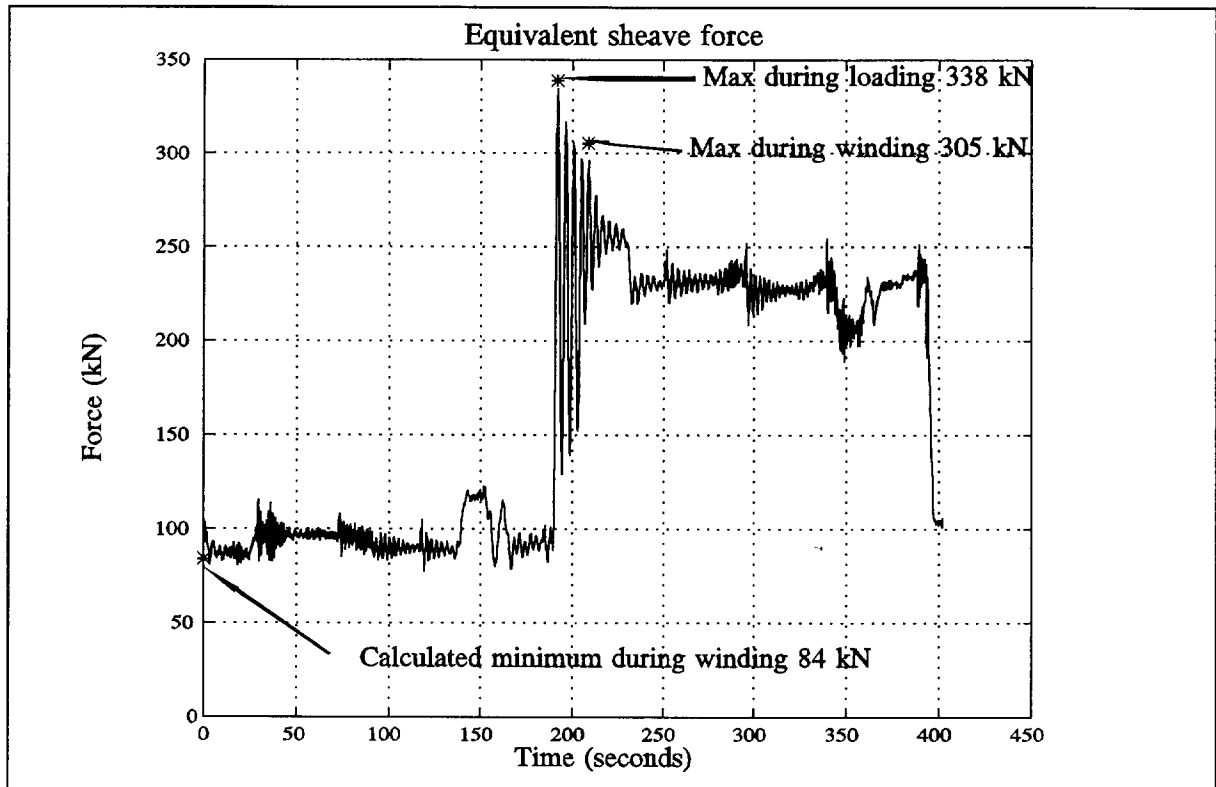
Figure 8   Maximum and minimum calculated values of equivalent sheave force

3.6   Load range - Method 4

In this method equation 10 is used, repeated here as equation 14. The measured skip force is separated into rigid body and dynamic components respectively, equation 14 is applied while the absolute winder velocity is above $0{,}5\text{m.s}^{-1}$. As a result of the inherent differences between man and rock winders the method is applied differently in each case:

(i)   Man winder

$$F_{sheave} = (F_{skip\ dynamic})D_r + (F_{skip\ rigid\ body})S_r$$

$$
\begin{aligned}
F_{sheave} &= \text{Calculated sheave force} \\
F_{skip\ dynamic} &= \text{Dynamic skip force} \\
F_{skip\ static} &= \text{Rigid body skip force} \qquad \ldots\ldots\ldots (14) \\
D_r &= 0{,}00948\eta^2 + 0{,}54426\eta + 0{,}9825 \\
S_r &= 1 + \eta \\
\eta &= \frac{\text{Suspended rope mass}}{\text{Conveyance mass}}
\end{aligned}
$$

The rigid body force is extracted from the measured conveyance force with a low band pass filter while the dynamic rope force is obtained by subtracting the rigid body force from the measured skip force. The ratio η is calculated by dividing the suspended rope mass with the attached mass. The rigid body ratio is $(1 + \eta)$, while the dynamic ratio is calculated in Equation 14. The steps of the method as applied to man winders are summarised as:

● Record conveyance force and position during the wind

This method is applied after every wind, therefore the data has to be stored so that subsequent calculations can be carried out.

● Identify data points where the absolute winder velocity is $> 0{,}5\text{m.s}^{-1}$

The method requires that the conveyance is freely suspended and that no step changes occur in the value of η (due to skip loading), it is therefore necessary to constrain the application of Equation 14 to the system when the winder is in motion.

● Separate the measured skip force into a rigid body and dynamic components using a low band pass filter and calculate the rigid body and dynamic force ratios during the wind.

The measured data points are filtered with a low band pass filter (as in Appendix F) to obtain rigid body force. The dynamic force is obtained by subtracting the rigid body force from the measured force signal. The rigid body force ratio and the dynamic force ratio are needed in Equation 14.

- Apply equation 14 to the measured data to obtain the sheave force estimate.
- Find the maximum and minimum sheave force from the estimate, and the rope weight when the minimum and maximum forces occur.

The rope weight at the maximum and minimum rope forces are needed to calculate the maximum and minimum equivalent sheave force.

- Subtract the rope weight from the maximum and minimum sheave force to obtain maximum and minimum values of the equivalent sheave force.
- The load range is calculated as the difference between the maximum and minimum equivalent sheave force.

(ii) Rock winder

When applying this method to the rock winder the maximum equivalent sheave force has to be corrected as maximum rope forces may occur during loading. The rope force measured at the conveyance is recorded during loading and the peak of this force is obtained. The peak rope force during loading is compared to the peak rope force during winding and if the loading force is higher than the force during winding then and adjustment is made to the maximum equivalent sheave force. The method applied to man winder is summarised in the steps:

- Record conveyance force and position during the wind
- Identify data points where the absolute winder velocity $>0,5\text{m.s}^{-1}$ and hence identify the loading (less than $0,5\text{m.s}^{-1}$) and winding part of the cycle (greater than $0,5\text{m.s}^{-1}$).
- Identify the maximum rope force during loading.
- Identify the maximum force during winding and calculate the ratio of the peak force during loading to the peak rope force during winding.

In a rock winder the maximum loading force may exceed the maximum winding force. The ratio of maximum loading force to maximum winding force is used to adjust the maximum equivalent sheave force.

- Separate the measured skip force into rigid body and dynamic components and calculate the rigid body force and dynamic force ratios during the wind.
- Apply equation 14 to the winding data to obtain the sheave force estimate.
- Find the maximum and minimum sheave force from the estimate, and the rope weights when the forces occur.
- Subtract the relevant rope weight from the maximum and minimum sheave force estimate to obtain maximum and minimum values of the equivalent sheave force.
- If the ratio of maximum loading force to maximum winding force is >1 then multiply the calculated maximum equivalent sheave force by this ratio.
- The load range is then calculated as the difference between the maximum and the minimum equivalent sheave force.

The method applied to rock winders is described in equation 15:

Maximum forces:

$$F_{\text{Max skip}} = 298\,\text{kN} \quad \text{(During loading)}$$
$$F_{\text{Min skip}} = 268\,\text{kN} \quad \text{(During winding)}$$
$$\text{ratio} = \frac{\text{Max loading force}}{\text{Max winding force}} = 1,11$$

Calculated forces:

$$F_{\text{Max sheave}} = \text{Max}\left[(F_{\text{skip dynamic}})D_r + (F_{\text{skip static}})S_r\right]$$
$$F_{\text{Min sheave}} = \text{Min}\left[(F_{\text{Skip dynamic}})D_r + (F_{\text{Skip rigid body}})S_r\right]$$

Equivalent forces:

$$F_{\text{Max sheave equivalent}} = F_{\text{Max sheave}} - \text{Rope weight}$$
$$F_{\text{Min sheave equivalent}} = F_{\text{Min sheave}} - \text{Rope weight}$$

$$\ldots\ldots (15)$$

If ratio > 1:

$$F_{\text{Max sheave equivalent}} = \text{ratio}\,(F_{\text{Max sheave equivalent}})$$

Load range:

$$\text{Load range} = F_{\text{Max sheave equivalent}} - F_{\text{min sheave equivalent}}$$

$$F_{\text{Max sheave}} = \text{Calculated maximum sheave force}$$
$$F_{\text{Min sheave}} = \text{Calculated minimum sheave force}$$
$$F_{\text{skip dynamic}} = \text{Dynamic skip force}$$
$$F_{\text{skip rigid body}} = \text{Rigid body skip force}$$
$$D_r = 0,00948\eta^2 + 0,54426\eta + 0,9825$$
$$S_r = 1 + \eta$$
$$\eta = \frac{\text{Rope mass}}{\text{Attached mass}}$$

In Figure 9 the conveyance rope force, when the winding (v > 0,5m.s^{-1}) and loading (v < 0,5m.s^{-1}) part of a rock winder cycle are shown.
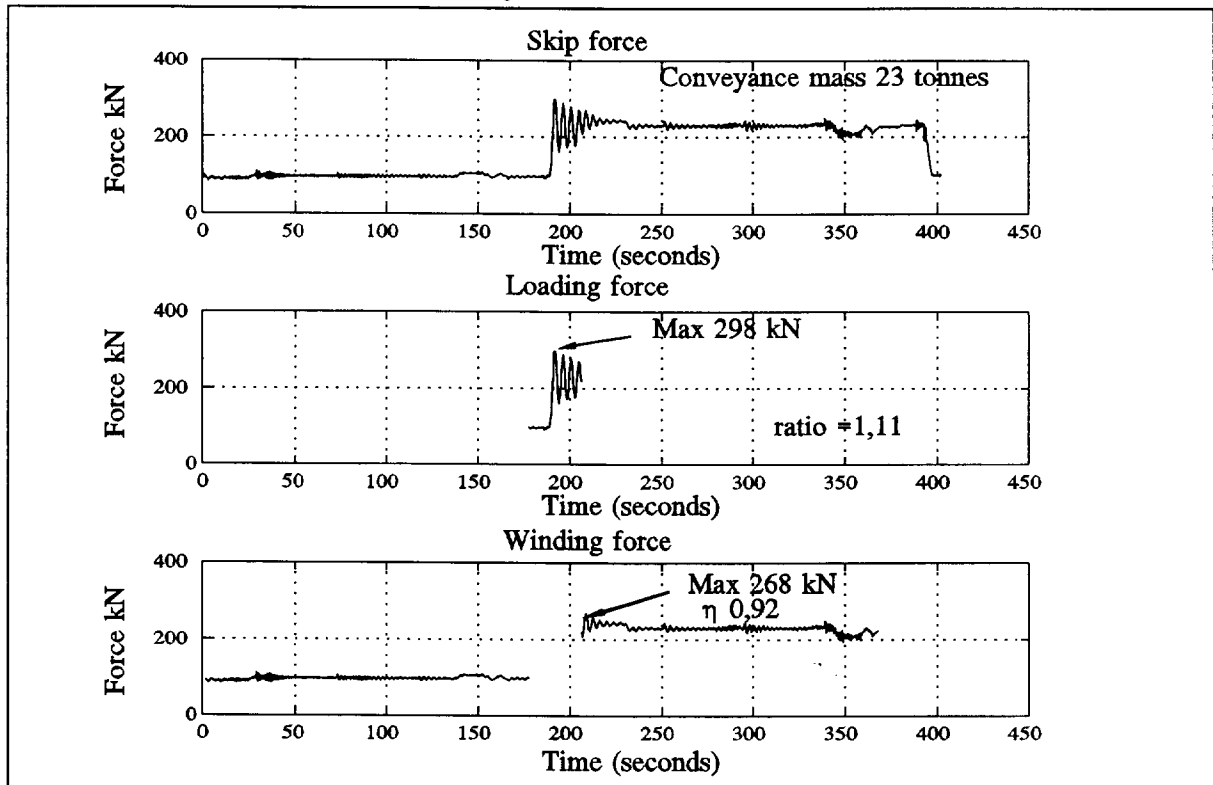
Figure 9   Skip force during loading and during winding

The load range calculated with method 3 is listed in table 1.

Force	Measured forces	Calculated forces
Maximum skip force	298	-----
Minimum skip force	84	-----
Maximum sheave force	545	-----
Minimum sheave force	83	-----
Maximum equivalent sheave force	335	330 *
Minimum equivalent sheave force	84	82 **
Load range	251	248

    *   Rigid body ratio 1,92
   **   Rigid body ratio 1,00

Table 2   Load range calculated by method 4

In Figure 10 and 11 the calculated and measured equivalent sheave force during the rock winder cycle are plotted.
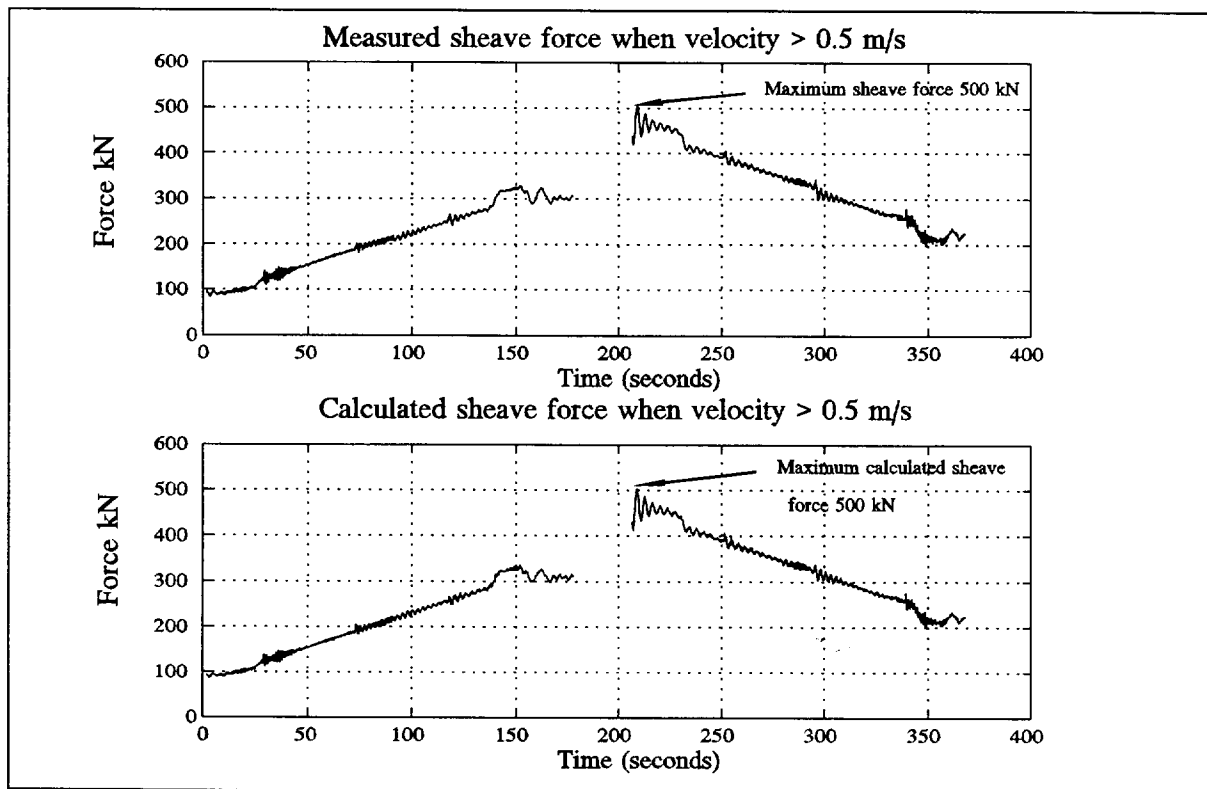
Figure 10   Measured and calculated sheave force for winder velocity $>0.5\mathrm{m.s}^{-1}$
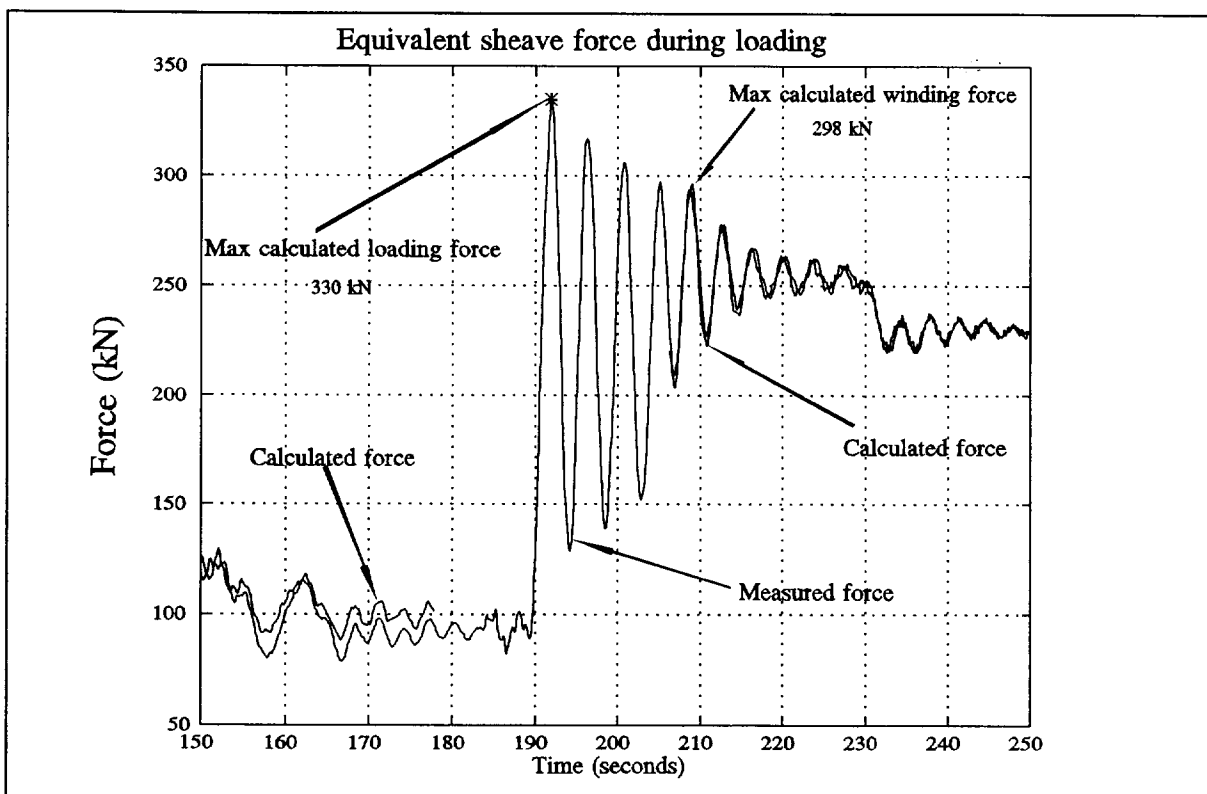
Figure 11   Equivalent sheave force during loading and acceleration from loading bay

4. CONCLUSIONS AND RECOMMENDATIONS

Load ranges during a winding cycle can be obtained from measurements at either the head sheave or the conveyance load cell. The improvement in accuracy of obtaining the load range from the head sheave (without any complicated manipulations) is offset by the decreased load cell accuracy at the head sheave.

If the load range is determined using the conveyance load cell then it is necessary to measure the conveyance position as well as the conveyance force as a function of time. A sophisticated recording system is required to carry out the data manipulations described in methods 3 and 4.

The methods proposed in this investigation were derived using measured data from a single rock winder, and a hypothetical man winder. Further development of each method may be required once applied to a winder system. The general equations will however not change.

5. REFERENCES

1.   van Zyl, M., "Load Ranges Experienced by Drum Winder Ropes", CSIR Contract Report No. MST(92)MC996, November 1992.

2.   Greenway, Dr.M.E., "Dynamic Loads in Winding Ropes - an Analytical Approach", Anglo American Mechanical Engineering department, February 1989.

3.   Greenway, Dr.M.E., "Dynamic Rope Loads Developed in Response to Instantaneous Winder Braking", Anglo American Mechanical Engineering department, June 1991.

APPENDIX A   ROCK WINDER DATA

Data from a South African rock winder was used in this investigation.

Double drum rock winder	
Winder Type Rope Speed (m.s^{-1}) Drum Dia. (m) Sheave Dia. (m)	DC Auto 16 5,54 5,54
Rock Mass (kg) Skip Mass (kg)	11 750 9 820
Rope Dia. (mm) Construction Steel area (mm^2) Tensile Grade (MPa) Mass/metre (kg.m^{-1}) Strength (kN)	48 6X32 1 053 1 800 9,75* 1 725
Suspended rope length (m) Length of wind (m) Catenary length (m)	2 204 2 196 73
Capacity Factor Safety Factor Load range Ratio	8,2 4,1 6,7

* The rope mass per metre reported was the actual rope mass and not the catalogued rope mass.

Table A1   Parameters of Rock winder used in investigation

Figures A1 to A3 show the rock winding cycle of the rock winder. A typical load recording obtained during the winding cycle is shown in Figure A1 (conveyance load cell) and Figure A2 (sheave load cell).
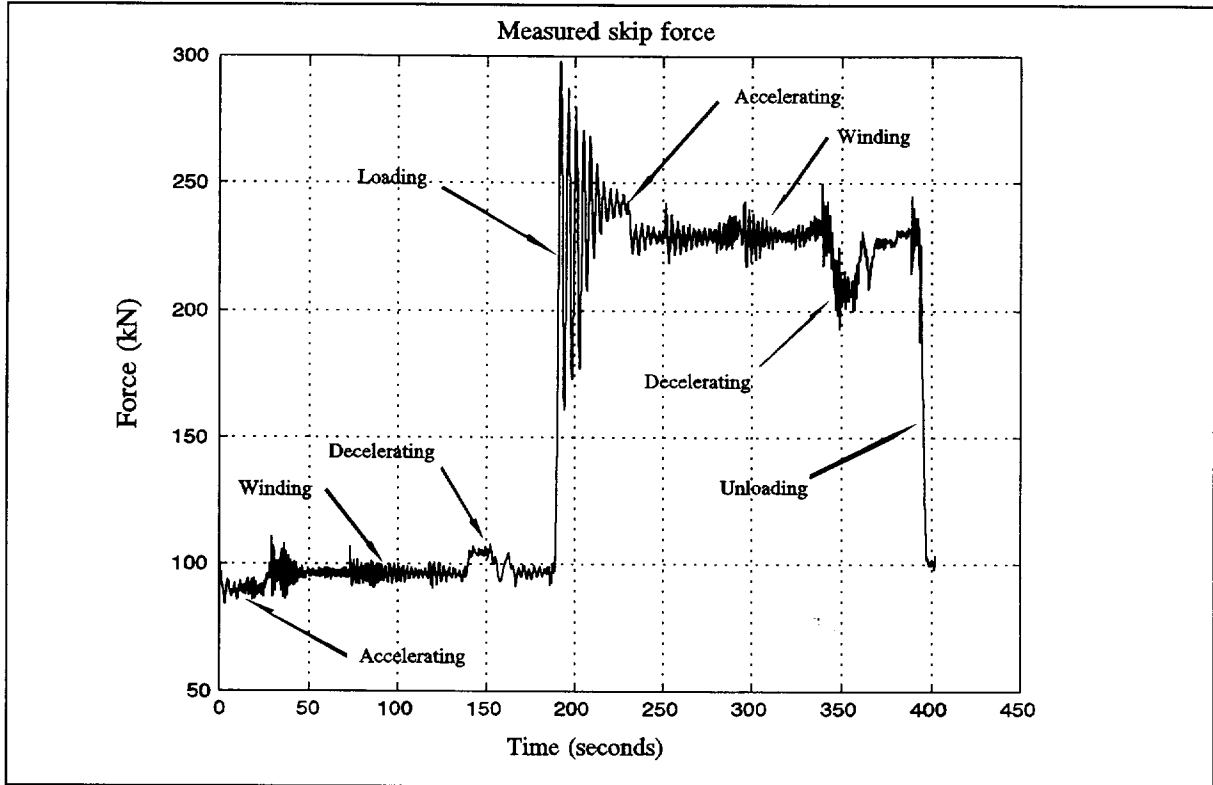
Figure A1   Measured skip force
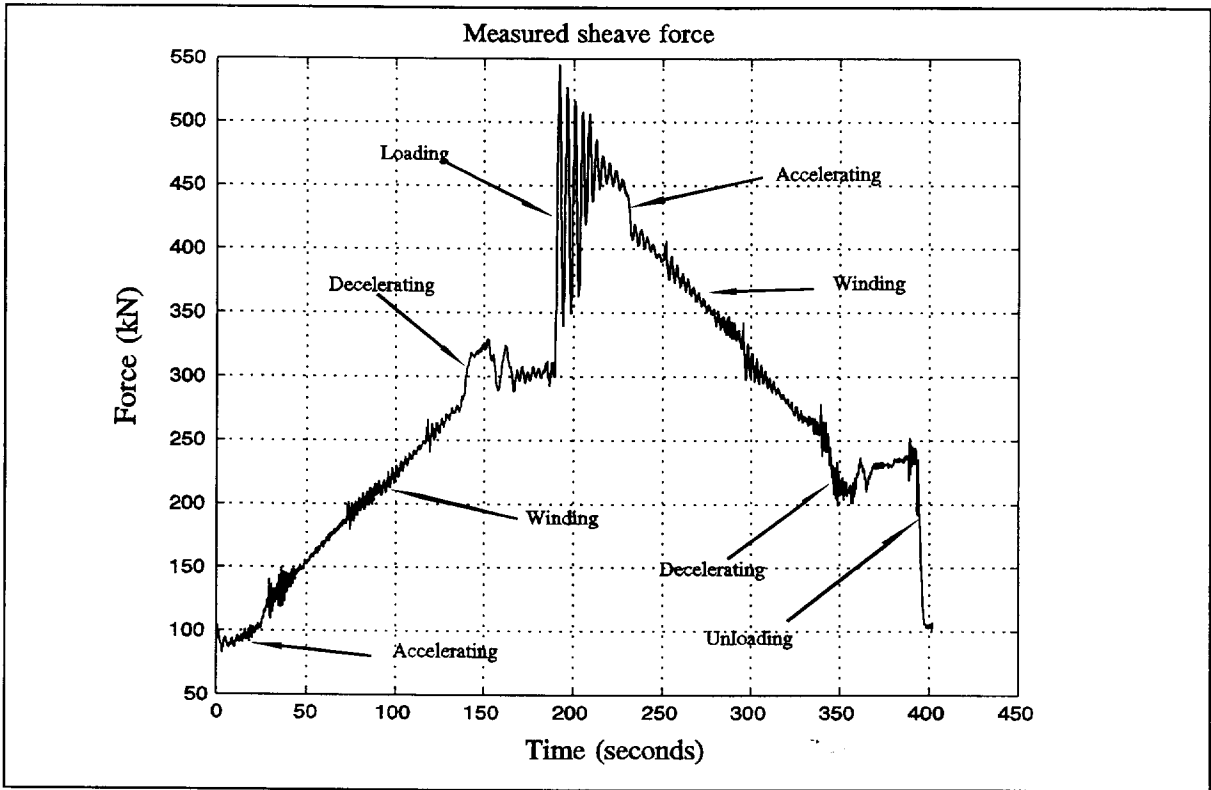
Figure A2   Measured sheave force

The suspended rope weight is calculated from the conveyance position. Figure A3 illustrates the suspended rope weight as a function of time. The rope mass multiplied by **g** (gravitational acceleration) yields the rope weight. The rope mass is obtained from the conveyance position as:

$$M_r = 1\rho_r$$

M_r = Suspended rope mass $\quad\cdots\cdots\cdots\cdots\cdots$ **(A1)**
  1 = Suspended rope length
  ρ_r = Rope mass per metre
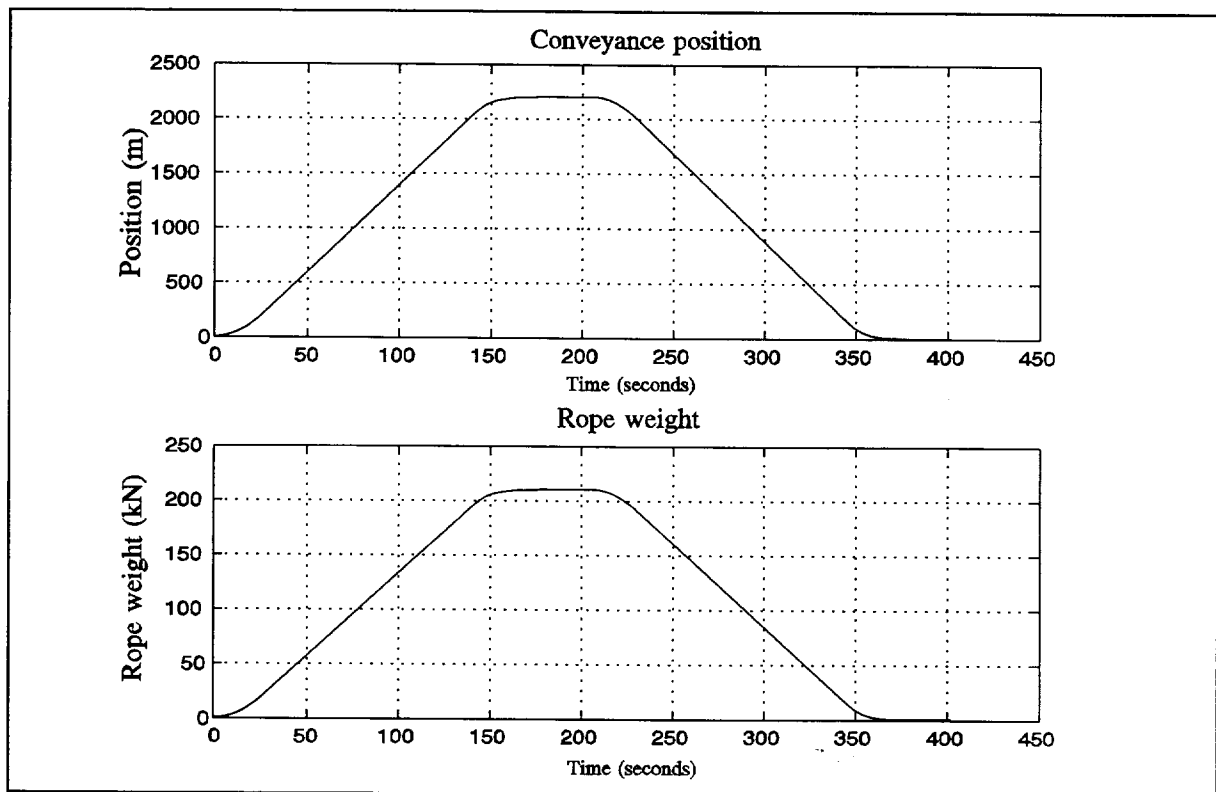
Figure A3   Conveyance position and rope weight

APPENDIX B   MAN WINDER PARAMETERS AND WINDING CYCLE

A hypothetical man winder cycle was used for this investigation. The cycle was calculated with a finite difference model. The man winder cycle was constructed using the same winder parameters as the rock winder cycle.

Rope Speed (m.s^{-1})	16
Drum Dia. (m)	5,54
Sheave Dia. (m)	5,54
Payload Mass (kg)	11 750
Conveyance Mass (kg)	9 820
Rope Dia. (mm)	48
Construction	6X32
Steel area (mm^2)	1 053
Tensile Grade (MPa)	1 800
Mass/metre (kg.m^{-1})	9,75*
Strength (kN)	1 725
Safety factor	4,1
Suspended rope length (m)	2 204
Length of wind (m)	2 196
Catenary length (m)	73

* The rope mass per metre reported was the actual rope mass and not the catalogued rope mass.

Table B1   Parameters of the hypothetical man winder
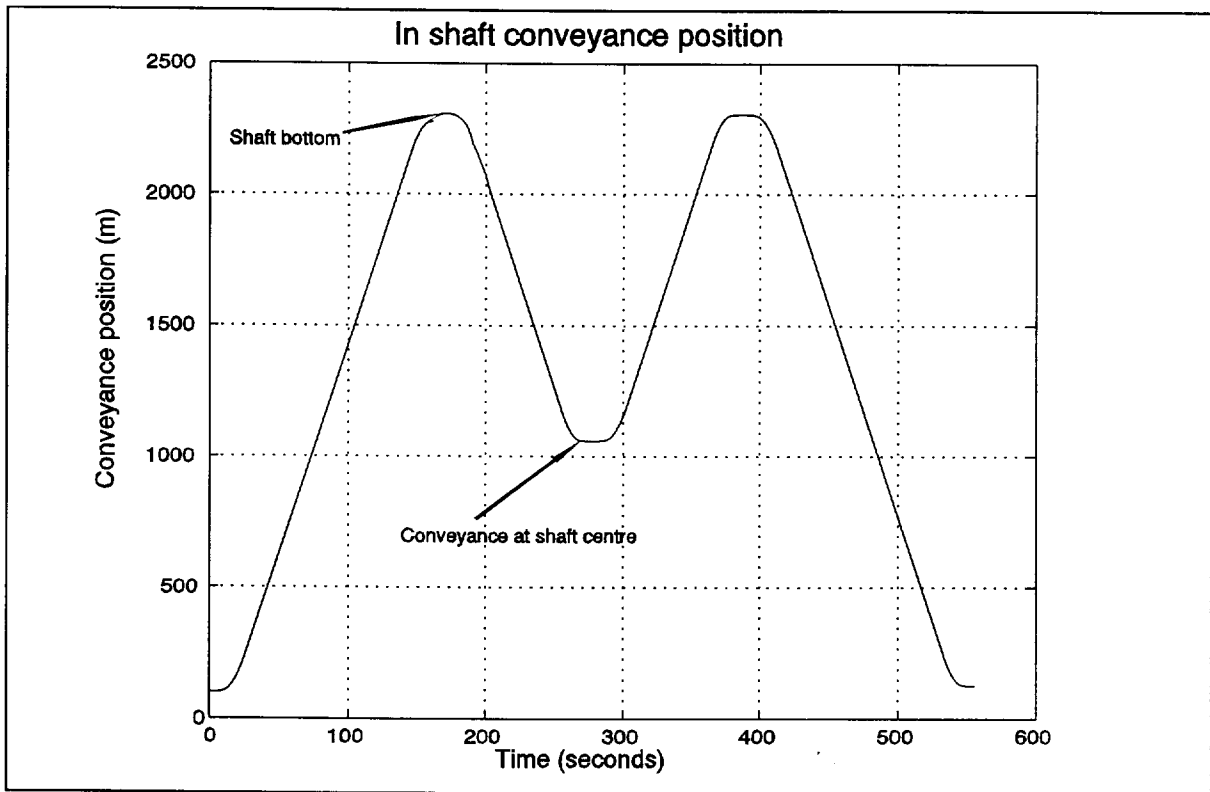
Figure B1   Conveyance position in shaft during winder cycle
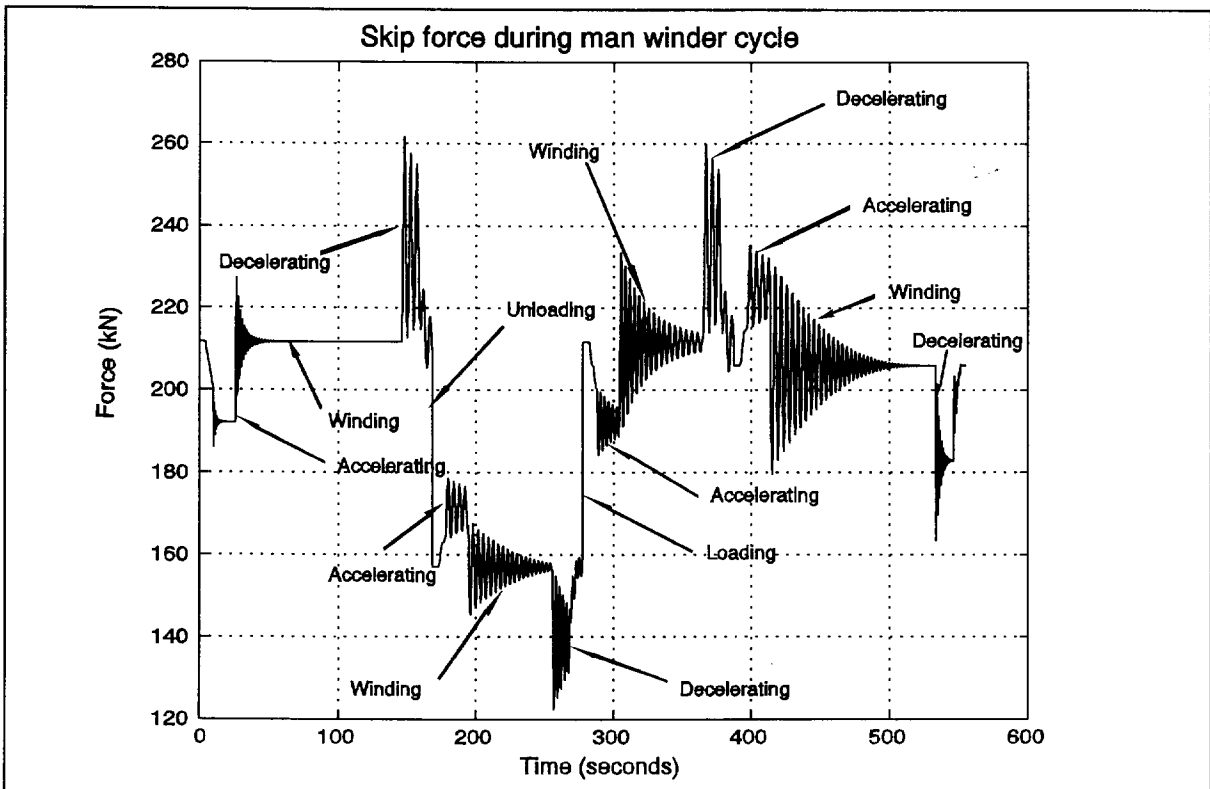
Figure B2   Calculated skip force of man winder cycle
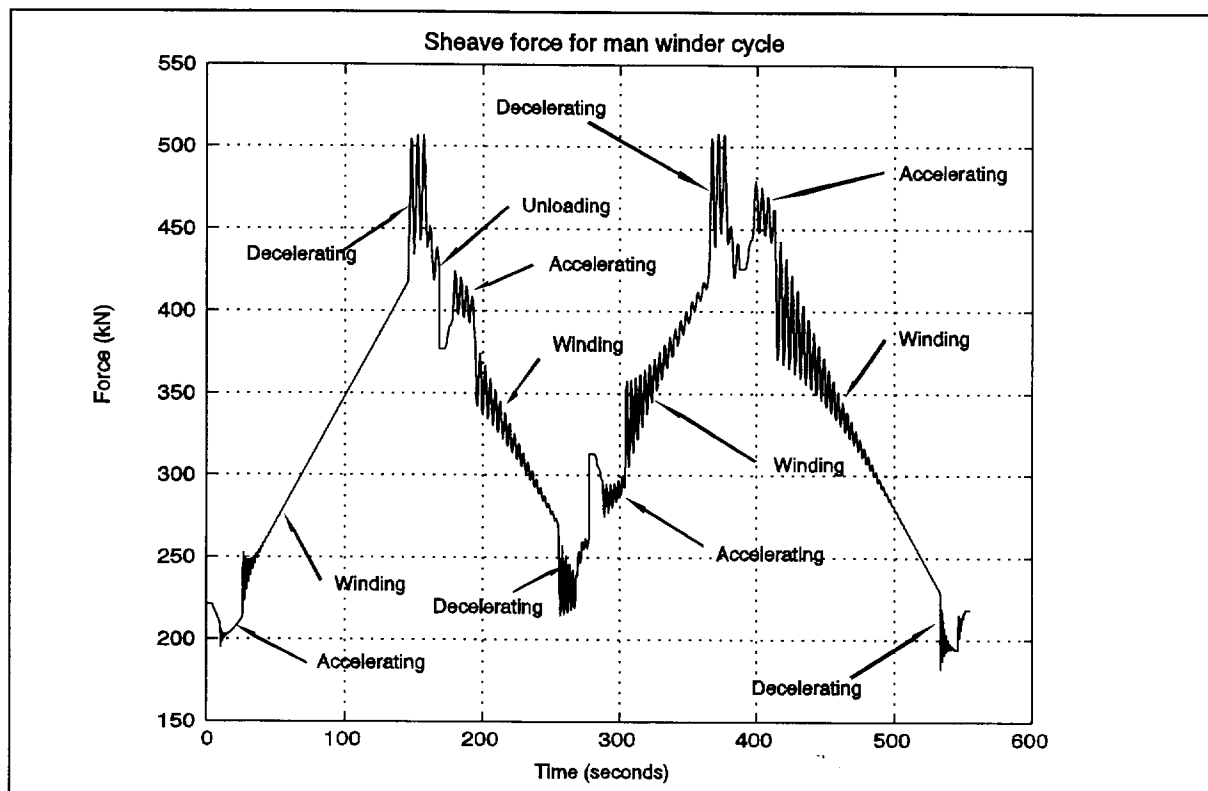
Figure B3 Calculated sheave force of man winder cycle

APPENDIX C   EQUIVALENT SHEAVE FORCE

Equivalent force calculation

The sheave force and the rope weight are a function of time. Figure **C1** shows the sheave force and the rope weight as a function of time during the winding cycle. The equivalent sheave force is calculated by subtracting the rope weight from sheave force signal while the conveyance is moving through the shaft.
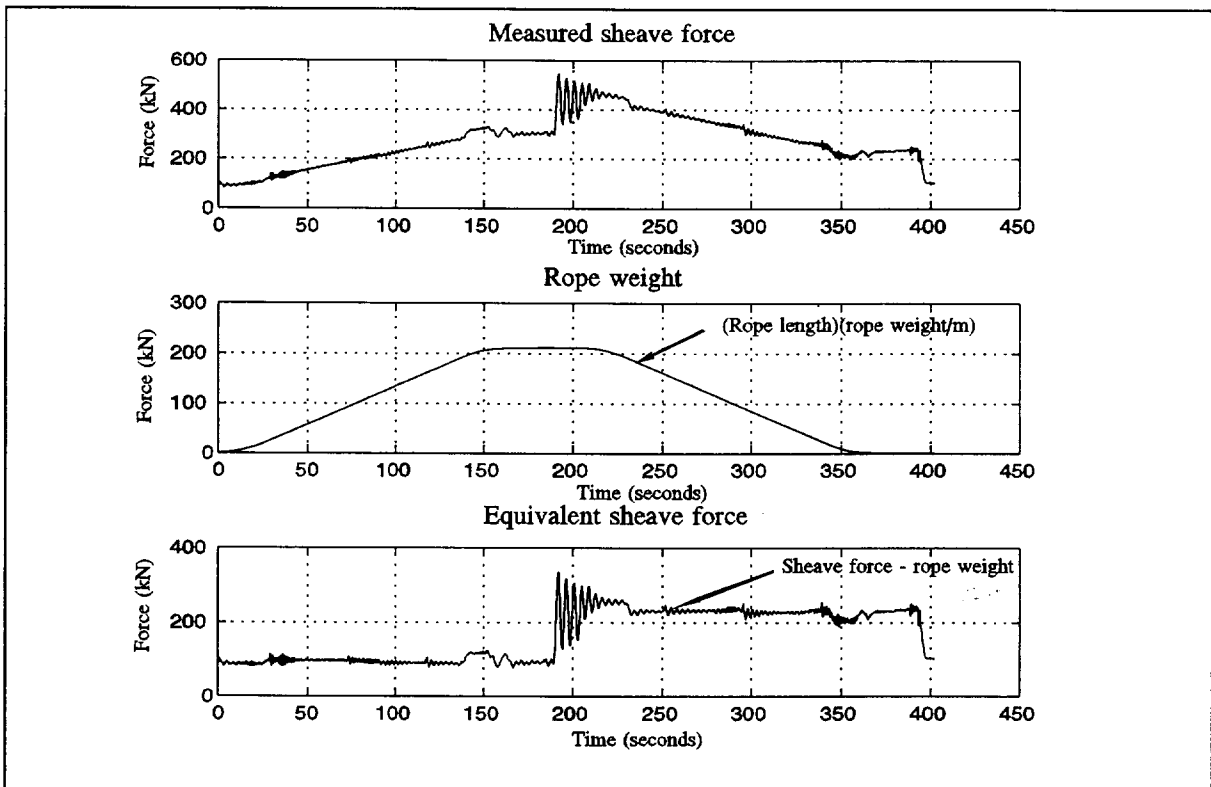
Figure C1   Equivalent sheave force

APPENDIX D   CALCULATION OF ATTACHED MASS AND PAYLOAD MASS

Conveyance load cell

The attached weight (and mass) is obtained by calculating the average conveyance force during each part of the winder trip. The average force is calculated as:

$$\text{Average weight} = \frac{\sum_{i=1}^{N} F_i}{N}$$

$$\dots\dots\dots\dots\dots\ A1$$

$$F_i = \text{Sampled force}$$

$$N = \text{Number of samples}$$

In Figure **D1** the attached weight of both the descending and ascending part of the winder cycle are calculated. The conveyance has to be in motion (absolute winder velocity greater than 0.5m.s^{-1}) when the sampled signal is averaged.
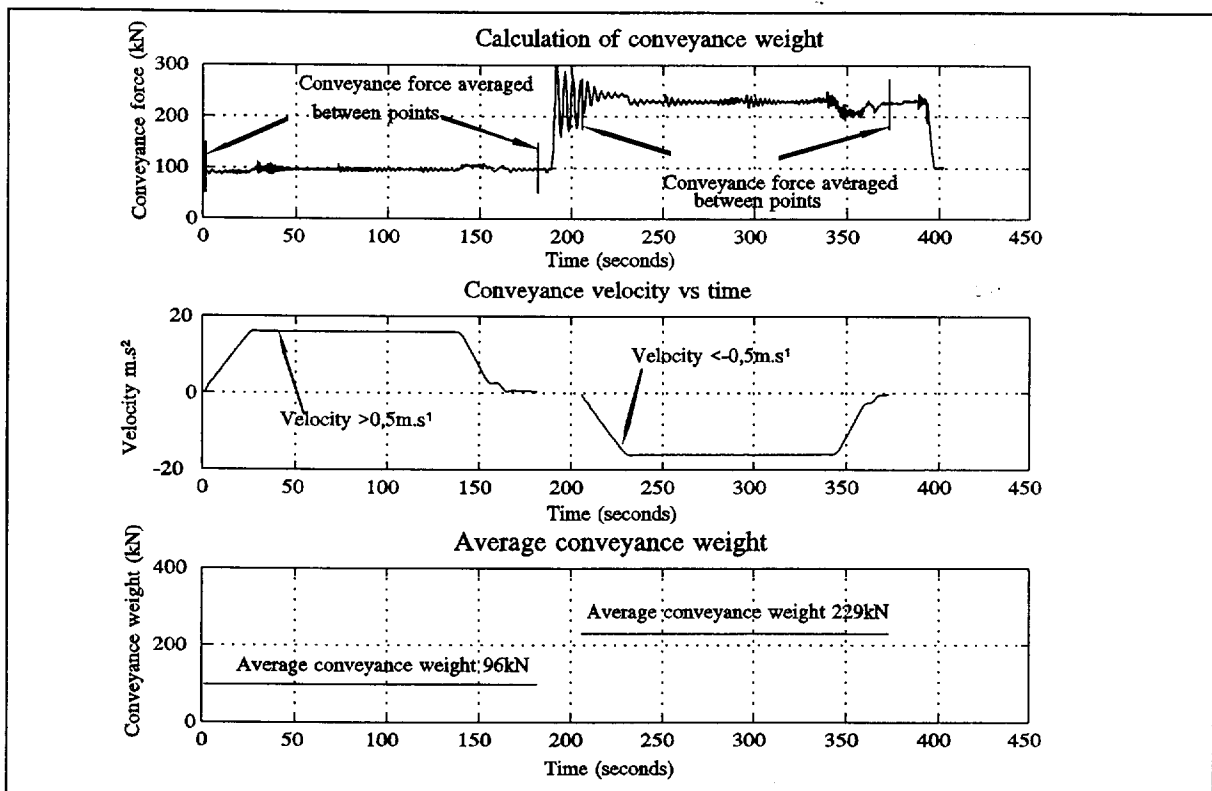
Figure D1   Conveyance weight

The calculation presented in this appendix requires that the force signal as well as the conveyance velocity is known. The force signal is averaged in the period that the conveyance is in motion. For a man winder the conveyance weight will be different for each

segment of the winding trip.

Sheave load cell

The equivalent sheave force derived in Appendix C is repeated in Figure **D2**. The attached weight may be calculated from the equivalent sheave force as well. The same method that is used for the conveyance load cell signal is used on the equivalent sheave force.
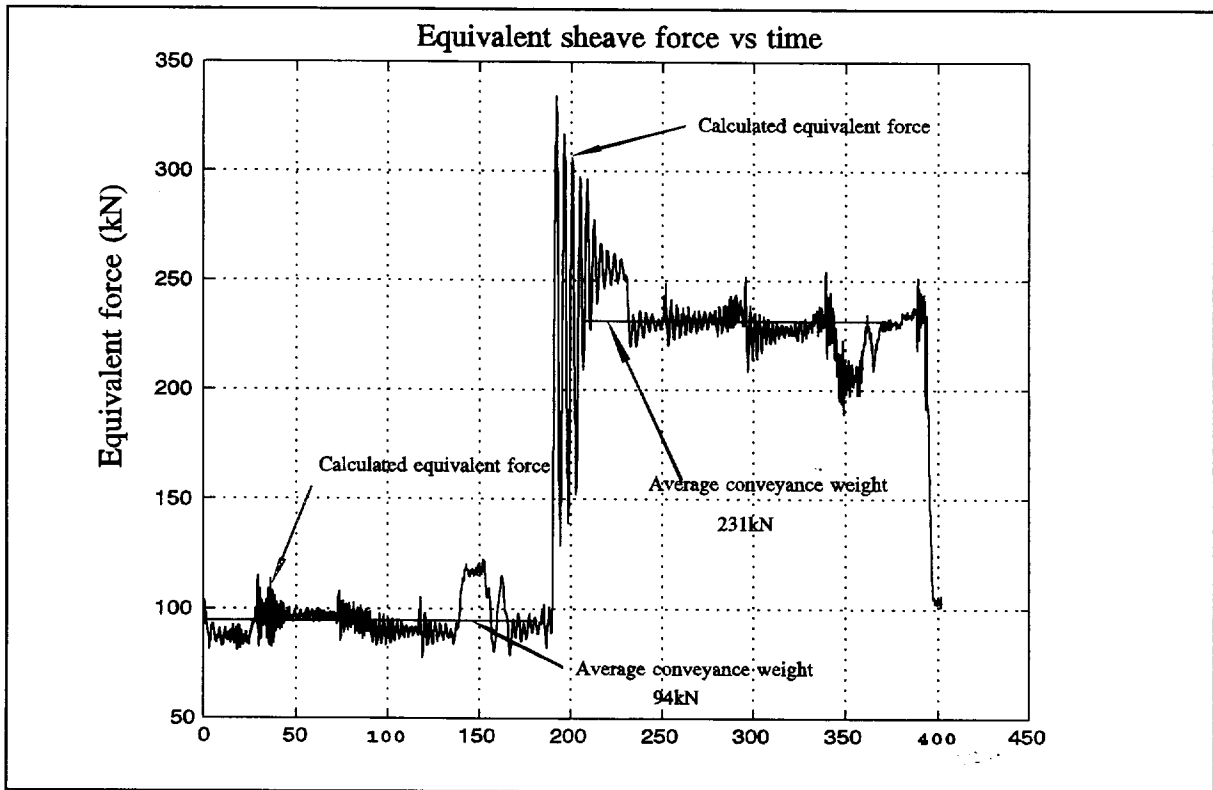
Figure D2   Conveyance weight calculated from sheave load cell

Accelerometer and conveyance loadcell

The attached mass can be determined using a conveyance loadcell and an appropriate accelerometer mounted on the conveyance. From dynamics:

$$M = \frac{F}{g + a_c}$$

where: . . . . **(A2)**

        M = Attached mass
        a_c = Conveyance acceleration
        g = Gravitaional acceleration

This method is appropriate during winding, or when the conveyance is not being loaded.

APPENDIX E   **PROPOSED WINDER COP APPENDIX LAYOUT: LOAD RANGE CALCULATIONS**

E1.   PREDETERMINED LOAD RANGE

The load range acting in a rope operating on a drum can be approximated as

$$\text{Load range} = M_p(g + 2a_m) + 3a_m(M_c + M_r)$$

Where:

$$
\begin{aligned}
g &= 9,8\,\text{m.s}^{-2} \\
M_p &= \text{Mass of payload} \\
M_c &= \text{Mass of conveyance} \\
M_r &= \text{Mass of rope} \\
a_m &= \text{Maximum winder acceleration}
\end{aligned}
$$

       . . . . E11

If the predetermined load range is used, the monitoring system shall record peak drum accelerations and payload. The controller shall log the load range to have been exceeded each time that the peak drum acceleration exceeds the value used in the above calculation.

E2.   LOAD RANGE CALCULATION FROM MEASURED BACK END ROPE FORCES

The monitoring system shall be equipped with a peak and trough hold facility for the rope force measurements from the head sheave for each rope (or set in the case of a BMR winder). The back end rope force shall be reduced by subtracting the product of the drum position and the mass per unit length and gravitational acceleration (g) to produce an equivalent rope force (if the rope is stationery the equivalent sheave force is then equal to the force acting in the front end of the rope). This equivalent rope force shall be fed into the peak and trough hold facilities. The equivalent rope force is the back end rope force minus the static weight of the suspended rope.

At the start of each winding cycle, each of the peak and trough hold facilities will be reset. At the end of the winding cycle, the load range shall be calculated by subtracting the trough of the equivalent rope force from the peak of the equivalent rope force.

E3. LOAD RANGE CALCULATION FROM MEASURED FRONT END ROPE FORCES: METHOD 3

E.3.1. Man winder

The monitoring system shall be equipped with a facility to record the conveyance force and the conveyance position at a rate of 10 samples per second as a function of time throughout the wind. The force monitoring system shall have adequate capacity to store the recorded signals for the duration of the wind and to carry out the required calculations. The signals shall be recorded during the wind and The load range shall be calculated using steps (1) to (7).

(1)   Record the conveyance position and conveyance force as a function of time during the wind, store the recorded values.

(2)   Using the recorded conveyance position data calculate the winder velocity as a function of time for the wind.

(3)   Using the calculated speed data, locate recorded force data (as a function of time or winder position) where the absolute winder velocity is larger than $0,5\text{m.s}^{-1}$.

(4)   Using the selected force data set (3) locate the maximum force and the skip position when the maximum force occurs.

(5)   Calculate the value of the suspended rope mass when the maximum rope force occurs by multiplying the conveyance position with the rope mass per metre.

(6)   Calculate the attached mass when the maximum rope force as shown in **E.3.3**

(7)   Calculate the value of $(1 + \eta)$ when the maximum rope force occurs

(8)   Using the selected force data set (3) locate the minimum force and the skip position when the minimum force occurs.

(9)   Calculate the value of the suspended rope mass when the minimum rope force occurs by multiplying the conveyance position with the rope mass per metre.

(10)   Calculate the attached mass when the minimum rope force occurs as shown in **E.3.3**.

(11)   Calculate the value of $(1 + \eta)$ when the minimum rope force occurs.

(12)   Using the maximum and minimum rope force calculate the maximum and minimum estimate sheave force using equation **E31**.

(13)   Subtract the rope weight that occurs at the maximum and minimum rope force from the maximum and minimum sheave force to obtain the maximum and minimum equivalent sheave force.

(14)   The load range is the difference between the maximum equivalent sheave force and the minimum equivalent sheave force.

$$F_{sheave} = (F_{Measured\ skip\ force})\ S_r$$

$$
\begin{aligned}
F_{Measured\ skip\ force} &= \text{Measured skip force}\\
S_r &= \text{Rigid body ratio}\\
S_r &= 1 + \eta\\
\eta &= \frac{M_r}{M_c + Mp}\\
M_r &= \text{Suspended rope mass}\\
M_c &= \text{Conveyance mass}\\
M_p &= \text{Payload}
\end{aligned}
\qquad \dots\dots\dots\ \textbf{E31}
$$

E.3.2 Rock winder

The monitoring system shall be equipped with a facility to record the conveyance force and the conveyance position at a rate of 10 samples per seconds as a function of time during the wind. Sufficient capacity shall be added to the force monitoring system to store the measured values throughout the wind and to carry out the required calculations. The load range shall be calculated using steps (1) to (10):

(1)   Record the conveyance position and conveyance force as a function of time during the wind, store the recorded values.

(2)   Using the recorded conveyance position data calculate the winder velocity as a function of time for the wind.

(3)   Using the calculated speed data, locate recorded force data (as a function of time or winder position) where the absolute winder velocity is larger than $0.5\,\text{m.s}^{-1}$ (loading force), and locate the recorded force data where the absolute winder velocity is less than $0.5\,\text{m.s}^{-1}$ (winding force).

(4)   From the selected force data set (3) find the maximum force during loading of the conveyance and find the maximum force during winding. Calculate the ratio of maximum loading force to maximum winding force.

(5)   Using the selected force data set (during winding (3)) locate the maximum force and the skip position when the maximum force occurs.

(6)   Calculate the value of the suspended rope mass when the maximum rope force occurs by multiplying the conveyance position with the rope mass per metre.

(7)   Calculate the attached mass when the maximum rope force occurs as shown in **E.3.3**

(8)   Calculate the value of $(1 + \eta)$ when the maximum rope force occurs

(9)   Using the selected force data set (winding (3)) locate the minimum force and the skip position when the minimum force occurs.

(10)   Calculate the value of the suspended rope mass when the minimum rope force occurs by multiplying the conveyance position with the rope mass per metre.

(11)   Calculate the attached mass when the minimum rope force occurs as shown in **E.3.3**.

(12)   Calculate the value of $(1 + \eta)$ when the minimum rope force occurs.

(13)   Using the maximum and minimum rope force calculate the maximum and minimum estimate sheave force using equation **E32**.

(14)   Subtract the rope weight that occurs at the maximum and minimum rope force from the maximum and minimum sheave force to obtain the maximum and minimum equivalent sheave force.

(15)   If the ratio of maximum loading force to maximum winding force is larger than 1 (3), then multiply the maximum equivalent sheave force with this ratio to obtain the adjusted maximum equivalent sheave force.

(15)   The load range is the difference between the maximum equivalent sheave force (or adjusted maximum equivalent sheave force) and the minimum equivalent sheave force.

This method applied to rock winders is described in Equation **E32**:

Maximum forces:

$$F_{max\ skip} = Max(F_{skip})...\ (Winding)$$

$$F_{max\ skip} = Max(F_{skip}...\ Loading)$$

Force ratio:

$$ratio = \frac{Max\ loading\ force}{Max\ winding\ force}$$

Equivalent force:

$$F_{Max\ sheave} = (1+\eta)F_{Max\ skip}$$

$$F_{Min\ sheave} = (1+\eta)(F_{Min\ skip})$$

E32

$$F_{Equivalent\ max} = F_{Max\ sheave} - Rope_{weight}$$

$$F_{Equivalent\ min} = F_{Min\ sheave} - Rope_{weight}$$

Adjust force:

$$F_{Equivalent\ max} = F_{equivalent\ max}(ratio)$$

Load range:

$$Load\ range = F_{equivalent\ max} - F_{equivalent\ min}$$

E.3.3 Attached mass and payload mass calculation

The attached mass is calculated for each segment of the winding cycle. The sampled conveyance force, or the sampled equivalent sheave force shall be used to determine the attached mass at each segment of the winder cycle. The attached mass shall be calculated from the average force while the winder velocity exceeds $0,5\text{m.s}^{-1}$.

$$\text{Attached mass} = \frac{\sum_{i=1}^{N} F_i}{N\,g}$$

where: E33

F_i = Sampled force
N = Number of samples
g = gravitational acceleration $(9,8\text{m.s}^{-2})$

The attached mass may also be calculated using an accelerometer and a conveyance force measurement. From dynamics:

$$M = \frac{F}{(a+g)}$$

where: E34

M = Attached mass
a = Conveyance acceleration
g = Gravitational acceleration $(9,8\text{m.s}^{-2})$

The acceleration measurement would be carried out with an appropriate accelerometer while the conveyance force is measured with the conveyance load cell.

The payload mass is obtained from the attached mass by subtracting the conveyance mass from the attached mass.

E4. LOAD RANGE CALCULATION FROM MEASURED FRONT END ROPE FORCES: Method 4

The monitoring system shall be equipped with a measuring system that shall record the skip force and the conveyance position at a sampling rate of 10 samples per seconds as a function of time during the wind. The monitoring system shall have sufficient capacity to store the data and to carry out the calculations described in this method. The sheave force shall be calculated according to equation **E41** using the steps described for the man and rock winder respectively.

$$F_{sheave} = (F_{skip\ dynamic})D_r + F_{skip\ static}S_r$$

$$
\begin{aligned}
F_{sheave} &= \text{Calculated sheave force} \\
F_{skip\ dynamic} &= \text{Dynamic skip force} \\
F_{skip\ rigid\ body} &= \text{Rigid body skip force} \qquad\qquad \textbf{E41} \\
D_r &= 0.00948\eta^2 + 0.54426\eta + 0.9825 \\
S_r &= 1 + \eta \\
\eta &= \frac{\text{Rope mass}}{\text{Conveyance mass}}
\end{aligned}
$$

E.4.1 Man winder

The load range occurring in the winding rope of a man winder shall be calculated as:

(1) Record the conveyance position and conveyance force as a function of time during the wind, store the recorded values.

(2) Using the recorded conveyance position data calculate the winder velocity as a function of time for the wind.

(3) Using the calculated speed data, locate recorded force data (as a function of time or winder position) where the absolute winder velocity is larger than $0,5 m.s^{-1}$.

(4) The data in (3) is next split into dynamic and rigid body forces. Rigid body forces are obtained by filtering the data in (3) with a digital or analog filter with a frequency response function as described in **E.4.3**. The dynamic force is obtained by subtracting the rigid body force form the measured force in (3).

(5) The rope mass is calculated by multiplying the conveyance position with the rope mass per metre. The attached mass is calculated as shown in **E.4.4**.

(6) The rigid body force ratio and the dynamic force ratio are calculated as shown in equation **E41**.

(7) The estimate sheave force is obtained by combining the measured conveyance force, the rigid body force ratio and the dynamic force ratio as shown in equation **E41**.

(8) Using the calculated sheave force data set (7) locate the maximum force and the skip position when the maximum force occurs.

(9)   Calculate the value of the suspended rope weight when the maximum rope force occurs by multiplying the conveyance position with the rope mass per metre and **g** ($9,8m.s^{-2}$), and hence calculate the maximum equivalent sheave force by subtracting the rope weight from the calculated sheave force.

(10)   Using the calculated sheave force data set (7) locate the minimum force and the skip position when the minimum force occurs.

(11)   Calculate the value of the suspended rope weight when the minimum rope force occurs by multiplying the conveyance position with the rope mass per metre and **g** ($9,8m.s^{-2}$), and hence calculate the minimum equivalent sheave force by subtracting the rope weight from the calculated sheave force.

(12)   The load range is the difference between the maximum equivalent sheave force and the minimum equivalent sheave force.

E.4.2 Rock winder

The load range occurring in the rope of a rock winder shall be calculated as:

(1)   Record the conveyance position and conveyance force as a function of time during the wind, store the recorded values.

(2)   Using the recorded conveyance position data calculate the winder velocity as a function of time for the wind.

(3)   Using the calculated speed data, locate recorded force data (as a function of time or winder position) where the absolute winder velocity is larger than $0,5m.s^{-1}$, and where the absolute winder velocity is less than $0,5m.s^{-1}$.

(4)   Find the maximum force during loading and the maximum force during winding and calculate the ratio of maximum loading force to maximum winding force.

(5)   The data in (3, winding) is next split into dynamic and rigid body forces. Rigid body forces are obtained by filtering the data with a digital or analog filter with a frequency response function as described in **E.4.3**. The dynamic force is obtained by subtracting the rigid body force form the measured force.

(6)   The rope mass is calculated by multiplying the conveyance position with the rope mass per metre. The attached mass is calculated as shown in **E.4.4**.

(7)   The rigid body force ratio and the dynamic force ratio are calculated as shown in equation **E41**.

(8)   The estimate sheave force is obtained by combining the measured conveyance force, the rigid body force ratio and the dynamic force ratio as shown in equation **E41**.

(9)   Using the calculated sheave force data set (7) locate the maximum force and the skip position when the maximum force occurs.

(10)   Calculate the value of the suspended rope weight when the maximum rope force occurs by multiplying the conveyance position with the rope mass per metre and **g** ($9,8m.s^{-2}$), and hence calculate the maximum equivalent sheave force by subtracting the rope weight from the calculated sheave force.

(11)   Using the calculated sheave force data set (7) locate the minimum force and the skip position when the minimum force occurs.

(12)   Calculate the value of the suspended rope weight when the minimum rope

force occurs by multiplying the conveyance position with the rope mass per metre and **g** (9,8m.s^{-2}), and hence calculate the minimum equivalent sheave force by subtracting the rope weight from the calculated sheave force.

(13)   If the ratio calculated in (4) is larger than 1 then the maximum equivalent sheave force is multiplied by the this ratio to obtain the adjusted maximum equivalent sheave force.

(14)   The load range is the difference between the maximum equivalent sheave force (or adjusted maximum equivalent sheave force) and the minimum equivalent sheave force.

E.4.3 Rigid body and dynamic measured force

The rigid body force ratio shall be calculated from the measured force signal by filtering the measured signal with a low band pass filter. The dynamic force shall be calculated from the measured skip force signal by subtracting the rigid body force from the measured force signal. The filter used on the measured data shall have a frequency response curve as shown in Figure E1.
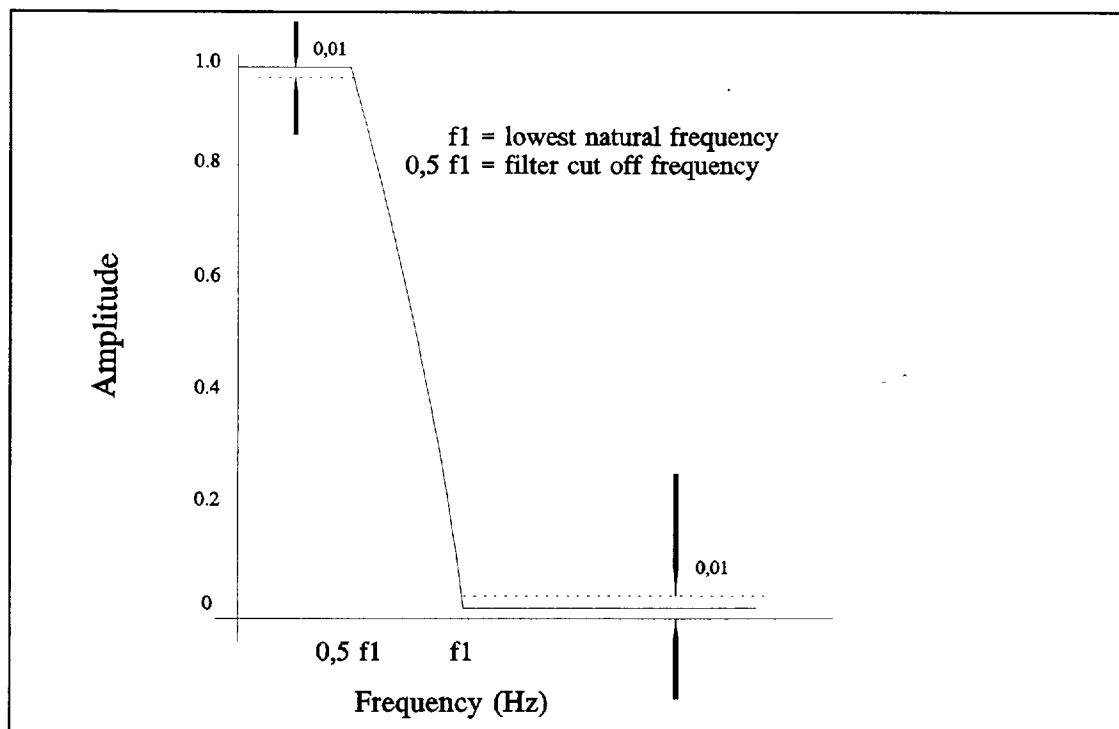
Figure E1   Frequency response function of filter

The cut off frequency shown on the frequency response diagram shall be a fraction of the lowest natural frequency of the winding system. The cut-off frequency shall be calculated as:

$$f_{cutoff} = 0,5f1$$

$$f1 = \frac{c}{2\pi L} \arccos\left[\frac{1}{0,00948\eta^2 + 0,54426\eta + 0.9825}\right]$$

where:

$$c = \sqrt{\frac{E}{\rho}}$$

$$E = 120\,GPa$$

$$\rho = 7800\,kg.m^{-3}$$

$$L = Shaft\ depth$$

$$\eta = \frac{L\rho_1 g}{(M_c + M_p)g}$$

$$\rho_1 = Rope\ mass\ per\ metre$$

$$M_c = Conveyance\ mass$$

$$M_p = Payload\ mass$$

E42

The rigid body and dynamic ratio shall be calculated as a function of the ratio η. All values of η, S_r, D_r, $F_{Sheave\ rigid\ body}$ and $F_{Sheave\ dynamic}$ shall be calculated as a function of time.

E.4.4 Attached mass and payload mass calculation

The attached mass is calculated for each segment of the winding cycle. The sampled conveyance force, or the sampled equivalent sheave force shall be used to determine the attached mass at each segment of the winder cycle. The attached mass shall be calculated from the average force while the winder velocity exceeds $0,5 m.s^{-1}$.

$$\text{Attached mass} = \frac{\sum_{i=1}^{N} F_i}{Ng}$$

where: E33
$$F_i = \text{Sampled force}$$
$$N = \text{Number of samples}$$
$$g = \text{gravitational acceleration} (9{,}8\text{m.s}^{-2})$$

The attached mass may also be calculated using an accelerometer and a conveyance force measurement. From dynamics:

$$M = \frac{F}{(a+g)}$$

where: . . . . . . (E34)
$$M = \text{Attached mass}$$
$$a = \text{Conveyance acceleration}$$
$$g = \text{Gravitational acceleration} (9{,}8\text{m.s}^{-2})$$

The acceleration measurement would be carried out with an appropriate accelerometer while the conveyance force is measured with the conveyance load cell.

The payload mass is obtained from the attached mass by subtracting the conveyance mass from the attached mass.

APPENDIX F   FILTER CHARACTERISTICS OF LOW-BAND PASS FILTER

This appendix describes the characteristics of a digital filter that is used during the investigation to calculate static and dynamic forces from the measured forces.

Cut off frequency

The cut-off frequency of the filter is set at 50% of the lowest natural frequency of the winding system in question. The lowest natural frequency of the system is obtained with the conveyance at maximum depth and with the licensed payload. Equation F1 is used to derive the first natural frequency of the winder system. The filter in question can be used as a low band pass as well as a high band pass filter. To obtain a high band pass filter the filtered signal obtained with the low band pass filter is subtracted from the unfiltered signal.

$$\omega_1 = 2\pi f1 = \frac{1}{L}\sqrt{\frac{E}{\rho}}\ \arccos\left[\frac{1}{0,00948\eta^2 + 0,54426\eta + 0,98250}\right]$$

$$\eta = \frac{\text{Maximum rope mass}}{\text{Maximum attached mass}} = \frac{21500}{23469}$$

$$L = \text{Maximum suspended ropelength} = 2204\,\text{m} \qquad \ldots\ldots \text{F1}$$

$$E = 210\,\text{GPa}$$

$$\rho = 7800\,\text{kg.m}^{-3}$$

$$\omega_1 = \text{First natural frequency (rad.s}^{-1})$$

$$f1 = \text{First natural frequency (Hz)}$$

Filter coefficients

The filter used is derived using an ideal low pass filter. A Lanczos window is used for smoothing the Fourier coefficients of the filter frequency response function. Equation F2 calculates the 2N+1 terms of the filter. The filter frequency response is obtained with Equation F3. Figure F1 shows the frequency response of the filter for a cut-off frequency of 0,5f1 and increasing values of N (N=24, N=49, N=74, N=100). Since the cut-off frequency is a small fraction of the sampling frequency, a large number of terms have to be included in the filter to ensure that the amplitude attenuation at 0Hz is 1. If too few terms are used then the attenuation of the signal amplitude is to large and errors are induced (e.g. the curve for N=24). The phase angle of the filter response is zero over the frequency range of interest as the filter coefficients are symmetric about the N+1'th term.

$$C_k = \sum_{k=-N}^{k=N} \frac{\sin(2\pi f_c k)}{\pi k} \frac{\sin\left[\dfrac{\pi k}{N}\right]}{\left[\dfrac{\pi k}{N}\right]} \quad \ldots\ldots\ldots\ldots\ldots \text{ F2}$$

$$f_c = 0.5 \frac{\text{Cut off frequency}}{\text{Sampling frequency}}$$

$$2N + 1 = \text{Width of the filter}$$

$$H(f) = 2f_c + 2\sum_{k=N}^{k=1} \sin\frac{(2\pi k f_c)}{\pi k} \frac{\sin\left[\dfrac{\pi k}{N}\right]}{\left[\dfrac{\pi k}{N}\right]} \cos(2\pi k f) \quad \ldots\ldots\ldots\ldots \text{ F3}$$

$$fc = 0.5 \frac{\text{Cut off frequency}}{\text{Sampling frequency}}$$
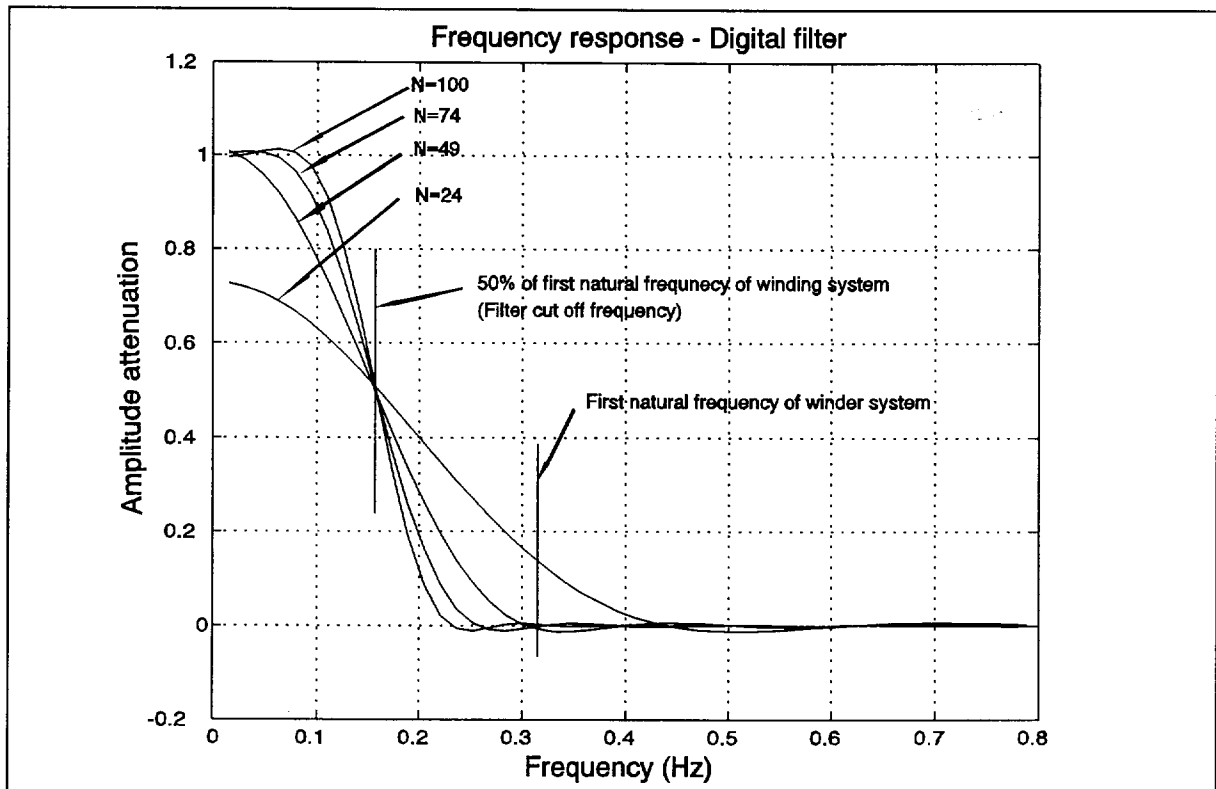
Figure F1   Frequency response of digital filter

Using the digital filter

The digital filter is used by convolving the filter coefficients with the measured readings. The convolution is obtained with equation **F4**. The digital filter derived in equation **F2** is calculated before the convolution can be carried out, the coefficients are a function of the winder parameters.

$$\text{For} \qquad i=1+N \text{ to } M-N$$

$$q(i)_{\text{filtered}} = \sum_{1}^{2N+1} C_K q_{(K+i-(N+1))}$$

End

$$\text{Where:} \qquad\qquad \ldots\ldots\ldots\ldots \textbf{F4}$$

$$M = \text{Size of measured signal}$$

$$N = \text{Size of filter}$$

$$C_K = \text{The } K'\text{th filter element}$$

$$q(i)_{\text{filtered}} = \text{The } i'\text{th filter element}$$

$$q = \text{The } i'\text{th measured element}$$

The first N and last N terms of the filtered signal cannot be calculated with the digital filter. The terms are calculated with **F5**. The filter width is $(2N+1)$ points the first calculable term is the $(N+1)$'th term, this means that a delay of $(N+1)$ times the sampling period is required before the first term of the filtered signal can be calculated. The width chosen for the filter $(2N+1)$ is dependent on the cut off frequency set for the filter.

$$q(i=1 \text{ to } i=N)_{\text{Filtered}} = q(N+1)_{\text{Filtered}}$$

and

$$q(i=(M-N+1) \text{ to } i=M)_{\text{Filtered}} = q(M-N)_{\text{Filtered}}$$

$$\text{Where:} \qquad\qquad \ldots\ldots \textbf{F5}$$

$$M = \text{Size of measured signal}$$
$$N = \text{Size of the filtered signal}$$

$$\text{Filter Delay} = (N+1)(\text{Sampling period})$$

$$\text{Sampling period} = \frac{1}{\text{Sampling Frequency}}$$

APPENDIX G   LOAD CELL ACCURACY REQUIREMENTS

In the winder Code of Practise a minimum accuracy of 1% of the rope breaking strength has been specified for measuring the rope force (and hence the load range). Measurement of the position of the conveyance is required to have an accuracy of 0,1% of the depth of the shaft. The choice of sheave load cell should therefore allow the calculated accuracy of the equivalent rope force to be greater than 1% of the allowable rope breaking strength.

The accuracy of methods 3, 4 and are to a larger extent limited by the accuracy of the load cell. In the controlled environment of this investigation the method accuracies were up to 2% of the maximum rope load range or 0,2% of the rope breaking strength. A load cell accuracy of 1% the rope breaking strength will therefore limit the accuracy of the applied method.

A sheave load cell accuracy of 0,25% the full scale (rope breaking strength) or 2,5% of the maximum rope load range. A skip load cell accuracy of at least 2,5% of the maximum load range is required.

A position measurement accuracy of 0,1% the shaft depth is recommended.

1

ROPE DETERIORATION:
FIELD STUDY REQUIREMENTS
AND RECOMMENDATIONS

by

G F K Hecker

CSIR Contract Report No. 950107
Job No. MC2450
March 1995

Submitted to:
      The Safety in Mines Research Advisory Committee

Prepared by:

Issued By:
      Mine Hoisting Technology
      Division of Materials Science and Technology
      CSIR
      Private Bag x28, Auckland Park, 2006

                                                                       G F K Hecker

      Telephone   (011) 726 7100
      Telefax   (011) 726 6418

SYNOPSIS

At the request of the Gold and Platinum Engineering Advisory group, a programme was drawn up to study the deterioration of ropes operating on drum winders. This report briefly describes the rope life histories and reasons for discarding ropes on several selected winders. Four winders have been selected for further field deterioration studies and a detailed study programme is proposed.

1. INTRODUCTION

The newly proposed rope safety regulations have been based on the information on rope deterioration that is currently available. The equation $SF = 25000/(4000 + L)$ for the required static factor was motivated on the basis that the load range acting in the rope is the only parameter that requires a limit. A statistical analysis[1] has, however, shown that there are many more parameters that influence rope life. Unfortunately the results of this study were very much affected by a lack of proper rope discard criteria. This problem is currently being addressed and a rigorous set of discard criteria is being introduced. Nonetheless there is still a lack of understanding of how various operating conditions affect rope deterioration. Consequently, the need for a test facility was expressed[2] to study simulated in-service rope deterioration. A feasibility study[3] has shown that there is not sufficient information available to compile adequate design specifications for such a test facility. It was concluded that further information on rope behaviour on winders was required before it could be assessed whether a test facility could be realised.

A different proposed strategy was to study rope deterioration on selected winders and to correlate the results of this study with the operating conditions of the rope. The main advantages of this approach are that no large capital expenditure is necessary and that several tests can be conducted concurrently. The major disadvantage is, of course, that the range of operating conditions will be limited to those set by current installations and that extrapolations must be done with circumspection.

This report describes the preliminary work done to identify winders on which rope deterioration could be studied and to draft a study programme.

2. SITE VISITS

The project started with visits to two winders where reportedly very good and very poor rope lives are being achieved respectively. The purpose of these visits was to assess the suitability of the winders for deterioration studies and to gain information on maintenance and operating procedures.

2.1 VISIT TO VAAL REEFS MINING AND EXPLORATION CO

Shaft: No 10
Date: 20 July 1994
Person met: Mr Derick Walters
              Shaft Engineer

The rock winder on the No 10 Shaft Rock/Vent Shaft was chosen as a possible suitable winder for this study because of a history of poor rope life.

Details of the winder and ropes are as follows:-

Permit No	6623	Rope diameter	62 mm
Serial No	D8603011602	Rope construction	6x33(15/12/6+3T)/F
Drum diameter	6,04 m	Static Factor	4,52
Sheave diameter	6,10 m	Capacity Factor	8,59
Rope suspended length	1814 m	Tensile grade	1800 MPa
Pay load	17,5 t	Rope mass	16,42 kg/m
Conveyance mass	15,5 t	Current ropes installed	93-11-21

The previous ropes were discarded after 24 000 cycles. They had used the new Anglo American discard criteria and had extended the life by a few months. The current ropes are still on and have already exceeded the life achieved by the previous ropes. Mr Walters expects that they will achieve a life of 100 000 cycles. He attributes the improvement in life to the incorporation of the Levelok™ device, which has given an immediate benefit in reduced spillage.

It is their ultimate aim to increase the payload to 21 tons with a possible reduction in conveyance mass. This will involve conforming to the codes of practice envisaged in present draft legislation[4]. They therefore propose to modify the winder to conform with all the requirements of the codes and newer Anglo design parameters such as the S shaped Lebus groove profile.

Meanwhile, they have been undertaking studies of winder parameters to correct existing deficiencies. One of these involves the risers on the present Lebus shells that appear to be giving problems with drum coiling associated with catenary vibration.

The winder was examined and found to run smoothly. The only problem that was obvious was a slight misalignment in the headgear sheaves. The plummer blocks were mounted on an inclined base that made it exceedingly difficult to achieve perfect alignment.

We were well received and cooperation in future activity seems to be assured as Mr Walters offered to carry out dynamic tests at any time, to suit the CSIR.

---

*   A device for clamping a conveyance during loading

2.2   VISIT TO WESTERN DEEP LEVELS - EAST MINE

Shaft: No 3 Tertiary
Date: 21 July 1994
Person met: Mr Grant Thorburn
                Relieving LTL Engineer

The rock winder on the No 3 Tertiary Shaft was chosen as a possible suitable winder for this study because of excellent rope life.

Details of the winder and ropes are as follows:-

Permit No	4071	Rope diameter	51 mm
Serial No	100/0790	Rope construction	6x32(14/12/6+3T)/F
Drum diameter	4,876 m	Static Factor	6,79
Sheave diameter	4,876 m	Capacity Factor	9,80
Rope suspended length	813 m	Tensile grade	1900 MPa
Pay load	12,25 t	Rope mass	11,12 kg/m
Conveyance mass	8,12 t	Current ropes installed	94-04-18

The winder was examined and found to run smoothly. The only problem that was obvious was a slight misalignment in the headgear sheaves and wear in the groove that has created a small shoulder. On the underlay rope there is a bang at the second layer crossover. The winder operates smoothly under automatic control.

The ropes had been in service for only a few months. Flattening of outer wires was noted but there was no evidence of wear.

The staff was helpful, but the disadvantage with this winder is the difficulty in visiting; it took 2 hours to reach the winder after arriving on the mine and it is only possible to leave at fixed times when there is cage availability.

It was proposed to examine rope test records kept by the rope testing technician before a decision is made regarding the study of this winder. There may be other winders with equally good rope life, but with easier access.

3. ANALYSIS OF ROPE LIVES AND REASONS FOR DISCARD

It is important to select winders that have sufficiently consistent rope lives so that it can be assumed that the life is determined by conditions that do not change significantly from rope to rope. It is also important that the reasons for discarding the ropes on each winder are consistent. It may then be assumed that similar deterioration modes may be expected once the proposed field deterioration studies commence.

3.1 DATA INSPECTION FROM WINDER STATISTICS

The data collected for a statistical analysis[5] was inspected to find those winders that gave consistent rope lives and reasons for discard. The data needed to be reduced to those winders where ropes were discarded because of "valid" reasons. Wherever discard reasons such as *bad rope manufacture*, *required life achieved* and *rope too short* were stated, it had to be assumed that the ropes could have remained in service longer. Naturally it is not known how long the potential life of such ropes would have been. Winders were thus excluded from the data set if such discard reasons were given for all ropes that operated on a particular winder. Ropes discarded because of corrosion were ignored because this deterioration mechanism will not be studied.

The consistency of the rope lives was evaluated by the sample standard deviation of the number of cycles completed by each set of ropes on the various winders. The sample standard deviation is given by

$$\sqrt{\frac{n \Sigma x^2 - (\Sigma x)^2}{n(n - 1)}}$$ with n the number of rope sets and x the rope life for each set,

and varies from the population standard deviation by a factor $\sqrt{\dfrac{n}{n - 1}}$.

Figure 1 shows the sample standard deviations as vertical lines with the upper end of each line representing the longest rope life achieved on each particular winder on a logarithmic scale. (The longest rope life on a winder was considered more important than the mean because it represents possible rope lives on that winder rather than actual rope lives). The data were sorted to have the smallest standard deviation, expressed as a percentage of the maximum rope life, on the left of this figure and the largest on the right. When selecting a short list of possible candidates from this figure, the following had to be kept in mind:

- A base winder was required with a very long maximum rope life, i.e. in the upper portion of the graph.

- Winders with rapid deterioration would show up at the bottom of the graph.
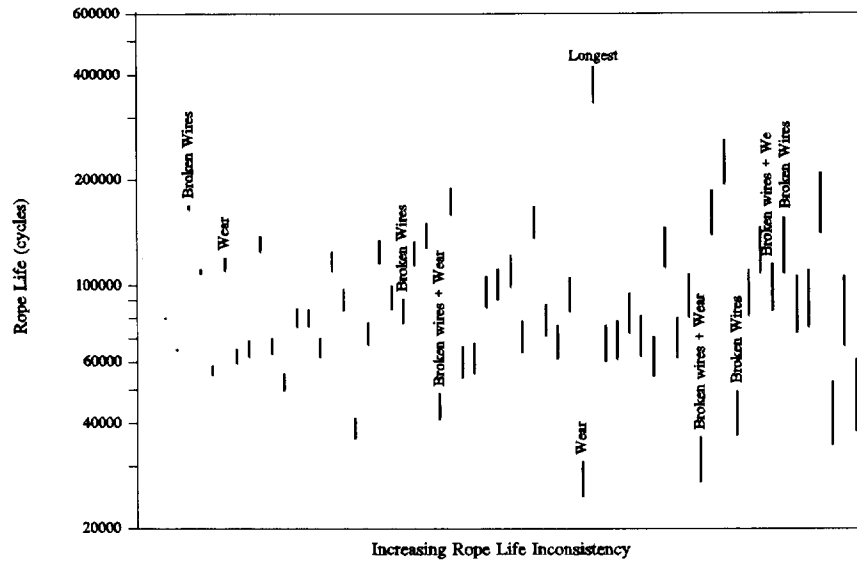
Figure 1: Sample standard deviations for rope lives on winders sorted according to increasing inconsistency

• From a possible selection of winders, those with the most consistent rope lives (i.e. to the left of the graph) would be preferred.

• Most important: The reasons for discarding the ropes should be clear. Wherever proper reasons for discard were found, these were labelled in Figure 1.

The following table is a short list of winders that, besides those visited on site, were considered for field trials. Whenever different reasons were reported for discarding different rope sets, the reason for that set that had the longest life is tabled.

Winder Type	Mine	Shaft	Depth (m)	Discard Reason	Maximum rope life (cycles)	Winder Permit
DD	St Helena	4	907	Rope too short	423470	2084
DD	Hartebeestfontein	4	2064	Normal wear	36280	6523
DD	West Driefontein	4	1463	Rope damaged	114500	3987
Blair	East Driefontein	2	2043	Broken wires	91000	4066
DD	President Brand	1	1158	Broken wires*	169196	2159
DD	Vaal Reefs	1 Sub	1067	Wear*	119985	4041B
Blair	Vaal Reefs	4	2073	Wear and broken wires	48557	6569
DD	Vaal Reefs	5	2161	Broken wires*	49327	6595
DD	Premier	1	608	Broken wires*	155671	4521

* These reasons for discard were consistent for all rope sets on the particular winder.
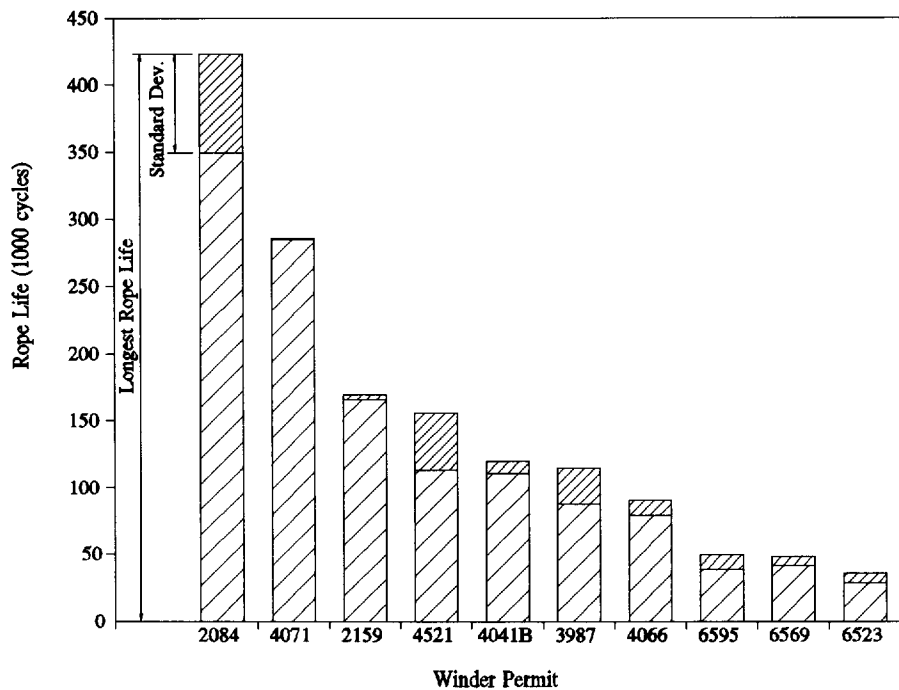
Figure 2: Rope lives on short list of winders

Figure 2 shows a bar chart of the verified rope lives on the short list of winders considered for the proposed field trials. The height of each bar shows the longest rope life achieved on each winder while the upper (finely hatched) section of the bar shows the population standard deviation of all the rope lives on that winder.

3.2 ROPE TEST HISTORY FROM CSIR DATABASE

Figure 3 shows the various ropes operating on the different winders as horizontal lines. Each line starts at the time when, according to the particulars supplied by the mine, the rope was installed. The vertical ticks on each line indicate the date on which a specimen of that rope was tested. The ropes have been grouped according to the winders that they operate on and the winder permit is shown on the left of the chart.

The following points can be observed from this chart:

- Apparently no rope tests were done during the period depicted by the left the chart. This is because the CSIR test database only started being recorded on computer during 1984.

- While the last test on most ropes was done before a new set was installed, it is interesting that, occasionally, rope specimens were tested *after* a new set was installed. Presumably such tests are on specimens of discarded ropes.

12 Months
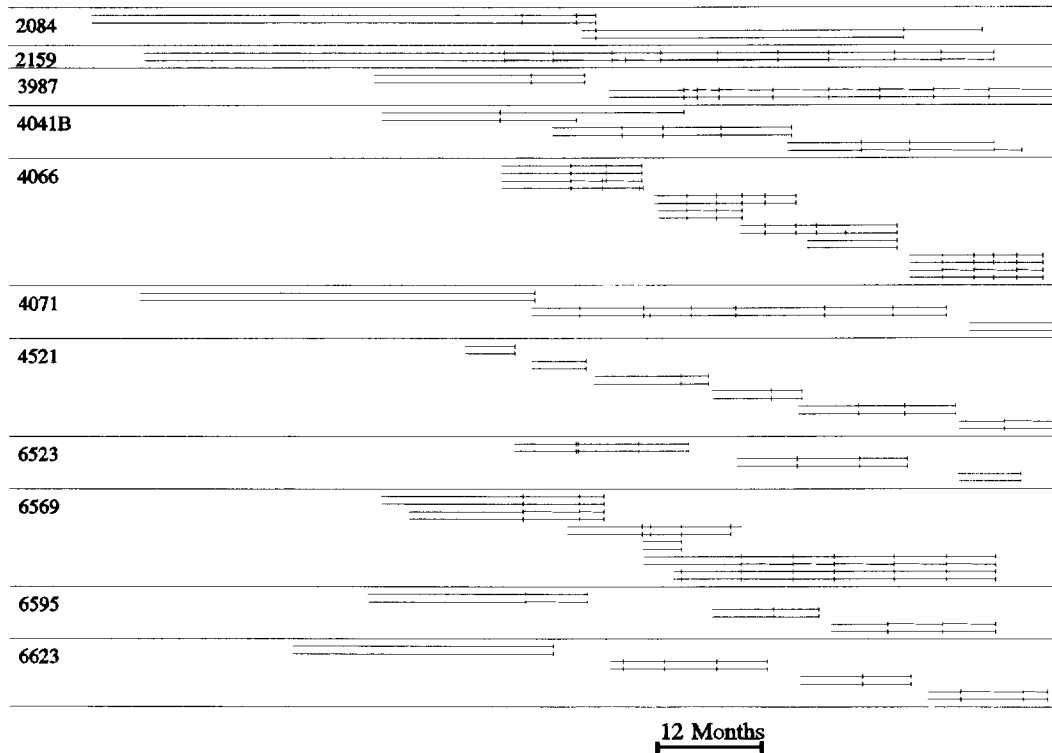
When this chart, which shows rope life on a time scale, is compared to Figure 2 which shows rope life in cycles, the differences are clear. The set of ropes operating on the winder with permit 2159, for example, is still the same set that was installed after the statistical data was being gathered. Winder 2084, on the other hand, is already on the second set but the number of cycles accumulated per set is much higher.

4. RECOMMENDATIONS

It must be borne in mind that the ultimate goal of rope deterioration studies is to understand the interaction between ropes and winders to such a degree that reliable rope life predictions can be made. Relationships between operating conditions and rope deterioration must therefore be derived.

It is recommended that a field deterioration study be done to establish the damage accumulated by ropes that operate on winders which subject the ropes to different modes of deterioration. The actual rope duties should be investigated and the performance of each rope should be traced throughout its life. Such a study should end with destructive strength tests on selected sections of each rope after discard.

Parameters like rope diameter, laylength and number of broken wires are recorded during routine rope condition assessments. This information should be made available to the investigators.

4.1 WINDER SELECTION

The previous sections have dealt with the extraction of a short list of winders that would be possible candidates for a field deterioration study. The following is a brief discussion of each of these. Interested readers may study the CSIR report on rope life prediction[1] that shows the predicted life of the ropes on these winders.

4.1.1 St Helena No. 4 shaft, Winder Permit 2084

Winder and rope details:

Drum diameter	4,267 m	Rope construction	6x32
Sheave diameter	4,267 m	Static Factor	7,4
Rope suspended length	907 m	Capacity Factor	12,0
Pay load	7,72 t	Tensile grade	1765 MPa
Conveyance mass	5,02 t	Rope mass	8,6 kg/m
Rope diameter	46 mm	Present rope installed	unknown

This winder has displayed the longest rope lives by far. Previous ropes have remained in service for between 3 and 8,5 years. Ropes have been discarded because they have shown wear. The set of ropes that was in use for over 423 000 cycles, however, was discarded because it became too short.

It is suggested that this winder be chosen as a reference winder, i.e. where very low deterioration rates are expected.

4.1.2 Hartebeestfontein No. 4 shaft, Winder Permit 6523

Winder and rope details:

Drum diameter	4,877 m	Rope construction	6x33
Sheave diameter	5,79 m	Static Factor	4,8
Rope suspended length	2064 m	Capacity Factor	10,9
Pay load	10,9 t	Tensile grade	1765 MPa
Conveyance mass	8,3 t	Rope mass	11,8 kg/m
Rope diameter	54 mm	Present rope installed	94-03-05

The ropes with the longest lives (28 000 and 36 000 cycles) on this winder were discarded because of normal wear. In other cases, however, broken wires appeared and ropes were discarded after 23 000 and 14 500 cycles. This winder would make an interesting study case because the ropes have the same tensile grade as those on the St Helena winder but attain less than one tenth of the number of cycles. If it can be assumed that broken wires no longer occur on ropes operating on this winder, it would be an ideal candidate to study rope wear. If, on the other hand, broken wires still occur, another winder should be chosen.

4.1.3   West Driefontein No. 4 shaft, Winder Permit 3987

Winder and rope details:

Drum diameter	4,876 m	Rope construction	6x31
Sheave diameter	4,267 m	Static Factor	5,5
Rope suspended length	1453 m	Capacity Factor	10,2
Pay load	9 t	Tensile grade	1750 MPa
Conveyance mass	7,19 t	Rope mass	9,3 kg/m
Rope diameter	46 mm	Present rope installed	90-10-14

The rope lives on this winder range between 51 000 and 114 500 cycles. The set of ropes that achieved the highest number of cycles was discarded because of damage and not because of normal deterioration. Other rope sets were discarded because of broken wires and/or wear. The number of cycles achieved with successive rope sets has steadily increased. This suggests changing operating conditions. Because of these inconsistencies, this winder is not recommended for a field deterioration study.

4.1.4   East Driefontein No. 2 shaft, Winder Permit 4066

Winder and rope details:

Drum diameter	4,267 m	Rope construction	6x30
Sheave diameter	4,267 m	Static Factor	4,8
Rope suspended length	2043 m	Capacity Factor	10,3
Pay load	17,25 t	Tensile grade	1800 MPa
Conveyance mass	13,02 t	Rope mass	8,7 kg/m
Rope diameter	45 mm	Present rope installed	93-09-19

The number of cycles achieved with ropes on this winder varied between 59 000 and 91 000. All the ropes were discarded because of broken wires, but one set also exhibited plastic deformation. This winder was therefore considered as a suitable candidate to study the onset and progress of broken wires.

4.1.5   President Brand No. 1 shaft, Winder Permit 2159

Winder and rope details:

Drum diameter	3,962 m	Rope construction	6x29
Sheave diameter	4,880 m	Static Factor	5,9
Rope suspended length	1158 m	Capacity Factor	9,5
Pay load	8,50 t	Tensile grade	1900 MPa
Conveyance mass	5,46 t	Rope mass	7,2 kg/m
Rope diameter	41 mm	Present rope installed	86-03-29

The information on only two sets of discarded ropes could be verified on this winder. Both sets were discarded because of broken wires. 162 000 and 170 000 cycles were achieved with the two sets respectively. Although these rope lives are consistent, there are only two samples. For this reason, and also because the rope lives are relatively long, it was decided not to choose this winder for field deterioration studies.

4.1.6 Vaal Reefs No. 1 sub-vertical shaft, Winder Permit 4041B

Winder and rope details:

Drum diameter	3,960 m	Rope construction	6x30
Sheave diameter	3,657 m	Static Factor	6,4
Rope suspended length	1067 m	Capacity Factor	10,2
Pay load	9,07 t	Tensile grade	1800 MPa
Conveyance mass	4,60 t	Rope mass	7,7 kg/m
Rope diameter	42 mm	Present rope installed	94-08-14

This winder has very consistent rope lives and all the ropes were discarded because of wear (although, unfortunately, the reason currently reported for discarding ropes is *end of useful life*). It is an ideal choice to study rope wear. Unfortunately it is located underground and is therefore not as easily accessible as surface winders.

4.1.7 Vaal Reefs No. 4 shaft, Winder Permit 6569

Winder and rope details:

Drum diameter	4,876 m	Rope construction	6x30
Sheave diameter	3,960 m	Static Factor	4,6
Rope suspended length	2073 m	Capacity Factor	10,0
Pay load	16,8 t	Tensile grade	1800 MPa
Conveyance mass	12,8 t	Rope mass	8,2 kg/m
Rope diameter	43,5 mm	Present rope installed	94-11-11

This winder is an excellent choice for a field deterioration study for the following reasons. The rope lives are short and consistent and the discard reason for all the rope sets is a combination of wear and broken wires (although the phrase *end of useful life* is currently used).

4.1.8 Vaal Reefs No. 5 shaft, Winder Permit 6596

Winder and rope details:

Drum diameter	5,486 m	Rope construction	6x32
Sheave diameter	3,658 m	Static Factor	4,9
Rope suspended length	2161 m	Capacity Factor	10,8
Pay load	11,5 t	Tensile grade	1950 MPa
Conveyance mass	6,0 t	Rope mass	9,9 kg/m
Rope diameter	48 mm	Present rope installed	94-01-08

All the rope sets on this winder were discarded because of broken wires. The variations in rope lives (19 000 to 49 000 cycles), however, cause reservations in selecting this winder for field deterioration studies.

4.1.9 Premier No. 1 shaft, Winder Permit 4521

Winder and rope details:

Drum diameter	3,965 m	Rope construction	6x32
Sheave diameter	4,800 m	Static Factor	6,9
Rope suspended length	608 m	Capacity Factor	8,7
Pay load	11,82 t	Tensile grade	2000 MPa
Conveyance mass	9,46 t	Rope mass	9,4 kg/m
Rope diameter	47 mm	Present rope installed	94-03-13

This winder could be a good choice for deterioration studies because its ropes accumulate cycles very quickly (due to its shallow depth of wind) and all ropes were discarded because of broken wires. The variations in rope life (30 000 to 156 000 cycles), however, preclude this winder from serious investigations.

4.1.10 Counterweight winders

The rope on the counterweight side of a counterweight drum winder is normally discarded together with the rope on the "working" side. It is generally accepted that the rope on the counterweight side deteriorates at a much lower rate than the "working" side rope. This can be ascribed to the fact that counterweight ropes experience very small load ranges.

Tracing the deterioration of counterweight ropes will support the study on the deterioration mechanisms of drum winder ropes, especially when the effect of load range on rope life is studied.

In summary, it is proposed to select the following winders for the proposed field deterioration study:

Winder	Study object
St. Helena No. 4 shaft	Longest rope life
Vaal Reefs No. 1 sub *or* Hartebeestfontein No. 4 shaft	Wear
East Driefontein No. 2 shaft	Broken wires
Vaal Reefs No. 4 shaft	Wear and broken wires
Counterweight winder (to be selected)	Low load ranges

4.2 STUDY PROGRAMME

Each winder selected in the previous section should be regarded as a rope fatigue test facility. It is proposed that the following test programme be followed on these winders:

4.2.1 Verification of winder parameters

Although the parameters of the chosen winders have been verified during the data collection for the statistical analysis[1], a brief check needs to be none to establish whether any parameters have changed during the last five years. If the original design duties of the winders are available, they should be compared with the duties that these winders have to perform today. Specific points that should be verified concern the layout of the winder, with reference to the items addressed in the winder code of practice, such as D/d ratios, tread pressures, catenary geometry and conveyance loading systems.

4.2.2 Corroboration of rope maintenance practice

The rope hygiene practices should be established through interviews (and verified during the subsequent field studies). Specific issues that are to be addressed include frequencies of front and back end cutting and the associated operations such as releasing rope torque, turning end for end and any operations on drums and sheaves. The interviews will also serve to learn about staff experience.

It may happen that winders with poor rope lives will have dramatic improvements once the staff members realise that they are under scrutiny. If this is the case, the investigators should attempt to understand what is being done differently once the study begins.

4.2.3 Winder behaviour measurement

A series of measurements must be done on each winder. These include measurements of winder dynamics and rope forces, fleet angles, drum flexure, rope slip and rotation as well as qualitative assessments of lateral rope oscillations in the catenary and in the vertical rope section. A data logger should be installed at each winder to record extraordinary events. Each time a winder is tripped or when unusually high or low rope forces occur, the data logger should store the history leading up to such an event. Parameters that should be recorded include drum position and speed, motor current and rope force (if such a measuring channel is available).

4.2.4 Rope inspections

Having selected winders based on fairly consistent rope lives, it is not considered essential to attend to a rope from the beginning to the end of its life. What is necessary, however, is to ascertain the onset and progression of rope deterioration. Rope inspections may therefore commence at any time, but they should include one whole life cycle. An installed set of ropes should therefore be monitored up to discard and the next set should be inspected until its age is at least that of the current set.

Studies on rope deterioration rates should concentrate on normal rope deterioration. Local damage and distortion of the rope should be noted but is not considered normal deterioration. Corrosion is a rope deterioration mechanism but it can in a way be controlled through lubrication of the rope and will not be considered as part of the mechanical degradation of a rope. If it is practical, sections near the two ends and at the middle of the ropes should be identified for detailed inspections. Such sections should be subjected to normal wear. If, on the other hand, it is not possible to find such locations on a rope, then a few rope sections with very little deterioration should be inspected regularly. This is necessary so that the minimum deterioration rate under a given set of operating conditions can also be ascertained.

Most of the parameters required during the deterioration studies are normally recorded during routine rope condition assessments. Besides the parameters that (according to the code of practice) are recorded during normal inspections, the following should be determined:

- The number of deformed and/or abraded wires should be counted and the width of the flattened section of each wire at a rope cross-section should be measured.

- If possible, replicates should be made of the rope's surface wherever detailed observations are recorded. Such replicates can be taken to the laboratory where measurements and microscopic examinations can be done.

The number of cycles completed by the set of ropes have to be recorded together with the above measurements. The way in which the cycles of a man-material winder will be counted has to be defined.

Other details obtained from the EM tests that are not directly relevant are relative loss in steel area from corrosion and from localised defects or distortion. These should be recorded for completeness of the study because these might eventually be the major reason for discarding the rope.

Further information on the relative position of the rope on the drum will be obtained from the recording of:

- Dates at which the back ends were pulled in and the length of rope pulled in.
- The dates at which the fronts were cut and the length of rope removed.
- Number of dead turns at rope installation.
- Number of dead turns at discard.
- If the rope was turned end for end, the date and lengths of rope cut at the ends.

Information on other factors that could influence the performance of the rope will be obtained from recording:

- the date and the conveyance positions whenever emergency braking occurred,
- when the ropes were re-lubricated,
- when the sheaves were re-profiled, and
- occurrences of slack rope and overwinds.

4.2.5 Evaluation of discarded ropes

Tensile tests on the rope after discard should be done on at least 10 specimens per rope. Specimens from the front, middle and back, near layer cross-overs on each layer, the section of rope that was the reason for discard and any specific sections that were observed in detail during the life of the rope should be included. The rope specimens should also be subjected to steel area measurements to determine variations in the amount of volume loss along the length of the rope.

Post test examinations are required to assess the damage mechanisms in detail. Such examinations should include microscopic examinations of deteriorated wires.

4.3 LABORATORY WORK

The investigations into the deterioration mechanisms of drum winder ropes should be augmented by simultaneously carrying out supporting laboratory investigations. The following are relevant and deals mostly with rope strength, internal rope stresses, and fatigue.

The work will initially be centred around triangular strand ropes, but every effort should be made to include other rope construction as well, especially if multi-layer strand ropes are to be used on drum winders.

4.3.1 Internal rope stresses

It has been shown[3] that the internal rope stresses generated by bending the rope over the sheave and on the drum could be much larger than the stress variations generated by axial load changes (the normal load range). If this is proved to be correct, it will have a great impact on the way in which rope deterioration is perceived.

Various researchers have done a great deal of work on internal rope stresses caused by loading and bending of the rope. The first task will therefore be to study the various papers published on this subject to determine their validity and to summarize the findings. If the information in the literature is inadequate, the project should be expanded to include the proper derivation of internal rope stresses.

The theoretical models and analyses should be verified by actual stress measurements on a rope. Stress measurements can be done on winder installations or in the laboratory.

The rope bending stresses generated by lateral oscillations of the rope in the shaft and in the catenary require investigation. The effect of lateral oscillations at the termination and at the tangent points on the sheave and drum also needs to be investigated. This could form part of the work on rope terminations. The rope stresses generated during the doubling down procedure can also be calculated. Coiling sleeves, rope turn cross-overs and layer cross-overs force the rope to follow a certain pattern. The bending stresses generated under these circumstances could then be addressed.

Another aspect that might need attention is the unsymmetrical distribution of stress in the rope: Some defects might not cause the breaking strength to change substantially (because of yielding of individual wires) but could greatly affect the stresses inside the rope in the elastic portion.

The following projects are proposed:

- Collect and study literature on internal rope stresses, especially bending.
- Measure the stress in ropes subjected to bending.
- Calculate rope stresses for lateral rope oscillations, doubling down and coiling arrangements.
- Investigate unsymmetrical rope stresses.

4.3.2 Contact stresses

Contact stresses are responsible for the plastic deformation of the surface of the rope, and are present where the rope is in contact with the sheave, at the contact on the surface of the drum, and rope on rope contact for multi-layer coiling on the drum.

The magnitude of the contact stresses depends on the tensile force in the rope, the radius of the contact surface (sheave or drum) and the area of contact. The area of contact presents the

biggest problem. As the rope is plastically deformed during use, the contact area increases. This, in turn, would result in decreased contact stresses.

The projects under this heading should concentrate on theoretical and practical studies to determine the minimum contact force required to cause plastic deformation for a rope with a given deformed surface (from new to fully deformed). Different rope constructions should be included in the study because they will have different contact areas, especially when new.

The findings of this investigation will be compared to the results obtained from the field deterioration studies of rock hoisting drum winders and counterweight winders. The ability to calculate the rate at which the surface of the rope deforms should result from these studies.

The influence and effect of repeated contact stresses should be studied. It is possible that the stresses are large enough to initiate cracks. The combination of backslip and contact stresses should be dealt with as well.

Proposed projects:

- Assess the contact stresses on rope surfaces through studying the contact geometry.
- Investigate the effect of repeated contact loading.

4.3.3 Rope fatigue

Both drum winder ropes and Koepe winder ropes are primarily discarded after excessive numbers of broken wires have developed with time. The formation of broken wires means that some fatiguing mechanisms have to be present in both winder systems for the initiation and propagation of wire cracks. Koepe winder ropes operate at larger load ranges than those on drum winders, while the deterioration of the surface of ropes is quite severe on drum winders and about non-existent on Koepe winders.

The load ranges experienced by Koepe winder ropes are considered large enough to generate broken wires. This has been illustrated during laboratory tests on new ropes. The presence of the surface deterioration on drum winder ropes makes it easier for cracks to initiate. The combination of the normal load range, together with the rope stresses generated by bending the rope over the sheave and drum, is large enough to propagate the cracks.

Reports on fatigue tests on Koepe winder ropes (mostly spin resistant ropes) have been reported on in the literature. Normal tension-tension tests and bending-over-sheave (BoS) tests are applicable. The relevant literature should be gathered, analysed and summarised to verify the state of the knowledge and whether it is fully applicable to Koepe winder systems. The results will suggest whether further work will be required.

Information on fatigue tests on triangular strand ropes, which are predominantly used on drum winders, is most probably quite sparse. A literature survey on this subject is also

required to verify the state of the knowledge and whether it is fully applicable to drum winder systems. The possible influence of the addition of bending stresses to axial stresses has to be looked at to assess the validity of the results from past projects.

The hypothesis that rope fatigue behaviour is independent of mean load can also be verified from the results of the literature surveys.

Preliminary investigations have suggested that earlier fatigue testing for drum winder ropes was done on new rope samples and at load ranges lower than those believed to act on ropes in reality. A series of fatigue tests would provide a better understanding of the formation of broken wires in drum winder ropes. Fatigue tests should be carried out on rope samples (of the same diameter) but at different stages of deterioration. Such samples can be cut from a discarded drum winder rope which will have greater deterioration at the back end than the front end. The test program should include BoS tests as well.

The test programme should be extended to include other rope constructions. Difficulty will be experienced in obtaining worn samples of construction other than triangular strand, because nearly all drum winders operate with triangular strand ropes.

If the rope deteriorates during a fatigue test, it will only be due to individual wires that develop cracks and fractures. It is not necessary to proceed with a fatigue test until failure of the rope, but a method of counting the number of broken wires and finding their locations is required. The remaining strength of the rope at any stage during a fatigue test can be estimated in this way. Fortunately, triangular strand ropes develop fractures in the outer wires of the strands, and are therefore visible. The rate at which broken wires develop during a fatigue test will be a first indication of the form of the envisaged "deterioration curve".

Proposed projects:

- Literature survey on rope fatigue tests.
- Analysis of results to verify the applicability of the test to local conditions.
- Decision on and planning of laboratory fatigue investigation.
- Tension-tension fatigue tests on triangular strand ropes (new and used).
- Study the influence of torque on the fatigue behaviour of triangular strand ropes.

4.3.4 Behaviour of ropes subjected to high loads

Industry has expressed its concern regarding the torque that will be generated by triangular strand ropes at depths greater than 2 500 m and at relatively low "safety factors". It is believed that the excessive torque generated could lead to rope behaviour problems. In order to start addressing these concerns, it is suggested to measure the torque in a rope on winder and to determine the torque-tension-twist properties of sections of rope from the front, middle and back of the rope.

The torque and twist in the rope will be measured and calculated, and will be compared to the lay length after the rope has been installed, how it changed during the life of the rope and what permanent set could be observed after the rope was discarded.

The newly proposed dynamic factor for drum winder ropes will allow the rope to be loaded to 40% of its breaking strength during normal emergency braking. This load level is close to the yield point of the rope. It is therefore possible that a section of a rope will yield during severe emergency braking. This would also be the case when the winder has to be brought to a halt in the shortest distance possible, or when the brake comes on fully because of a brake controller malfunction.

The subsequent behaviour of a yielded rope section on a drum winder is not known. It may be possible that the rope could deteriorate very rapidly after it has been yielded. Possible rope property changes caused by the yielding of the rope could result in unacceptable local laylength or diameter distortions. It is therefore not possible to prescribe what should be done after such an event has occurred, i.e. if the rope has to be discarded immediately, after a while, or not at all.

A basic investigation is required to find out whether rope properties (elastic modulus and torque behaviour) of a yielded rope is any different to a normal rope.

Proposed projects:

- Fatigue tests on rope specimens (new and used) that have been loaded past their yield strength.
- Torque-tension-twist tests on rope specimens that have been loaded past their yield strength.

REFERENCES

1. Van Zyl,M.N. *A Life Prediction Model for Drum Winder Ropes* CSIR Contract Report MST(91)MC662, February 1991

2. Kuun,T.C. *Single Lift Shafts: Limits of Winding Rope Application* Anglo American Corporation ref.TS/TCK/IS/A702/5, May 1988

3. Hecker,G.F.K., Van Zyl,M.N. *Drum Winder Rope Test Facility: a Feasibility Study* CSIR Contract Report MST(93)MC1233, January 1993

4. Hecker,G.F.K., Van Zyl,M.N. *STATUS REPORT: Safety Standard for the Performance, Operation, Maintenance and Testing of Mine Winding Plant* CSIR Contract Report MST(94)2281 No 940248, November 1994

5. Van Zyl,M.N. *Information on 99 drum winders and 711 discarded ropes* CSIR Contract Report MST(90)MHT3, May 1990